UNIVERSITY OF OKLAHOMA

GRADUATE COLLEGE

EXPERIMENTAL STUDY OF PROPPANT TRANSPORT IN HORIZONTAL AND DIRECTIONAL WELLS

A THESIS

SUBMITTED TO THE GRADUATE FACULTY

in partial fulfillment of the requirements for the

Degree of

MASTER OF SCIENCE

By

SOHAM PANDYA
Norman, Oklahoma
2016

EXPERIMENTAL STUDY OF PROPPANT TRANSPORT IN HORIZONTAL AND DIRECTIONAL WELLS

A THESIS APPROVED FOR THE
MEWBOURNE SCHOOL OF PETROLEUM AND GEOLOGICAL ENGINEERING

BY

_____
Dr. Subhash N. Shah, Chair

_____
Dr. Ramadan Ahmed

_____
Dr. Maysam Pournik

To my beloved Grandfather.
You will always be in our hearts.

Acknowledgements

The encouragement of the people close to me is what made this research a successful endeavor. I would like to take this opportunity to thank all of those who, whether directly or not, assisted with the completion of this thesis.

I am immensely grateful to my family for their unwavering support and encouragement; they have not only provided me with invaluable resources but have also constantly inspired me to strive for excellence. For this, I am deeply indebted to them.

I express my deepest appreciation and gratitude toward Dr. Subhash N. Shah for his guidance, support, and invaluable knowledge. His mentorship throughout my Master's program has been crucial to my development as a researcher.

I would also like to thank Dr. Ramadan Ahmed for his commitment to helping me and his faith in the quality of my work, which served to refine my ideas. I am also grateful to Dr. Maysam Pournik for investing his time in my work by serving as a committee member, despite his busy schedule.

I would like to extend a special thanks to Jeff McCaskill for his technical support with lab equipment. I would like to thank my fellow lab mates Vineet, Abhishek, and Harsh, who graciously contributed time by conducting experiments, lending insight, and engaging in technical discussion. You guys actually made learning science to be fun. I am also thankful to Sarvesh for conducting the study that served as a foundation for this research. I am especially grateful to Maulin for his assistance in particle size analysis test.

I would also like to acknowledge all my friends including Nidhi, Sumeer, Abhijeet, Tabish, Anvit, Nauman, Mounraj, Aman, Kritika, Fatema and Richa for making this place a home away from home with their love and emotional support. Thank you guys for always being there during my highs and lows.

Last but not the least, thank you Science!! You taught me that every experiment proves something. If it didn't prove what I wanted it to prove, it proved something else.

Table of Contents

List of Tables

List of Figures

Abstract

Wellbore cleanouts represent the main application of the coiled tubing (CT) industry. A typical cleanout operation designed to remove solids from the wellbore using stationary circulation method involves tripping the CT to a target depth, and circulating the fluid to erode the solids bed and suspend particles into the flow stream up to the surface. Theoretically, the wellbore can be cleaned out completely by circulating a high density fluid at very high flow rates. However, this would result in high bottom-hole pressure that may exceed the fracture pressure of the formation. Thus, the circulation process is associated with limitations of maximum achievable flow rate and equivalent circulating density of the fluid. Hole cleaning is a function of multiple variables including but not limited to fluid properties, flow rate and wellbore deviation. The efficiency of hole cleaning operation is crucial to the industry. Therefore, we seek answers to how these variables influence the hole cleaning efficiency.

Efficiency of fluid was quantitatively studied by bed erosion tests conducted in a 34 ft test section of 5½-in. OD (5-in. ID) outer transparent pipe and 2.375-in. OD inner tubing. The reduction in bed height as a function of circulation time, fluid rheology, flow rate, and wellbore inclination was investigated. Fluids incorporated in this study were water, and 10 lbm/Mgal and 20 lbm/Mgal Guar fluids. Proppant used in the study was light-weight 20/40 mesh size ceramic proppant. Proppant bed was deposited using freshwater. Bed erosion was carried out at flow rates from 80 to 120 gpm and within inclination of 45° to 90°.

To quantitatively describe proppant transport efficiency, two parameters were used as the target variables in this study –

i. Normalized Bed height: indicates the vertical height of the stationary proppant bed in the annulus with respect to the initial vertical bed height.
ii. Cleanout efficiency: measure of the weight percentage of proppant cleaned out of the test section at end of 30 minutes.

Bed erosion curves were generated to analyze the data with respect to the reduction in bed height with time for various parameters. Efficiency plots were analyzed to determine the range of critical inclination within which efficiency of all fluids is similar. An important consideration in designing cleanout operations is the proper selection of the pump rate and circulation fluid. Higher turbulence generated by low viscosity fluid (water) assisted in better lift of particles from the stationary bed. However, higher viscosity fluids tend to transport particles in the flow stream to a greater distance due to its greater carrying capacity. It was observed that the low viscosity fluids like water performed better at higher inclinations whereas, higher viscosity fluids performed better at lower inclinations due to their relatively superior particle carrying capacity. In general, it is recommended that cleanouts should be conducted using high viscosity fluids for wellbore inclination less than 70° (critical inclination). Experimental results were analyzed by non-linear regression technique to establish a functional relationship among different parameters. Empirical bed decay model was developed to incorporate the effect

of change in circulation time, flow rate, and fluid rheology for each inclination. Field application of the developed correlation can aid in optimized cleanout practices.

CHAPTER 1

INTRODUCTION AND SCOPE OF RESEARCH

1.1 Introduction

Complex structure wells like horizontal well, multilateral well, and extended reach well are becoming the preferred well profiles, especially for low permeability formation such as shale. With increasing target depth and longer lateral length in the directional and horizontal wells, effective hole-cleaning becomes critical for successful drilling and completion operation. Movement and accumulation of solid particles can have a considerable impact on fluid flow within the wellbore.

Buildup of the solid particles in the wellbore significantly hinders the oil and gas production. To regain productivity of the well, removal of accumulated solids to the maximum possible extent is necessary. This inhibition in production is commonly dealt with CT intervention. Coiled tubing stands out as a viable option because it is relatively easier to rig up/rig down as compared to a conventional workover rig. Moreover, tripping time is considerably less than that for a jointed tubing string used by conventional workover rigs. Nearly half of all CT operations consist of well cleanouts to remove debris such as produced sand or residual proppant from hydraulic fracturing treatments (Rolovic et. al. 2004). Despite a long history of CT hole-cleaning methods, advancement in technology, and good amount of experience, many cleanout operations are frequently considered inadequate. This leads to frequent protracted interventions and prevents timely return of the wells to production.

Wellbore cleanout operation is always associated with non-productive time and significantly adds to the operational cost of a rig. The complexity of the wellbore cleanout process presents a challenge in terms of how various associated parameters affect the solids transport mechanism. In order to minimize the operational cost, it is of utmost importance to understand the solids transport mechanism within the wellbore and the parameters affecting it.

Figure 1.1 depicts a typical wellbore cleanout operation with CT. Coiled tubing is a continuously milled tubular pipe that is spooled on a reel. The CT is nominally straightened during a trip in process and is recoiled back for spooling on reel during trip out. The elimination of making any pipe connection reduces the chance of spillage and the number of personnel required. The most common technique for inclined and horizontal wellbore cleanout uses a jetting tool conveyed downhole by CT. While pumping cleanout fluid down the tubing, the tool is lowered into the wellbore until it tags the top of the sand column or other debris, often termed as fill. The CT is further run into the hole to a target depth while jetting into the solids. The nozzles create high velocity jets which cause agitation, mixing, and local suspension of particles at the end of the string. The jetting nozzles are designed to create turbulence that aids in mobilizing and suspending the solid particles. The turbulence decreases as the distance from the nozzles increases. Consequently, the solid particles settle on the low side of the annulus in the inclined wellbores. With continuous particles settling, a “solids bed” is formed at the low side of annulus. With increasing solids bed height, less of the wellbore cross sectional area is available for the clean fluid to flow. As a result, the fluid velocity across the surface

of the bed increases until a critical velocity is attained. The erosion and deposition processes equalize at this velocity and this leads to an equilibrium condition in the wellbore. The lateral or upward distance traveled by particles before settling is influenced by the fluid properties (viscosity and density), solid properties (size, density, and concentration), flow rate, wellbore geometry, and pipe eccentricity (Xiaofeng et al. 2013). Fluid viscosity and flow rate are two common parameters that are carefully controlled to improve cleanout operation without over-pressurizing the formation. High flow rate can produce a higher bottom hole pressure gradient that exceeds the fracture gradient of the formation. This limits the increase in flow rate during cleanout operation. Hence, in many cases, the maximum flow rate achievable during a cleanout job may be insufficient to erode the bed.

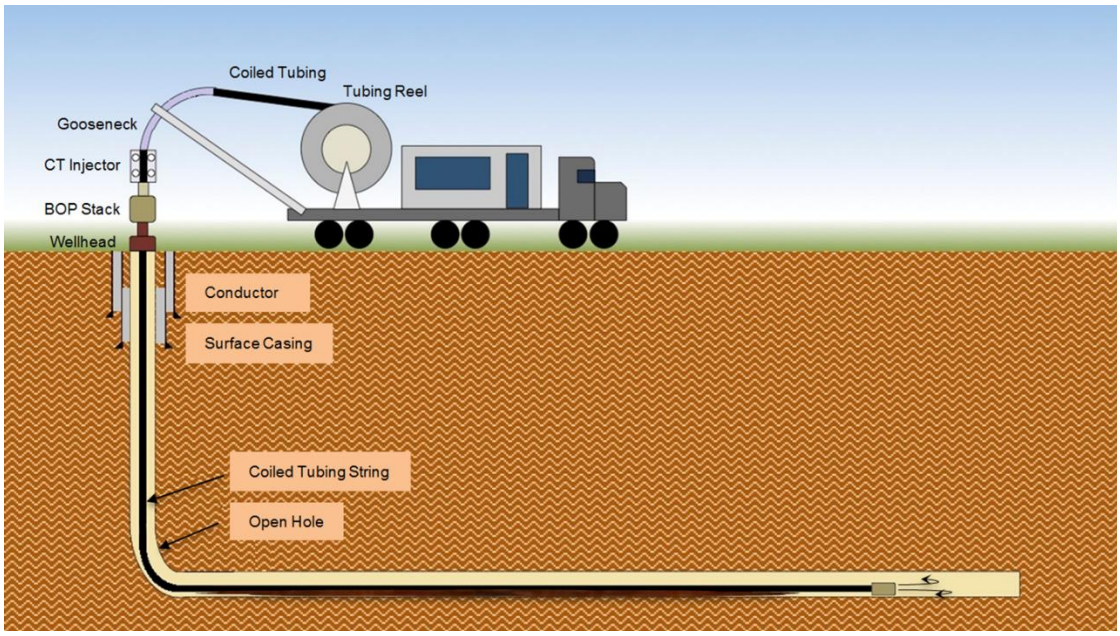

Figure 1.1: Wellbore cleanout process using CT (Naik, 2015)

The procedure mentioned above is termed as stationary circulation since the position of CT is fixed during the entire cleanout process. The stationary circulation method generally involves a CT of large diameter, higher flow rates and using costly bio-polymeric fluids. Although such a method has proven to be efficient, it can be time consuming and costly. Alternatively, a common industry practice, termed as 'wiper trip', is carried out for hole-cleaning. Wiper trip, as defined by Li et al. (2008), is the movement of the CT and the bottom hole assembly out of the hole up to a certain distance or to surface, while continuously circulating cleanout fluid through the upward-facing, low-energy nozzles of the specialized downhole cleanout tool. The cleanout process during the wiper trip is similar to that of a stationary circulation except that the CT string is also in motion. As the jetting tool moves upward along with CT, turbulence generated by nozzles helps to lift and suspend the solids, transporting it up the hole until solids once again settle out of the flow stream. The cycle repeats, displacing the bed up the hole as the CT is pulled out. Depending on the job type, a single or multiple wiper trips may be required to clean the hole.

Coiled tubing cleanout provides two circulation modes to remove solids: forward and reverse circulation mode. In forward circulation, the fluid is pumped through CT and solids are transported through the annulus between casing/open hole and CT. In some cases, size of available CT limits the maximum achievable flow rate during forward circulation. In reverse circulation, the fluid is circulated through the annulus and the solids are transported through CT. Due to smaller cross sectional flow area, it is possible to

achieve higher fluid velocity inside CT and efficient cleanout can be conducted by circulating fluid up the CT.

Despite numerous studies carried out to understand the solids transport mechanism, varied and ambiguous experimental results have been reported by researchers. Due to the complexity of solids transport mechanism, the oil and gas industry has accepted certain rules of thumb that are used to compensate for the incomplete understanding of solids transport. For example, one common procedure is to circulate two hole volumes at target depth; which may be insufficient to clean the wellbore (Li and Luft, 2014).

Different studies have conflicting views on whether fluids with high viscosity or low viscosity perform better, or whether circulating the clean fluid for longer time results in better cleanout. Thus, it can be stated that the solids transport is not entirely understood, partially because of the inter-dependence of different parameters affecting cleanout. This study focuses on cleanout of proppant from the wellbore using water and low viscosity polymer fluids. Proppants are natural or man-made solids used in hydraulic fracturing to keep the generated fracture open once pumping stops.

1.2 Problem Statement

The success of a cleanout operation using a specific fluid depends on the circulation rate and time. However, high-rate circulation for a long time increases non-productive time. Hence, it is important to optimize these factors. The vital parameters to be considered during optimizing a cleanout operation are fluid, flow rate and circulation time of the operation. Many theoretical and experimental studies have been conducted on the solids

transport mechanism in the past. However, most of them mainly focus on the transport of drilled cuttings through drilling muds. Moreover, only few of the previous studies have related the cleanout parameters to the inclination angle of the well. The models generated to predict the cleaning efficiency are often complex and cannot be applied in the field.

With rapid increase in fracturing treatments being conducted, it is vital to understand the transport behavior of proppant in the wellbore. Proppant settling in the wellbore can be a result of screen out during fracturing treatment or proppant backflow during initial stages of production. The resultant solids bed formed can significantly lower the hydrocarbon production. Previous study carried out by Naik (2015) summarized the effect of flow rate and fluid rheology on the erosion of proppant bed. This research carries the study forward to determine the type of fluid to be used based on the specific inclination of the wellbore. Moreover, previously developed correlations have been improved to optimize the results by incorporating the effect of flow rate and fluid rheology.

1.3 Scope of Research

This research aims to gain an insight into the wellbore cleanout operations using water and low viscosity polymeric fluids pumped at different flow rates and for various inclinations of the wellbore. A review of the effects of fluid rheology and flow rate on solids cleanout in horizontal and inclined wells is discussed; followed by the determination of critical inclination angle at which all tested fluids exhibit approximately a similar cleanout performance. This will help field engineers to design a cleanout fluid

according to the well profile. Finally, the previous empirical correlations developed by Naik (2015) have been improved to incorporate the effect of fluid rheology and flow rate.

The previously fabricated experimental setup used for wellbore cleanout study was modified to improve the quality of data. The modified setup was used to repeat some of the previously conducted tests to check for repeatability. Moreover, tests at the inclination of 50° and 70° were conducted for the accurate determination of critical inclination. The cleanout fluids selected were water, 10 lbm/Mgal guar, and 20 lbm/Mgal guar. Solids used to deposit the bed were 20/40 mesh ceramic proppant. A total of 30 tests were conducted including 12 repeat tests and 18 new tests. Overall, the data was obtained at flow rate of 80, 100 and 120 gpm and inclination of 45, 50, 60, 70, 75 and 90°.

Guar gum is a unique galactomannan based bio-polymer processed from endosperm of cluster bean. Chemically, guar gum is a polysaccharide composed of the galactose and mannose. Both sugars have the same chemical formula of $C_6H_{12}O_6$; however, they are structurally different. The backbone of guar gum is a linear chain of β 1,4-linked mannose residues to which galactose residues are 1,6-linked at every second mannose, forming short side-branches as shown in **Fig. 1.2**. The molecular weight of the polymer ranges from 5×10^5 to 8.0×10^6 g/mol. It is commonly used in the form of liquid gel concentrate as an additive in various oilfield operations like hydraulic fracturing, jet perforations and hole cleaning. The predominant use of guar is attributed to its ability to form strong hydrogen bonds with water molecule. It is a hydro-colloidal and remains stable in solution over a pH range of 5-7. Thus, it is chiefly used as thickener and stabilizer. Guar gum used

in this study was in the form of liquid suspension. The activity of the polymer was 4 lbm per gallon of slurry.

The solids used in this study are TerraProp Plus light weight 20/40 mesh ceramic proppant supplied by Baker Hughes, Inc. It is a synthetic product of bauxite and hence, its major constituent is aluminum oxide. This proppant has an average diameter of 630 microns and a relative density of 1.75.

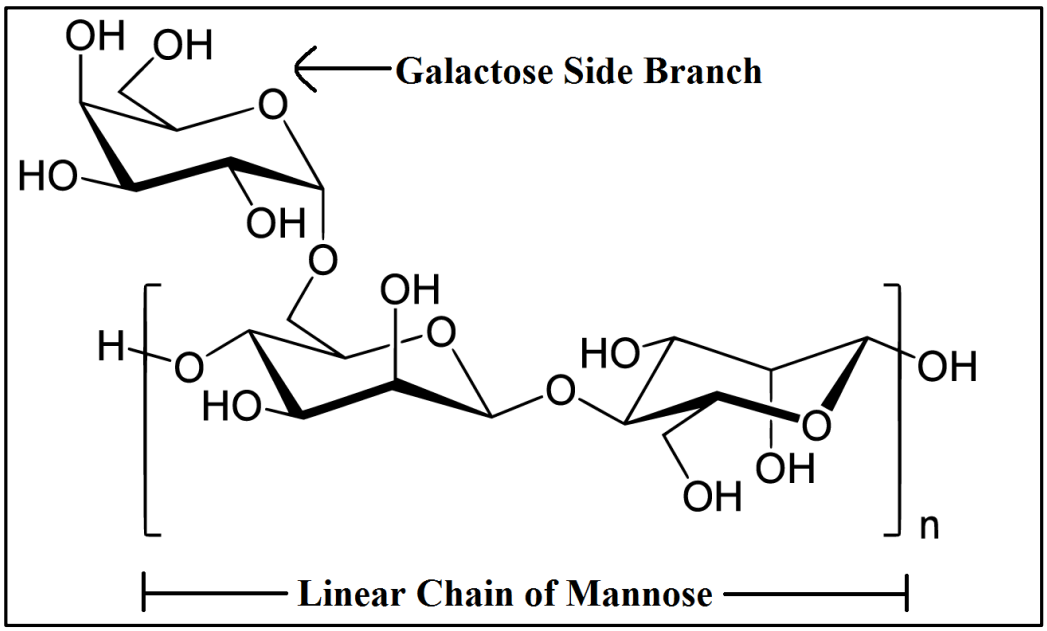

Figure 1.2: Chemical structure of guar gum

Auxiliary tests to check for the variation in proppant size were also carried out. Proppant used to deposit the bed during tests was dried and reused in successive tests. Also, due to minor loss of proppant in the flow lines during each test, a new batch of unused proppant was periodically mixed with the remaining proppant. Consistency in the size of proppant was investigated to prevent variation in solids properties. Laser particle size analysis was

carried out on a sample of unused proppant, sample of proppant from the batch after 36 tests, and sample of proppant from the batch after 60 tests. The equipment, test procedure, and results of the particle size study are discussed in Appendix A.

1.4 Approach

Solids bed erosion tests were conducted with various fluids and using 20/40 mesh proppant to investigate the effect of flow rate and fluid rheology at different inclination. Solids bed was deposited in the annulus using measured weight of proppant followed by a re-circulation of cleanout fluid at a constant flow rate to erode the bed. A filter was placed downstream of the test section to separate solids. The weight of solids removed was used to determine the cleanout efficiency for each case. The solids bed height with time was recorded for each experiment at 42 locations (21 on each side) along the wellbore.

Data was plotted as solids bed height versus time and an exponential equation was fitted using non-linear regression analysis. The results indicated that low viscosity fluids (water) performed better in near horizontal well profiles (high inclination angle). However, as the inclination angle is reduced from 90° to 45°, the polymeric fluids (10 lb/Mgal guar and 20 lb/Mgal guar) exhibited better cleanout efficiency as compared to water after some particular inclination. In order to determine the critical wellbore inclination, additional data points were generated using the procedure described above.

1.5 Objectives

The primary objective of this study is to perform experimental studies on wellbore cleanout in directional wellbores using CT. Specific objectives are as follows:

1. Conduct solid erosion tests with fresh water, 10 lb/Mgal and 20 lb/Mgal guar fluids, each at flow rate of 80, 100 and 120 gpm and inclination of 50° and 70°.
2. Determine the critical inclination angle beyond which the high viscosity fluid exhibits better cleanout efficiency than the low viscosity fluid.
3. Improve the empirical correlations previously developed by Naik (2015), which relates solid bed height reduction to circulation time for a given flow rate and fluid rheology at various inclinations.
4. Extend the empirical correlations to incorporate the effect of flow rate and fluid rheology on bed height reduction in addition to circulation time.

1.6 Overview of Thesis

This thesis is divided into 7 chapters. Chapter 1 underlines the objectives for this study and the approach taken in order to meet the objectives. Chapter 2 details the physical phenomena of particle transport in an inclined annular section under various conditions. The various parameters that play a vital role in wellbore cleanout are discussed. Moreover, studies conducted by previous researchers are summarized as literature review. The description of experimental setup, test procedure and data analysis is provided in chapter 3. Experimental results, data analysis, and discussion on these results is detailed in chapter 4. In chapter 5, the development of empirical correlations to incorporate the effect of fluid rheology and flow rate is discussed. This is followed by the

limitations and range of applicability of this model. The field application of the study is discussed in chapter 6. The conclusions and recommendations from this study are discussed in chapter 7. Results of auxiliary tests conducted to verify the consistency in proppant size throughout the tests are provided in Appendix A.

CHAPTER 2

THEORY AND LITERATURE REVIEW

A review of theoretical and empirical models available to study the solids transport is detailed in this chapter. Solids transport mechanism in the wellbore is widely a function of fluid and solids properties, and wellbore geometry. A discussion on sensitivity of these parameters on solids transport is also presented here.

2.1 Theory

Figure 2.1 shows a solid particle on the low side of the wellbore wall in an inclined well with inclination angle, θ. Various forces acting on the particle in an inclined wall system are forces due to gravity, buoyancy, and hydrodynamic drag and lift.

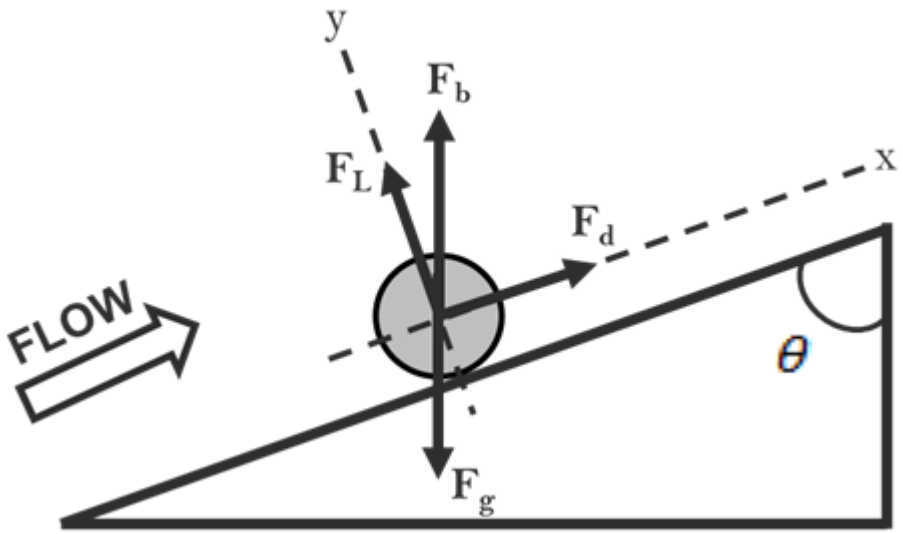

Figure 2.1: Forces acting on a solid particle

Force due to gravity is a function of the mass of particle and is expressed as:

$$F_g = mg$$

If the mass of particle is expressed in terms of the particle density and volume, then:

$$F_g = \rho_s V_s g$$

$$F_g = \frac{1}{6}\pi d_s^3 \rho_s g \qquad (2.1)$$

where,

$F_g =$ force due to gravity;

$m =$ mass of the particle;

$\rho_s =$ density of particle;

$V_s =$ volume of particle;

$d_s =$ diameter of particle;

$g =$ acceleration due to gravity.

Buoyancy is an upward force exerted by a fluid that opposes the weight of an immersed object and is expressed as:

$$F_b = m\left(\frac{\rho_f}{\rho_s}\right) g$$

or, in terms of particle diameter as:

$$F_b = \frac{1}{6}\pi d_s^3 \rho_f g \tag{2.2}$$

where,

$F_b =$ force due to buoyancy;

$\rho_f =$ fluid density.

The hydrodynamic lift force acts perpendicular to the fluid flow axis and tends to lift the solid particle off the low side wall of the annulus. The drag force is the frictional force acting on the particles parallel to the fluid flow axis. The hydrodynamic lift and drag on the solid particle are given by:

$$F_L = \frac{1}{2} C_L \rho_f u^2 A_p \tag{2.3}$$

$$F_d = \frac{1}{2} C_D \rho_f u^2 A_p \tag{2.4}$$

where,

$F_L =$ lift force;

$F_d =$ drag force;

$C_L =$ lift coefficient;

$C_D =$ drag coefficient;

A_p = projected area of particle over a mean bed surface;

u = fluid velocity.

The coefficient of drag C_d and lift C_L are determined experimentally by varying conditions.

It is important to note that during a cleanout operation, the lift force, drag force, and buoyancy force tend to transport the particles downstream of the flow while gravity tends to move the particles downwards.

For a nearly vertical well profile, the dominating forces acting on particles are the gravitational force and drag force. Hence, the drag force must exceed the gravitational force for the particle to be transported out of the wellbore.

In deviated wellbore, for particle transport mode to be in suspension, the combined vertical component of lift and drag forces must be greater than that of gravitational force. To transport the particles by rolling or sliding them along the low side of the wellbore, the drag force must exceed the axial component of gravitational force. In general, when hydrodynamic forces exceed the static forces (buoyant and gravity), the particles tend to roll along the bed. The dynamic forces generally increase with fluid velocity.

2.2 Parameters affecting Wellbore Cleanout Efficiency

Well cleanouts are by far the most common operation performed with CT and also one of the most complex operation due to many operational variables involved. Hence, it becomes necessary to understand the effect of major factors involved in a well cleanout

design in order to optimize the process. Cleanout design and performance are functions of the following parameters.

2.2.1 Wellbore geometry

For a given flow rate, the CT completion annular area is dictated by the casing size or diameter of the open hole and the external diameter of the inner tubing. Large internal diameter of the completion makes it more challenging to obtain an adequate annular fluid velocity. Correspondingly, large size of the internal tubing string will help achieve higher annular velocity for cleanout operation. Moreover, larger pipe size of tubing makes in feasible to pump at a higher flow rate for a given pressure drop inside the tubing assisting in the cleanout efficiency and providing a better control over the operational life of tubing. However, the selection of higher OD tubing is limited to certain extent. For a constant ID of casing, a higher OD tubing will provide a smaller cross sectional area for the flow which will induce higher annular friction pressure. Another limiting factor, especially for larger OD CT is the logistics and safety. Hence, the selection of completion size including the ID of outer hole and OD of the inner tubing, and pump rate should be optimized.

Becker and Azar (1985) studied the effect of drillpipe diameter on the concentration of cutting generated during drilling process. A general observation made was that the volumetric cuttings concentration increases slightly with increase in drillpipe diameter. Another study conducted by Jalukar (1993) suggested that cuttings transport velocity requirement increases as the hydraulic diameter for flow increases. However, this effect

is insignificant if the wellbore inclination is between 30° and 45°. Both the studies had a major limitation that all the tests were carried out with a nominal fluid velocity of 2.5 ft/s. For the specified configurations of experimental setup used, this velocity results in a laminar flow regime. However, the cleanout process is well within the turbulent regime. Hence, it was not conclusive of the effect of wellbore configuration in hole cleaning within turbulent flow regimes.

2.2.2 Particle properties

The properties of particles being lifted from the bottom and transported to the surface might not be entirely known in some cases. The sphericity of particle is often neglected in cleanout studies but is an important factor affecting the fluid kinematics acting on particles. The viscous force acting on particle is more uniform and maximized in the case of perfectly spherical particle. The spherical particle has maximized surface area per volume ratio that helps it being transported much readily than angular particle. Moreover, the fluid induced rotation on spherical particle negligibly hinders the inertia or ability to move as it spins. Not only are the angular particles difficult to lift from a stationary bed, but they continuously accelerate and decelerate or even stop as they rotate along their own axes. Hence, for the same amount of distance transported, the angular particles require more time for circulation and more energy to be imparted by the fluid.

The density of solid particle has a direct impact on the weight of particle. The weight of particle and the density difference between fluid and particle determines the subsequent lifting of particle from the stationary bed into flow stream. As expected, a heavier particle

is more difficult to transport. Li and Wilde (2005) carried out tests with four different 20/40 mesh proppant densities. The specific gravity of proppant tested varied from 1.25 to 3.6. It was concluded that for a given flow rate, higher density solids deposit easily to form a solids bed. It was also concluded that for a constant flow rate, the solids were easier to transport in vertical wellbore than in the horizontal wellbore. This conclusion is only partially correct since the fluid employed for hole cleaning dictates the efficiency in vertical and horizontal wellbores. It is observed in this study that more viscous fluids perform better in vertical wellbores whereas low viscosity fluid such as water perform better in horizontal sections.

Many studies have been conducted to study the effect of particle size. Larsen (1990) tested different cuttings size distribution: large (0.275 in.), medium (0.175 in.) and small (0.09 in.). It was concluded that smaller cuttings were difficult to transport at higher inclination. However, on reducing the inclination, the smaller sized cuttings of the same shape are easier to clean. Li and Wilde (2005) investigated three different particle sizes and concluded that velocity required to prevent solids from settling into the bed (critical velocity) initially increases with increase in particle size (up to 0.5 mm). On further increasing the particle diameter, the critical velocity decreases. This is attributed to the reason that for large particles the shear stress at the interface of upper fluid flowing layer and lower stationary bed layer increases with increasing particle size. The results obtained are fairly consistent with other studies carried out to study the effect of particle size on hole cleaning efficiency.

2.2.3 Wellbore Inclination

The wellbore inclination is an important parameter affecting solids transport. Different modes of solids transportation are encountered based on the inclination angle. Three different ranges of inclination angle have been identified according to the mode of transport associated to it. The regions are:

1 Low (0 to 30°)

2 Intermediate (30 to 60°)

3 High (60 to 90°)

Under no flow conditions, the solids bed tends to slide downward in a deviated wellbore and accumulate at the 'heel'. During fluid flow, this is avoided by the drag force of the fluid. In order to keep the solids in suspension, the fluid velocity should be increased in the intermediate inclination wellbore section. Usually, with an inclination angle between 30 to 60°, the solids bed slides down since the gravity acting on solids bed overcomes the friction force between bed and wall boundaries and fluid forces. Another phenomenon which comes into play is the Boycott effect, which states that settling in stagnant fluid is higher in inclined sections (between 40° and 50°) than in vertical.

Tomren et al. (1986) conducted a total of 242 tests by varying the angles of inclination, pipe/hole eccentricity and fluid flow regimes. It was concluded that solids bed is formed at inclination more than 35°. The authors haven't clearly demarcated this critical inclination in terms of the flow regime. Clearly, in a turbulent flow regime with higher in-situ velocity, there must be a different critical angle of inclination. Peden et al. (1990) studied the Minimum Transport Velocity (MTV) as a function of different operational

parameters. Based on experimental results, MTV required to transport the solids by rolling mechanism within the annulus increased initially as the hole angle increased but reached a maximum value, after which it decreased. The critical angle was found to be in the range of 40 to 60° from vertical. The solids bed at these critical angles was unstable and the authors reported local agitation of particles.

2.2.4 Fluid Characteristics

Fluid characteristics are extremely important in effective cuttings transport behavior. Fluid rheology is a characteristic that requires the most attention. Fluid must be designed in a way to incorporate the highest pump rate with smallest possible friction pressure. High viscosity fluids perform better in vertical or near vertical wells whereas highly deviated and horizontal wells benefit more from low viscosity fluids. Li and Walker (1999) found similar results from their experiments. The authors compared three different fluids (water, HEC, and Xanvis polymer). It was concluded that for the vertical/near vertical wellbore, hole cleaning is more efficient if a high viscosity fluid is pumped in laminar flow regime than a low viscosity fluid in turbulent flow. The shear stress at the solids bed and liquid interface, for a near horizontal wellbore, plays the key role in transport of solids. Low viscosity fluids help generate higher shear rate at the tubular walls and develop a turbulent flow pattern more readily. The turbulence helps in lifting the particles from a stable bed into the flow stream.

Li et al. (2005) studied the cleanout efficiency with various bio-polymers. These bio-polymers had high Low Shear Rate Viscosity (LSRV) and were shear thinning in nature.

These fluids exhibit relatively low viscosity at the fluid-solid interface due to high shear at the interface. As a result, turbulence is generated and it lifts the particle into the flow stream. The fluid element in the flow stream is exposed to a relatively low shear rate as compared to that at walls, and hence maintains high viscosity. Due to this, once the particle is lifted from a stationary bed, the viscous fluid is able to carry it to longer distance before it re-settles. It was recommended that the LSRV should be higher for better suspension capabilities. To summarize, high viscosity fluids are better in carrying the suspended particles whereas low viscosity fluids are more efficient in lifting the particles from a stationary bed. However, high viscosity fluids can be more costly and complex as compared to low viscosity fluids.

The increase in fluid density increases solids suspension capacity of fluid by reducing the settling velocity of particle (or increasing buoyancy). Despite the fact that fluids with higher density increase buoyancy effects, they are difficult to pump in turbulent flow regime. Another disadvantage with ‘weighted’ fluids is the tendency of the weighting material to settle out of the fluid phase, which is known as ‘sag’. The purpose of fluid density is to exert hydrostatic pressure, and hence is not generally changed for improving hole cleaning. However, a small increase in density was found to improve cuttings transport (Sifferman and Becker 1992).

Hence, an optimally designed and supervised fluid increases efficiency of an entire operation, improving the hole cleaning efficiency and considerably decreasing operational time and cost.

2.2.5 Fluid Velocity

Fluid flow velocity is the most important design parameter in order to obtain effective cleanout. With the steady increase in cleanout depth and completion size, higher flow rates are required to achieve necessary fluid velocity. Many experimental studies have been conducted to determine the effect of fluid velocity in hole cleanout efficiency. A high fluid velocity exerts high shear stress on the solids bed, which improves rate of solids transport. Moreover, higher velocity also increases the fluid drag and lift force that aids in greater transportation of suspended solids. It was generally observed that a critical velocity exists, below which the solids will form a bed on the low side of an inclined wellbore or will start settling vertically downwards in case of a vertical well (Li and Walker, 1999).

The cross-sectional velocity profile within the wellbore is much more indicative of a cleanout efficiency since it depends on fluid rheology and shear stress in addition to the flow rate. In practical terms, a fluid can be subjected to either a laminar or a turbulent flow regime, depending on the combination of the inertial forces and frictional forces. A dimensionless ratio of inertial and viscous forces, called Reynolds number, determines the fluid flow regime.

$$Re = \frac{inertial\ force}{viscous\ force} = \frac{\rho_f u d_h}{\mu}$$

where,

$Re =$ Reynolds number, dimensionless;

ρ_f = density of fluid, kg/m^3;

u = mean velocity of fluid, m/s;

d_h = hydraulic diameter, m;

μ = dynamic viscosity of fluid, kg/(m.s).

Laminar flow occurs at low Reynolds number, where viscous force is dominant, and is characterized by smooth, constant fluid motion, which leads to stability. Turbulent flow occurs at high Reynolds number and is dominated by inertial force, which tends to produce chaotic eddies, vortices and other flow instabilities.

It is also important to discuss the flow conditions occurring within a boundary layer. Boundary layer occurs at the solid-liquid interface having a characteristic of fluid velocity reduction to zero, irrespective of the flow velocity and fluid flow regime distant from this interface. This is often termed as “no-slip” condition. In simpler words, no-slip condition states that the fluid adheres to the surface of the solid in a boundary layer.

In laminar flow, the fluid molecules follow the path of streamlines. These streamlines do not cross each other in laminar flow regime. The combined effect of smooth and stable flow in laminar regime plus the no slip condition inhibits the lifting of particles from the solids bed. On the contrary, a large number of eddies are developed when the fluid is well within the turbulent regime.

The size of eddies can vary from very large ones crossing several streamlines to much smaller ones that are limited to near the walls. In terms of fluid kinematics, these eddies superimpose on the main flow stream and reshape it. As shown in **Fig. 2.2**, the fluid element experiences rotation due to the momentum transfer from eddies that cross the streamline they follow. The larger eddies are limited to the center of the flow stream.

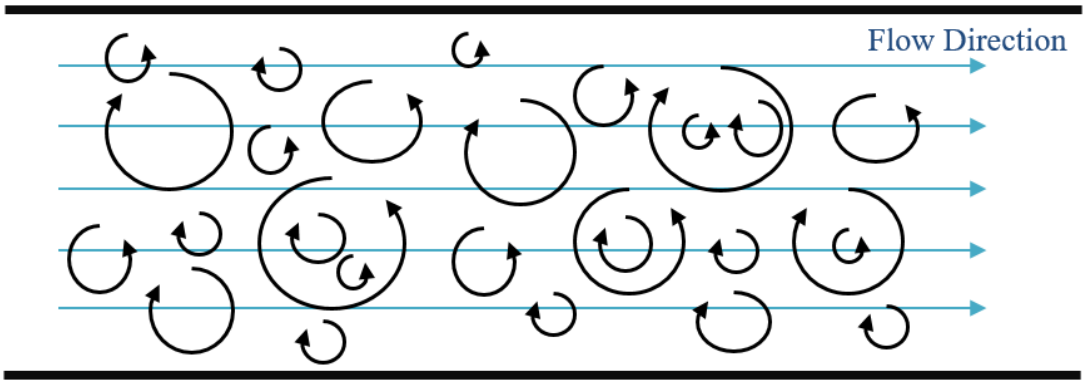

Figure 2.2: Turbulent flow and eddy behavior

The viscosity or apparent viscosity of a fluid (more adequate for a power law fluid) is an important property in the analysis of fluid motion and behavior within the boundary layer. **Figure 2.3** illustrates the velocity profile of turbulent and laminar flow regime within a pipe. It should be noted that the velocity profile for the turbulent flow regime indicates average velocity profile. In real scenario, the streamlines are not as smooth as in laminar regime.

Substantial amount of momentum is transferred from the center of the pipe towards the pipe walls in case of turbulent flow regime as compared to laminar regime. This results in a much more flat velocity profile. Within the boundary layer, the velocities closer to

the wall are much higher in turbulent region as compared to that in laminar region. However, as the magnitude of turbulence increases, this boundary layer gets thinner and the momentum can be directly applied to particles, moving them back into the flow stream.

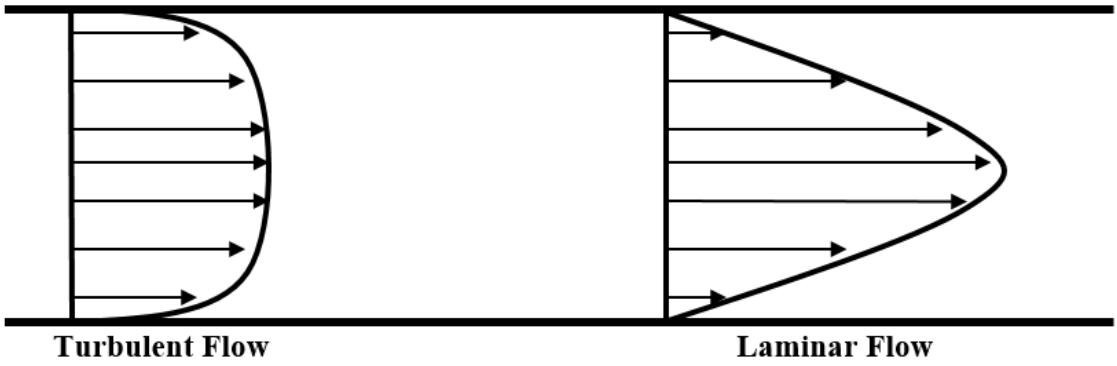

Figure 2.3: Velocity profile in pipe

2.3 Mechanistic and Experimental Models

Researchers have been investigating the solids transport mechanism in wellbore for several decades. Since the development of technology that allows a well to be drilled directionally and horizontally, considerable efforts have been expended on understanding the movement of solids in such profiles. Numerous efforts have been made to study the effects of each parameter and its sensitivity to the cleanout efficiency. Moreover, attempts have been made to develop an accurate model that determines the optimum parameters to be considered for a specific cleanout job design. These studies follow two major methodologies:

1. Theoretical approach is based on analyzing the forces with the use of mass balance and momentum balance equations. These equations are numerically solved with physical or mathematical assumptions and a mechanistic model is developed as either a two-layer or three-layer model.
2. Experimental approach involves investigating solids transport behavior by means of data obtained from experiments conducted using lab scale models. Several correlations have been obtained empirically using dimensionless analysis or semi-theoretical reasoning that involves force analysis on a particle.

The literature can be broadly divided into two categories, depending on the approach adopted.

2.3.1 Mechanistic Models

Mechanistic models can be categorized into one-layer, two-layer and three-layer models. One layer model describes the system as particle settling in stationary fluid. Two layer and three layer models are illustrated in **Fig. 2.4**. Two-layer models assume that the particle movement occurs in two distinct layers. A layer of nearly stationary solids bed forms on the low side of the wellbore. Another layer of clean fluid with or without suspended solid particles overlays the bottom layer. The three-layer model consists of a stationary solids bed, above which exists a moving bed of solids. The top layer is a fluid layer which may have a suspension of some solid particles.

These mechanistic models are based on mass balance equations for solids and fluids and momentum balance equations for the different layers assumed; resulting in a system of coupled algebraic equations. Boundary conditions are generally applied to these sets of equations in order to obtain a solution.

The two-layer and three-layer models primarily vary in terms of the following:

1. Solids distribution in the heterogeneous solid-liquid layer
2. Interfacial friction between the fluid and moving solids bed
3. Terminal settling velocity of particles in fluid
4. Fluid friction between the fluid and pipe walls.

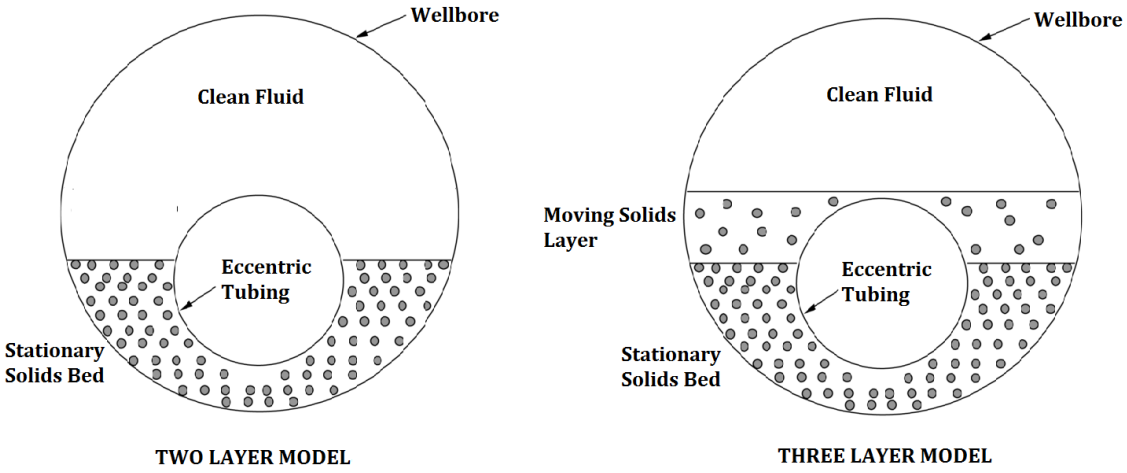

Figure 2.4: Illustration of two-layer and three-layer model

One-Layer Models

Settling behavior of suspended particles in inclined vessel was first observed by Boycott (1920). During the settling process, the particles approach the inclined wall and form a concentrated high density slurry. Since, the slurry becomes significantly heavier than the clear fluid above it, it slides along the inclined wall until it reaches the bottom of the vessel. Boycott observed that the settling rate of particles in inclined vessels is higher than in vertical vessels.

Acrivos and Herbolzheimer (1978) developed a theory for quantitatively describing the Boycott settling of particles in inclined vessels. A two-layer approach was used to model this theory. The study suggested that irrespective of the inclination, the particles initially suspended in the flow stream settle vertically until they reach the stationary bed layer. It was concluded that vertical settling rate of particles is a function of particle Reynolds number and Grashof number. This study was further extended to anticipate the downward sliding of the solids bed in a manner similar to natural convective motion of a heated or cooled fluid layer (Nir and Acrivos, 1989). Conditions suitable for steady state motion were determined. The fluid motion is considered to be in steady state when the combined effect of settling and shear induced particle suspension create a particle concentration distribution such that the accumulation of particles in the inclined section is prevented. However, the studies conducted were limited to laminar flow and Newtonian fluids. Direct application of these results to real scenarios is difficult as the cleanout operations

in field are conducted with non-Newtonian fluids and the flow is well within turbulent flow regime.

Jia and Michaelides (2007) used the Lattice Boltzmann Method (LBM) to simulate the Boycott settling of particles in inclined vessels. They concluded that as the inclination is increased from 0° to 45°, the particles reach the low side of the vessel very quickly. This trend changes at angle of inclination higher than 45° as the driving force for the particles to slide and settle in the bottom (gravity) becomes weaker.

The rate of change of amount of solid particles in the annulus is a clear indication of cuttings transport efficiency. Studies have been conducted to represent the amount of annular cuttings in the form of equivalent solids bed height, solids concentration, annular bed area, and the ratio between the mass of suspended particles and initial mass of the deposited cuttings.

Two-Layer Models

Gavinet and Sobey (1986) studied the cuttings transport mechanism in an inclined annulus as a two-layer system. Modes of particle transport studied were saltation and sliding. Saltation occurs when the particle at the solid-fluid interface is lifted into fluid stream due to drag force, and sliding occurs when solids bed travel up or down the wellbore, depending on the magnitude of forces exerted by the fluid. A model based on this study was developed to correlate wall stresses and interfacial stresses with the pressure drop in layers. A limitation of this model was an assumption that the pressure

drop is equal in both layers. If the stresses are known, the bed height becomes a function of flow rate and inclination. The study, however, did not account for stationary bed formation that generally exists at low fluid velocity in near horizontal wells.

Another mechanistic model similar to the previous one was presented by Martins et al. (1992 and 1998) to describe the stratified flow in eccentric annuli. Their model assumed the top layer as a heterogeneous suspension unlike Gavinet and Sobey model. The model was applied to several flow patterns that characterize the solid-liquid horizontal flows. The concentration of the particles in suspension was calculated using the diffusion equation. Well cleaning in terms of reduction in bed height, solids concentration and pressure loss due to friction was evaluated to be a function of a modified Lockhart and Martinelli parameter, and the flow regime of the top layer. However, the procedure for calculating solids dispersion coefficient in the diffusion equation was not provided. The predictions from this model were not compared with experimental or field data.

An extension of this model was presented by Martins and Santana (1998) to include specific correlation for interfacial friction factors depending on five different rheological models studied. This new model also incorporated the formulation of porous media to account for the fluid flow through the solids bed. The conclusions made in the study emphasized the importance of fluid rheology on solids transport. However, the study was conducted with an assumption of no-slip at the solid-liquid interface. This assumption becomes invalid at lower inclinations.

Clark and Bickham (1994) developed a mechanistic model to account for solids transport behavior across the entire wellbore from the surface to the nozzle/bit, by studying the minimum transport velocity. It was observed that solids transport mode is settling mechanism in vertical wells, lifting mechanism in wells with low inclination, and by rolling and lifting mechanism in high inclination or horizontal wells. The predicted results of this study were compared with experimental data obtained from 5 and 8-in. flow loop at University of Tulsa. The critical flow rate values from the model predictions were lower than the experimental data. The difference between model predictions and experimental values was because critical velocity was recorded based on visual observation during experimental studies, whereas pressure drop was the criteria used to determined critical velocity obtained from the model.

Ford et al. (1996) developed a computer package that predicts the minimum transport velocity required to ensure efficient hole cleaning in deviated wells. The predictions are based on a force balance on particle assuming a two-layer model. The authors concluded that the minimum transport velocity is a function of fluid rheology, well inclination, and radial distance from the drill pipe. The study suggests that the mode of solid transport is dominated by rolling at higher inclination if the flow velocity is higher than minimum transport velocity. On the contrary, the particle transport by suspension is dominant near 60° inclination if the minimum transport velocity is exceeded.

Three-Layer Models

Nguyen and Rahman (1998) presented a three-layer model to predict different modes of solids transport in highly deviated and horizontal annuli. The three layers comprised of a solids bed with uniform solids concentration, a dispersed layer with variable solid concentration, and a top layer comprised of either clear fluid or a turbulent suspension. The presence of a dispersed solid layer at the interface of uniform solids layer was an improvement over the stationary cuttings bed. The authors proposed five different modes of transport depending on the operating conditions. The transition from two-layer to three-layer flow or vice-versa depending on operating conditions was presented. However, the procedure for calculating solids concentration in the heterogeneous layer was not provided. There was no comparison of the model predictions with experimental or field data. The different mechanism of transport such as rolling or lifting was not discussed. The settling velocity of particle was ignored, which limited the application of the model to horizontal or highly deviated wells.

Kamp and Rivero (1999) developed a mechanistic model to predict cuttings bed build-up during drilling. The model prediction is based on settling and re-suspension of solids at the interfacial layer. The model could be extended to account for slip velocities by using separate momentum equations for fluid and solid in heterogeneous layer or by using drift flux law. However, this model was shown to over predict cuttings transport in comparison to the model derived by Larsen (1990) and Jalurkar (1993). This is attributed to the reason that cuttings concentration profile in the heterogeneous layer is not flat and this was neglected by the authors.

Ramadan et al. (2005) presented a three-layer model for solids transport in horizontal and inclined pipes. This model can predict the annular pressure loss and average solids transport rate with Newtonian and power law fluids. It considered the settling behavior of particles to determine the solids concentration in the suspension layer. The authors compared the model predictions with their experimental data. The model predictions deviated from the experimental results for small particles with both Newtonian and power law fluids at near critical flow rates. This deviation at near-critical flow rates was attributed to formation of dunes and ripples, which was neglected in the model.

Cho et al. (2001) presented a three-layer model for two phase incompressible flow in annuli. The model modified the single particle settling velocity with concentration effects to account for hindered settling. The model predictions were compared with the experimental results of Tomren et al. (1986). It was suggested that the conventional mechanistic models are unable to properly characterize the cuttings transport mechanism based on the inclination angle since the dominant factors controlling hole cleaning efficiency varied with wellbore inclination. The annular fluid velocity and fluid rheology were found to be the most important parameters for solids transport. A new two-layer was developed as it was concluded that any three layer model does not reduce to a two layer model at high fluid velocity.

2.3.2 Experimental Models

In order to study the effect of various parameters on hole cleaning, many flow loops have been established to conduct lab scale experiments. The following experimental research indicates that the flow rate, fluid rheology and density, inclination, pipe rotation, and particle size and density have certain effects on solids transport. In addition, multi-factor interactions affecting the transport mechanism were also observed.

Larsen (1997) studied the effect of fluid rheology, eccentricity, inclination, solids size, and flow rate by conducting more than 700 tests in a 35 ft, 5-in. x 2.375-in. annulus with varying pipe eccentricity and inclination range of 55 to 90°. An empirical correlation to predict critical transport velocity was developed. Critical transport velocity was defined as the minimum fluid velocity required to maintain upward movement of cuttings, irrespective of the mode of transport. The CTFV was reported in the range of 3 to 4 ft/s depending on the value of various parameters, such as the fluid rheology, drilling rate, pipe eccentricity, and drillpipe rotation. A correlation for predicting solids bed area at sub-critical flow rates was also developed. Jalukar (1990) extended this correlation to account for different annular geometries. Adari (1999) proposed an exponential decay relationship for reduction in bed height as a function of time during bed erosion. This equation was limited to a fixed combination of flow rate, fluid rheology and high inclination. This study is one of the few transient state studies, like that of Adari, carried out so far.

Walker and Li (2000) quantified the effects of particle size and fluid rheology on solids transport mechanism. The studies pertaining to fluid rheology indicated that high viscosity fluids like Xanvis and HEC have better solids carrying capacity but are inefficient in eroding a stationary bed as compared to water. Hence, hole cleaning is efficient in vertical or near vertical wellbores if high viscosity fluids are pumped in laminar flow regime. In addition, for the tested particle size range from 0.15 mm to 7 mm, an average size of 0.76 mm was the hardest to clean with water. These results were consistent with those obtained by Martins et al. (1993).

Kelessidis and Mpandelis (2004) studied the solids transport mechanism with water and aqueous solutions of Carboxy-Methyl-Cellulose (CMC) in a recirculating flow loop with a non-rotating concentric annulus. The characteristics of the flow patterns and the particle-liquid interactions at various flow rates were visually observed. It was found that particles form a moving bed at low flow rates. This moving bed can be eroded if the flow rate is increased. At higher flow rates, but not sufficiently high for full solid suspension, the solids do not deposit on the wall but flow in streaks near the bottom wall of the annulus.

Ozbayoglu et al. (2004) conducted extensive experiments in a 100 ft flow loop of 8-in. diameter test section. The effects of major parameter, such as flow rate, fluid density, viscosity, gas ratio, cuttings size and density, wellbore inclination, and eccentricity of the CT on cuttings transport efficiency were analyzed. The major findings of this study mentioned that the flow rate or the average annular velocity is the most dominating

parameter on wellbore cleaning. Cuttings properties, wellbore inclination and eccentricity have some influence on cuttings transport. In addition, it was concluded that as the viscosity of fluid is increased, the thickness of cuttings bed developed increases significantly. Hence, turbulent flow is better for preventing the bed development. These tests were conducted in the test sections at high inclination or horizontal profile. Thus, limiting the use of data obtained. Later tests conducted by Ozbayoglu et al. (2008) in a 15 ft long test section of 4-in. diameter indicated that stationary bed is established when the flow velocity is less than 6 ft/sec, and a critical flow velocity of 8 ft/sec is essential to establish a no-bed condition.

Duan et al. (2008) conducted flow loop tests using three different particle sizes and various fluids including water. Results indicated that water was efficient in cleaning out large sized particles. Pipe rotation and fluid rheology were mentioned to be crucial factors in cleanout of smaller particles. Viscous fluids like 0.25 lbm/bbl PAC solution proved to be more efficient in cleaning smaller particles. The data obtained by authors deviate to up to 80% from that obtained by Ozbayoglu et al. (2004)

Further experiments conducted by Duan et al. (2009) determined the critical conditions for efficient transport of solids in horizontal and high-angle wells by defining critical deposition velocity (CDV) and critical re-suspension velocity (CRV). CDV was defined as the minimum fluid velocity required to prevent bed formation and CRV was defined as the minimum velocity to initiate bed erosion. It was found that the critical deposition velocity is two to three times larger than the critical resuspension velocity. Results also

indicated that water is better at eroding the bed. The results were consistent with those obtained by Martins et al. (1993) and, Walker and Li (2000).

CHAPTER 3

EXPERIMENTAL SETUP

This chapter describes the individual components of the test setup used to conduct the cleanout experiments. Subsequently, description of the experimental procedure followed for all tests is detailed. Finally, the parameters used for the analysis are defined and the procedure for obtaining these parameters is reported.

3.1 Design details

The tests presented in this report were conducted in a 34 ft annular section comprising of 5.5-in. OD x 5-in. ID outer acrylic pipe and a 2 3/8-in. OD inner CT. **Figure 3.1** shows the schematic of the setup. **Figures 3.2** and **3.3** show the photograph of the setup in horizontal and inclined position. The different segments of experimental setup used for conducting bed erosion tests are categorized as follows.

3.1.1 Support Structure

The support structure makes up the base of the test section. It was fabricated to provide stability to the setup under all operating conditions. The support structure comprises of the hinge and I-beams resting on the base frame (**Fig. 3.4**). The base frame was 12 ft long and 5 ft wide. The setup was designed to study hole cleaning at various inclinations. For this purpose, the base frame was mounted on a set of rollers that aids in smooth linear movement of the entire structure. The hinge system facilitates rotation of the test section at the inlet end during inclined tests. It consists of two hinges placed 4.5 ft apart

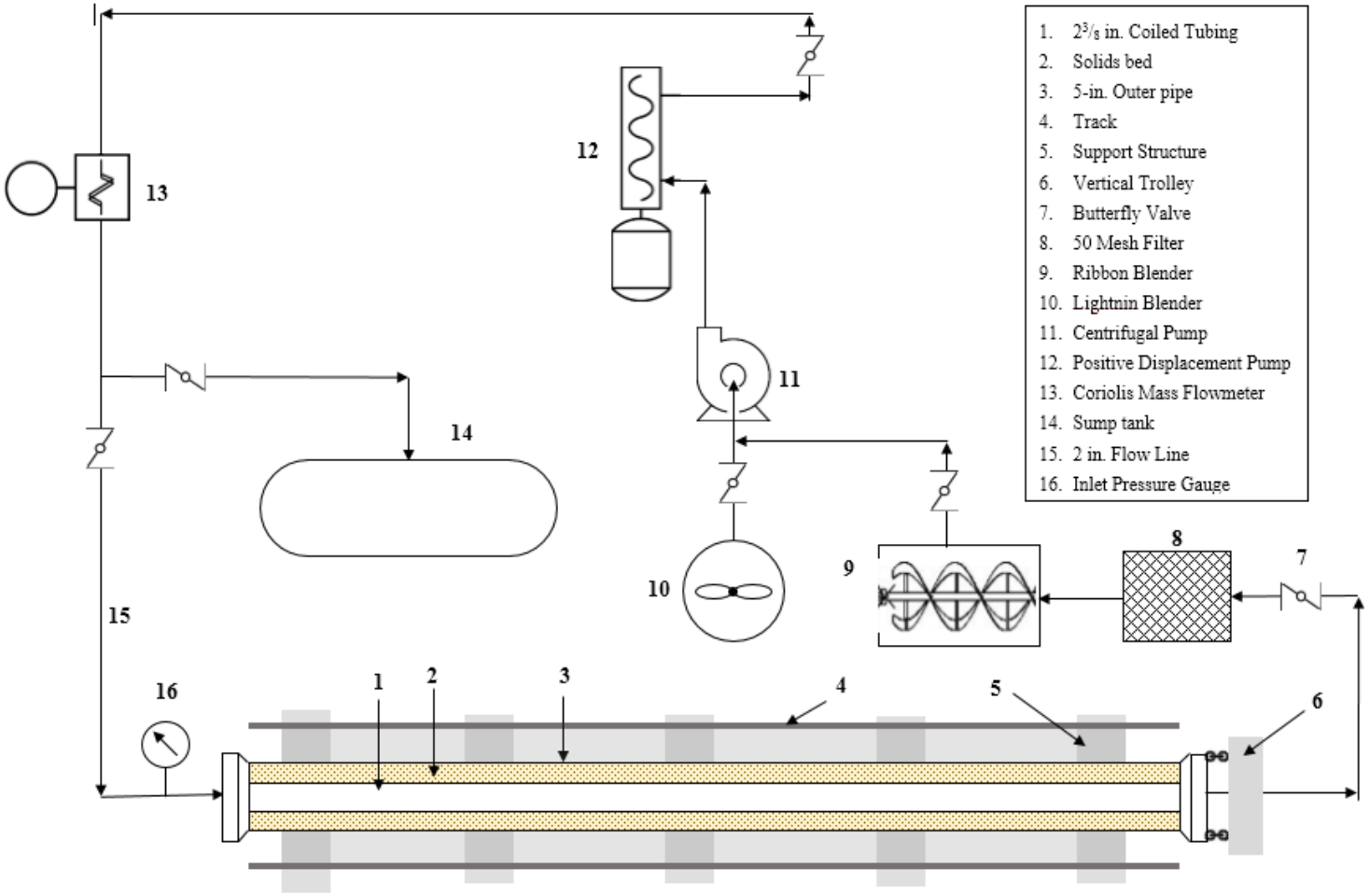

Figure 3.1: Schematic of the experimental setup

Figure 3.2: Photograph of the wellbore cleanout setup in horizontal position

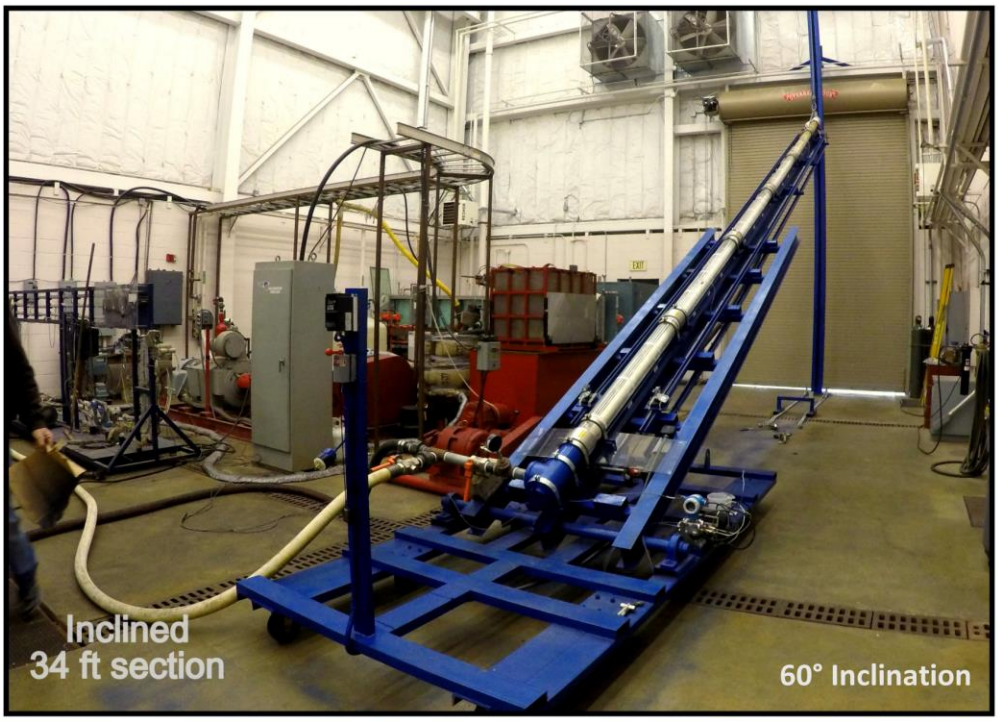

Figure 3.3: Photograph of the wellbore cleanout setup in inclined position

with a solid iron shaft (2 7/16-in. OD). This iron shaft couples the movement of test section as the hinge system rotates. The test section is clamped to a 34 ft long central I-beam. The free end of the I-beam at the discharge end can be raised with pulley-winch hoisting system for conducting experiments in the inclined position whereas the base frame remains on ground at all times. Two tracks made of 34 ft long channels are welded on either side of the test section to enable a linear movement of the cameras mounted on the chain.

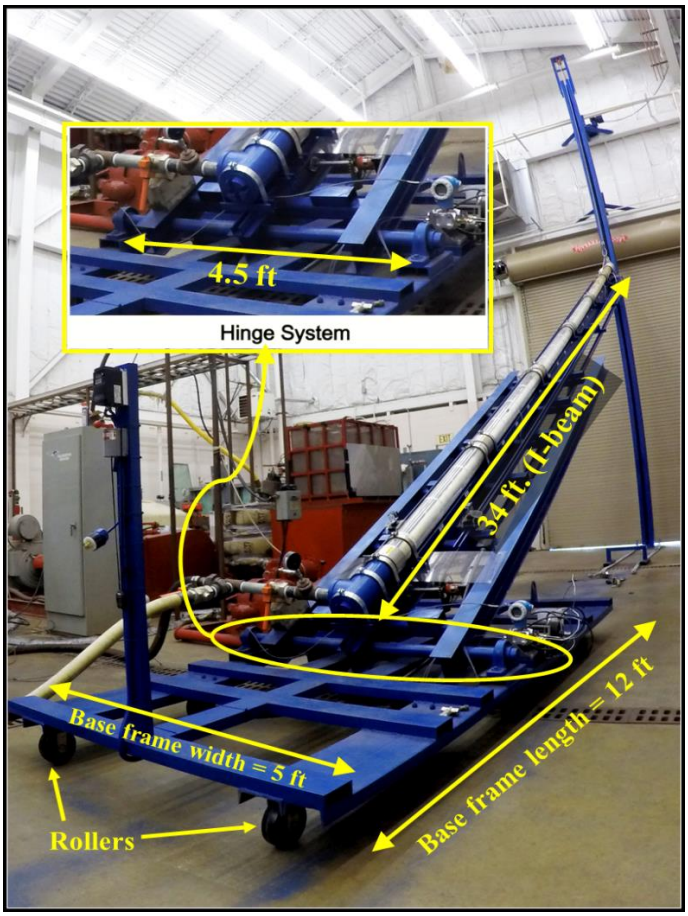

Figure 3.4: Components of the support structure

3.1.2 Hoisting system

The hoisting system consisted of a vertical beam, roller arrangement and pulley-winch system. The vertical beam is a 32 foot long hollow square beam with 1 ¾-in. seam cut on one side. A roller was placed inside the vertical beam to guide the vertical movement of central I-beam. It consisted of two 6-in. diameter wheels coupled with a 3/4-in. OD shaft. The free end of central I-beam was connected to a pulley (mounted on top of a vertical beam) by a steel rope to hoist the section.

3.1.3 Test Section

The test section consisted of a 34 ft acrylate outer pipe with dimensions of 5.5-in. OD x 5-in. ID dimensions, clamped to the central I-beam (**Fig. 3.5**). Several sections of the outer acrylic pipe were coupled using a Straub connection to form a single tight seal. A 2 3/8-in. OD CT was placed eccentrically inside the outer pipe. The inner CT was painted white for better flow visualization. Blinds were welded at ends of the inner tubing to ensure that the flow is restricted to the annular section between the outer pipe and inner tubing. A T-connection was attached on both ends of the test section to connect the inlet and discharge line. The inner CT exerted considerable amount of load at the inlet T-connection, especially at lower inclination. Hence, the T-connection made of cast iron was installed at the inlet. On the contrary, the T-connection at the discharge end of the test section was made of PVC to minimize the weight to be lifted by pulley and winch system. Gate valves were used for isolating the test section and diverting the flow to the bypass line.

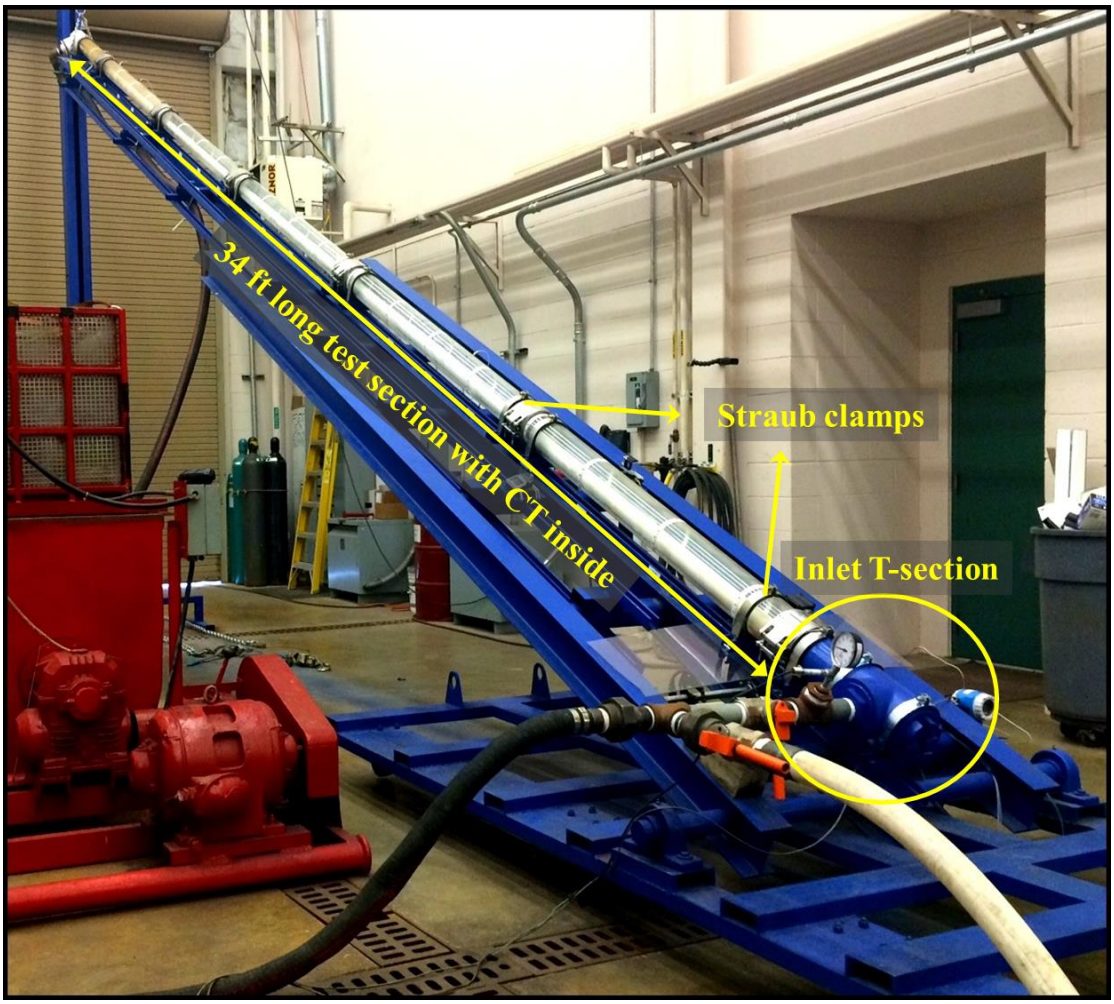

Figure 3.5: Test Section

3.1.4 Separator

A sieve was fabricated to collect the proppant from discharge line. The fabrication was carried out in two stages. Firstly, a 3.5 ft X 2.75 ft X 3.25 ft frame was constructed by welding pieces of 0.5-in. square tubing together. This frame was then used to support the 50 US mesh size screen that was seamed with the frame to avoid any leak from the edges. The seams were made using high strength Kevlar thread. **Figure 3.6** shows the fabricated sieve and seams. This separator was tested to be efficient in handling the slurry of viscous

fluid and proppant pumped at flow rate of 140 gpm. Moreover, metal sheets were wrapped around the separator to avoid any spillage on the floor.

Figure 3.6: Solid/Liquid separator

3.1.5 Mixing system

A 50 gallon capacity tank equipped with a Lightnin blender was used to mix proppant and water during the bed deposition. A 200 gallon ribbon blender was used to store and mix the fluid for bed erosion tests.

3.1.6 Pumping System

During deposition of the bed, a Halliburton style 5M Deming centrifugal pump (Sr. No-BHPS10012), controlled by a variable frequency drive (VFD) was used to recirculate the slurry of proppant and water through the test section (**Fig. 3.7**). This centrifugal pump was equipped with a 25 HP, 1770 RPM motor. The centrifugal pump was used for fluid circulation through the flow loop at lower flow rate. As shown in **Fig. 3.8**, a 6P10 Moyno progressive cavity pump (Sr. No. 011385-1) was used in series with the centrifugal pump

to perform the tests at higher flow rate. This pump has a 100 HP, 1780 RPM, 3 phase 60 Hz motor. The upper limit of operation of the Moyno pump is approximately 140 gpm at 600 psi.

Figure 3.7: Centrifugal pump used during experiments

Figure 3.8: Progressive cavity pump used during experiments

3.1.7 Instrumentation and Data Acquisition System

A Coriolis mass flow meter (Endress Hauser Proline Promass E 200) placed downstream of the circulation pump was used to measure flow rate, fluid density, and fluid temperature. This flow meter is capable of measuring mass flow rate up to 2570 lb/min and fluid density with an accuracy of ±0.0005 g/cc.

A differential pressure transducer (Endress Hauser Deltabar S PMD75) was used to measure friction pressure loss across the test section for a fully developed flow. The pressure range for this transducer was set to 0 - 1.5 psi.

A track system with a chain and sprocket arrangement was fabricated and installed on both sides along the entire length of test section (**Fig. 3.9**). Two video cameras for flow visualization were maneuvered along the track using this chain and sprocket arrangement. A motor was used to drive chain into linear motion across the length of test section. The speed of this motor was controlled by a variable frequency drive (VFD) coupled with a switch used to change the direction of motion. These cameras recorded the bed arc length readings measured using paper scales attached across the test section. The scales were placed 1.5 ft apart along the test section

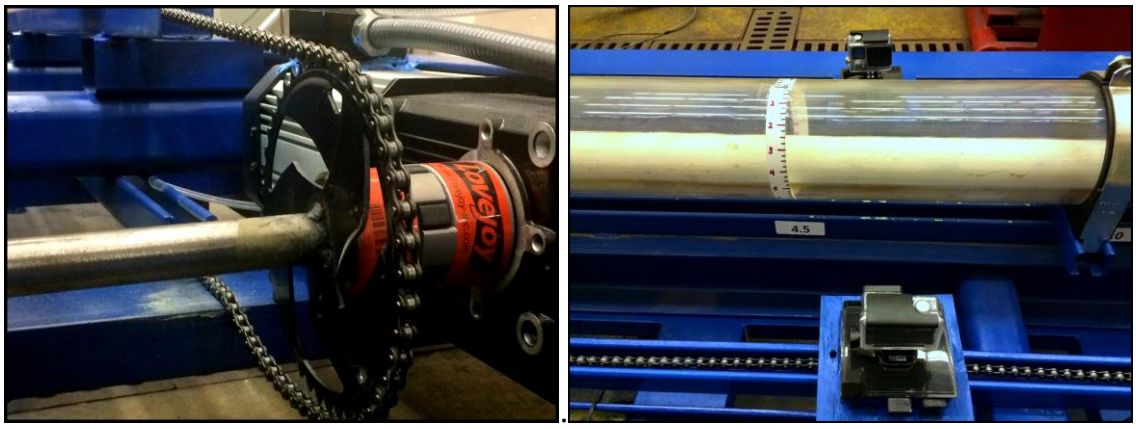

Figure 3.9: Camera motion using chain and sprocket mechanism

The data acquisition system (NI CompactDaq model NI cDAQ-9188) was used to transmit the measurements from mass flow meter to a wireless logger that provides the flow data such as temperature, flow rate and density of fluid (**Fig. 3.10**). The system has

dedicated channels for gathering different output signals from various instruments; 32 channels for voltage, 16 channels for current, 4 channels for thermocouple and 8 channels for frequency input. Data are transferred to main computer through a wireless data logger.

Figure 3.10: Data Acquisition System (NI cDAQ-9188)

3.2 Test Procedure

The procedure for solid bed erosion test consists of the following steps:

Step 1. Deposition of solids bed in the test section

1. Water from the 55 gal blender was re-circulated through the test section at 50 gpm.

2. Once the test section was filled with water, 200 lbm of sand was slowly added to the blender while re-circulating through test section. Previous tests conducted by Naik (2015) indicated that 200 lbm of proppant ensured the inner pipe in the 34 ft section was completely covered with solids. The total volume of the loop was approximately 100 gal.

Hence, the solids re-circulation was at the concentration of 2 lbm/gal initially and it reduced as the bed started forming in the test section.

3. Sand settles slowly in the test section forming a solids bed. The sand bed height was sufficient to completely cover the inner pipe, thereby simulating a worst-case scenario.

4. The test section was then isolated using valves, and bypass lines were flushed with water.

Step 2. Fluid Preparation

1. Two hundred gallons of fresh water was filled in the ribbon blender.

2. For a polymeric fluid test, the required amount of polymer was added to fresh water while agitating the fluid at moderate speed.

3. The fluid was mixed for an hour to ensure complete polymer hydration.

4. Fluid rheology measurements were performed using 6 speed, model 35 Fann viscometer equipped with $1/5^{th}$ spring.

Step 3. Erosion of solids bed

1. After depositing solids bed, the test fluid was pumped through the loop and bypass lines at a low flow rate of 10 gpm to displace water.

2. The test section is then raised to the desired inclination and bed perimeter readings were recorded at 42 locations (21 location on each side), each 1.5 ft apart using paper

scale affixed on the test section. The recording was done by a camera traveling along the track. These readings are the initial bed height.

3. The test fluid was then diverted to the bypass line where the flow rate was increased to a desired value.

4. After attaining the desired flow rate, the flow was diverted back to test section and the stop-watch was started.

5. The bed perimeter was recorded 1 min after the flow through test section followed by recording at every 2 mins. The bed perimeter was the average of 42 readings taken along the test section. The bed height was calculated from bed perimeter using mathematical relations discussed in Section 3.3.

6. The test was continued for 30 mins and then the flow was diverted to the bypass line.

7. The final bed perimeter (average of 42 readings) was then recorded.

The sand collected in the filter upon completion of test was dried in an oven and weighed. This weight was recorded as cleanout weight. Water was then pumped through the test section to flush polymeric fluid and the remaining sand. The remaining sand was dried and weighed and was recorded as the weight of sand flushed out. This procedure was repeated for each test.

3.3 Definition of Parameters

To quantitatively describe cuttings transport efficiency, two parameters are used as the target variables in this study.

'Bed height' indicates the vertical height of the stationary proppant bed in the annulus. The bed perimeter reading was recorded on both sides of the section along the circumference. This reading, 'a', is recorded from the top of the outer pipe. The bed perimeter (along the circumference) from the bottom is $b = 8.64 - a$, where 8.64 is half-circumference of the outer pipe (**Fig. 3.11**). The relationship between the radius, bed perimeter, and central angle (when measured in radians) is: $b = r.\phi$.

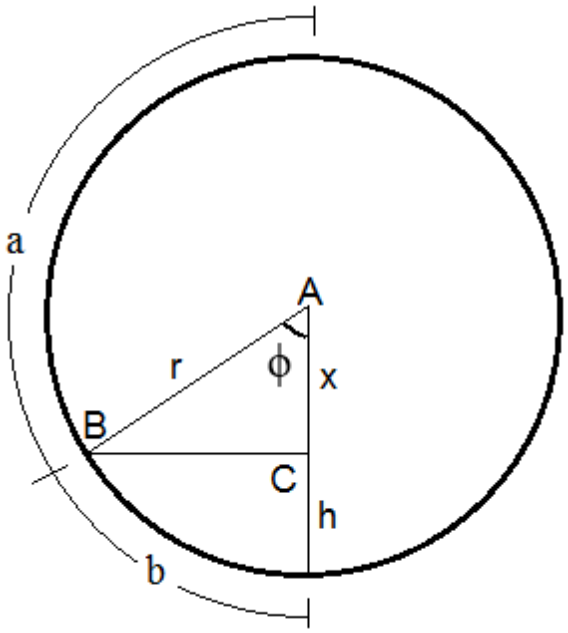

Figure 3.11: Bed height calculation

The triangle ABC in Fig. 3.11 is a right-angled triangle and hence, using trigonometric relations, we get, $cos\ \phi\ =\ x/r$.

Thus,

$h\ =\ r\ -\ x$

$h\ =\ r\ -\ r\ cos\ \phi$

or,

$h\ =\ r\ -\ r\ cos\ (b\ /\ r)$. (3.1)

The correct bed-height is obtained by accounting for the thickness of the outer pipe. Hence, subtracting the thickness of 0.25-in. of the outer pipe from the calculated bed height, we obtain:

$h_c\ =\ (h\ -\ 0.25)$-in. (3.2)

For example, if the bed height reading recorded at a given time is $a\ =\ 5.24$-in. then,

$b\ =\ 8.64\ -\ 5.24$

or,

$b\ =\ 3.50$-in.

The corrected bed height is given by,

$h\ =\ 2.75\ -\ 2.5\ cos\ (3.50\ /\ 2.75)$

$h = 1.92$-in.

$h_c = 1.92 - 0.25$

or,

$h_c = 1.64$-in.

The ‘bed height’ was then converted to the ‘normalized bed height’ in order to set the same initial condition of bed height for comparison purpose.

Another parameter, ‘cleanout efficiency’ is defined as the ratio of the dry weight of the proppant collected in the filter at the end of cleanout test and the dry weight of total amount of proppant collected at the end of cleanout and flush.

$$Cleanout\ Efficiency = \frac{m_{30}}{(m_{30} + m_{flush})}$$

where,

m_{30} = dry weight of proppant cleaned out during the 30 min test

m_{flush} = dry weight of proppant flushed out from test section after the test

The denominator of this parameter is different from the feed weight (200 lbm) since some amount of proppant is lost in the flow lines during deposition of bed as well as flushing of the test section.

CHAPTER 4

RESULTS AND DISCUSSION

As mentioned earlier, this study is a continuation of that carried out by Naik (2015). A total of 54 test data was analyzed, 30 of which was generated out during this study.

4.1 Rheological Characterization

As discussed earlier, three different fluids (water, 10 lbm/Mgal guar and 20 lbm/Mgal guar) were employed in the tests conducted. Water is a Newtonian fluid and its viscosity is independent of shear rate. Guar fluids are non-Newtonian fluids and their viscosity depends on the applied shear rate. The rheology of polymeric fluids was determined at ambient conditions employing model 35 Fann viscometer with $1/5^{th}$ spring (**Fig. 4.1**). This rotational viscometer was used for rheology measurements and quality control of gelled fluid collected before and after the test. The test fluid is contained in the annular space between two cylinders. The rotation of outer cylinder (sleeve) at known velocity causes the fluid to exert a viscous drag, which in turn imparts a torque on inner cylinder or bob. This torque causes the deflection in the dial reading of viscometer. The measurements were carried out at respective test temperature and ambient pressure. However, there was marginal increase in temperature while conducting rheology measurements before and after the test due to the shear applied to the fluid during flow test. The viscometer used was equipped with R1B1 bob and cup geometry. The dimensions and specifications are presented in **Table 4.1**.

Table 4.1: Specifications of Viscometer

Instrument	Geometry	Dimensions, mm	Shear Rate Range $(sec)^{-1}$
Fann 35 Viscometer	Diameter of Bob	$D_b = 34.49$	5.1 – 1022
	Diameter of Cup	$D_c = 36.83$	
	Ratio (β)	$D_b / D_c = 0.9365$	

The power law model or Ostwald-de Waele model adequately described the test fluid behavior over a wide shear rate range. The relationship of wall shear stress and wall shear rate for power law fluids is given by,

$$\tau_w = K_v \dot{\gamma}_w{}^n \tag{4.1}$$

where,

$\tau_w =$ wall shear stress (lbf/ft^2);

$\dot{\gamma}_w =$ wall shear rate (sec^{-1});

$K_v =$ viscometer flow consistency index ($lbf\text{-}s^n/ft^2$);

$n =$ flow behavior index (dimensionless).

The power law parameters, n and Kv were determined from the regression of the wall shear stress and wall shear rate data on a log-log plot. The wall shear stress and wall shear

rate were calculated from the viscometer dial readings (θ) and speed of the rotating sleeve of viscometer (rpm) using following equations:

$$\tau_w = 0.01066 N \theta_i \quad (4.2)$$

$$\dot{\gamma}_w = 1.703(rpm) \quad (4.3)$$

where,

$N =$ spring number (0.2 for 1/5th spring);

$\theta_i =$ dial reading at ith rpm.

The apparent viscosity was calculated using the formula,

$$\mu_a = 47880\ K_v(\gamma_w)^{n-1} \quad (4.4)$$

where,

$\mu_a =$ apparent viscosity (cP).

Tables 4.2 and **4.3** list the average values of n, K_v and μ_a measured for the guar based fluids before and after the tests. There was some variation in the apparent viscosity of the same fluid since the ambient temperature varied for every test. It can also be seen that the viscosity of a specific fluid has a relatively wider variation. This is attributed to the fact that the tests were conducted within the ambient temperature range of 58° F to 72° F. Average value of rheological parameters for guar fluids is given in **Table 4.4**. The

Reynolds numbers of all tests were above 4500 and hence, the fluid regime in all tests was turbulent.

Table 4.2: Rheological characterization of 10 lbm/Mgal guar fluid

Fluid	Inclination	Flow rate (gpm)	Flow behavior index, n	Fluid consistency index, K_v ($lbf.sec^n/ft^2$) ($x10^{-4}$)	Apparent viscosity μ_a @ 511 sec^{-1} (cP)	Ambient Temperature (°F)
10 lb/Mgal Guar	90°	80	0.670	7.67	4.69	67.82
		100	0.673	7.63	4.74	58.46
		120	0.637	8.94	4.49	59.54
	75°	80	0.664	8.60	5.03	67.10
		100	0.660	7.81	4.50	71.96
		120	0.652	7.89	4.31	68.18
	70°	80	0.568	18.52	6.01	61.52
		100	0.712	7.21	5.71	60.26
		120	0.683	9.14	6.07	58.28
	60°	80	0.654	8.75	4.85	68.54
		100	0.646	8.85	4.66	70.52
		120	0.670	9.37	5.72	63.14
	50°	80	0.568	18.52	6.01	60.44
		100	0.589	15.55	5.74	58.28
		120	0.671	9.29	5.74	56.66
	45°	80	0.657	10.93	6.17	60.98
		100	0.548	21.26	6.09	60.98
		120	0.663	8.63	4.99	70.52

Table 4.3: Rheological characterization of 20 lbm/Mgal guar fluid

Fluid	Inclination	Flow rate (gpm)	Flow behavior index, n	Fluid consistency index, K_v ($lbf.sec^n/ft^2$) ($x10^{-4}$)	Apparent viscosity μ_a @ 511 sec^{-1}, (cP)	Ambient Temperature (°F)
20 lb/Mgal Guar	90°	80	0.576	33.22	11.31	68.54
		100	0.512	64.15	14.60	60.44
		120	0.639	25.88	12.99	72.32
	75°	80	0.567	35.63	11.48	70.34
		100	0.577	38.53	13.17	70.88
		120	0.596	33.33	12.45	71.42
	70°	80	0.609	34.11	14.29	63.68
		100	0.611	34.19	14.51	62.24
		120	0.616	34.13	14.88	63.14
	60°	80	0.606	28.60	11.60	70.52
		100	0.583	35.59	12.63	71.60
		120	0.577	42.04	14.39	63.50
	50°	80	0.563	42.18	13.23	61.88
		100	0.596	36.33	14.01	61.34
		120	0.595	36.55	13.98	64.58
	45°	80	0.527	56.40	14.13	66.56
		100	0.536	51.59	13.71	67.10
		120	0.601	36.12	14.35	61.88

Table 4.4: Average rheological properties of guar fluids

Fluid	Average flow behavior index, n	Average fluid consistency index, K_v ($lbf.sec^n/ft^2$) ($x10^{-4}$)	Average apparent viscosity μ_a @ 511 sec^{-1}, (cP)
10 lb/Mgal Guar	0.644	10.19	5.31
20 lb/Mgal Guar	0.574	41.43	13.47

4.2 Bed Erosion Curves and Cleanout Efficiency for Various Flow Rates

Bed erosion curve is defined as the plot of solids normalized bed height reduction as a function of time. The cleanout efficiency is defined as the ratio of the solids collected in filter at the end of cleanout test to the total amount of solids collected at the end of cleanout and flush. The cleanout efficiency is useful for determining the performance of different fluids at inclination of 50° and 45°, where no stationary solids bed exists. At these inclinations, most of the solids in the test section were either in form of sliding bed or in suspension.

The bed erosion curves for different fluids at 80, 100 and 120 gpm and at various inclination are shown in **Figs. 4.1 through 4.4** (for water), **Figs. 4.6 through 4.9** (for 10 lb/Mgal guar), and **Figs. 4.11 through 4.14** (for 20 lb/Mgal guar), respectively. With increasing flow rate, the solids erosion rate increases for each fluid at all inclinations. Increase in flow rate improves interfacial stress acting on the solids bed. Higher interfacial stress indicates higher force acting to transport solids, leading to improved solids

transport. The fluid drag on suspended solids also increases with increasing flow rate leading to improved solids transport. The rate of solids erosion increases with flow rate for all fluids and at all inclinations considered. **Figures 4.5, 4.10 and 4.15** show the cleanout efficiency of water, 10 and 20 lb/Mgal guar at different inclination and flow rate, respectively. It is observed that cleanout efficiency increases with flow rate for all fluids and inclinations considered.

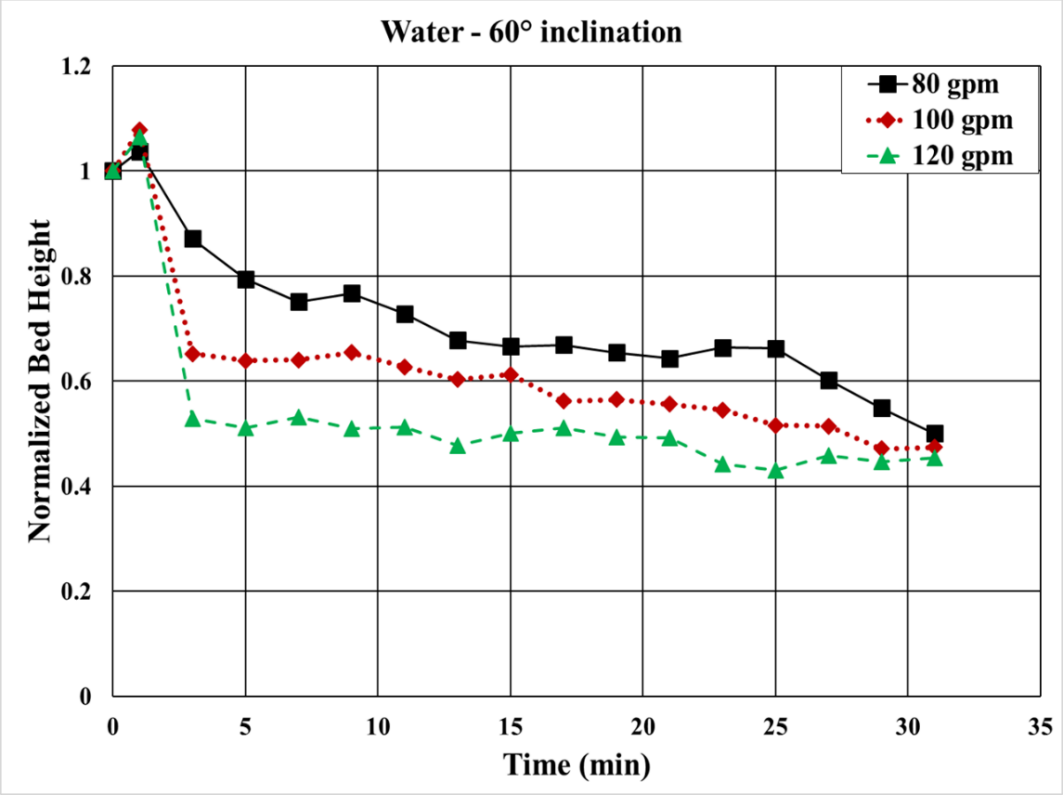

Figure 4.1: Bed erosion curves for water at 60° inclination

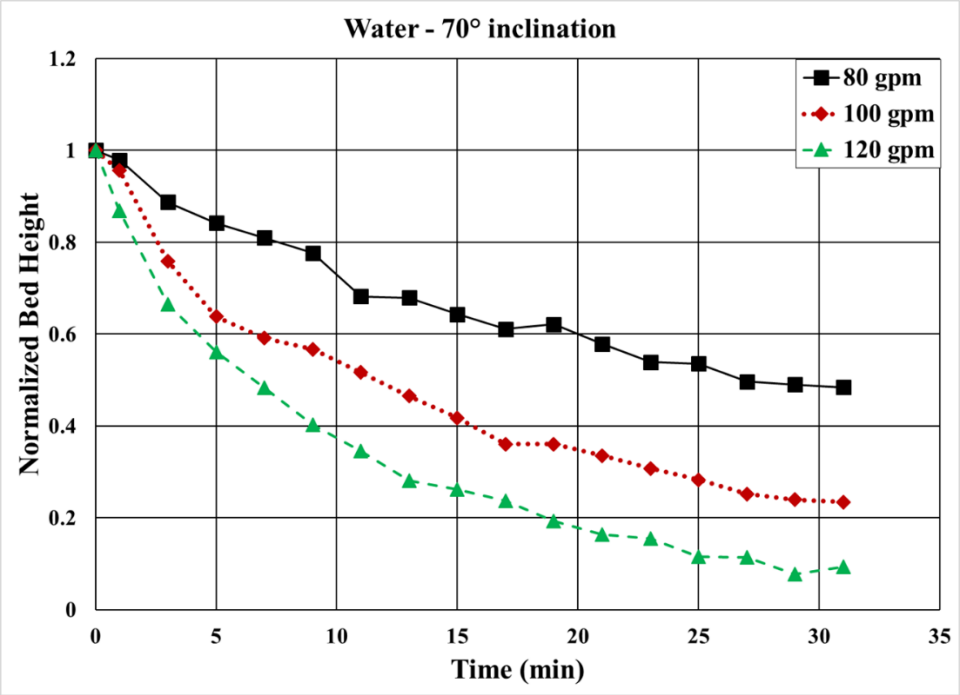

Figure 4.2: Bed erosion curves for water at 70° inclination

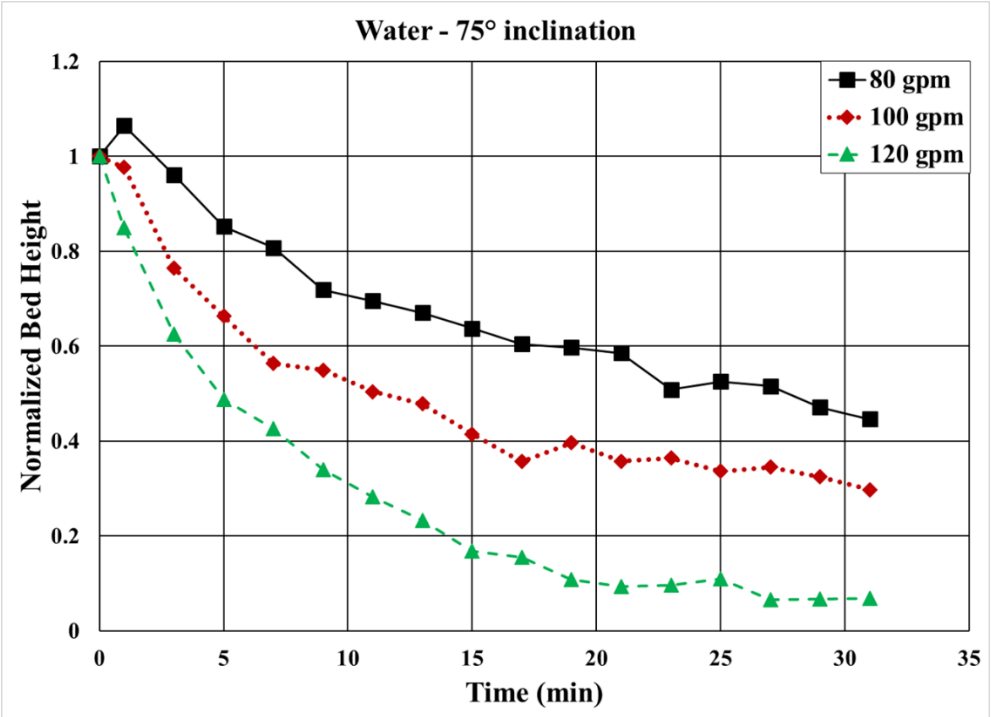

Figure 4.3: Bed erosion curves for water at 75° inclination

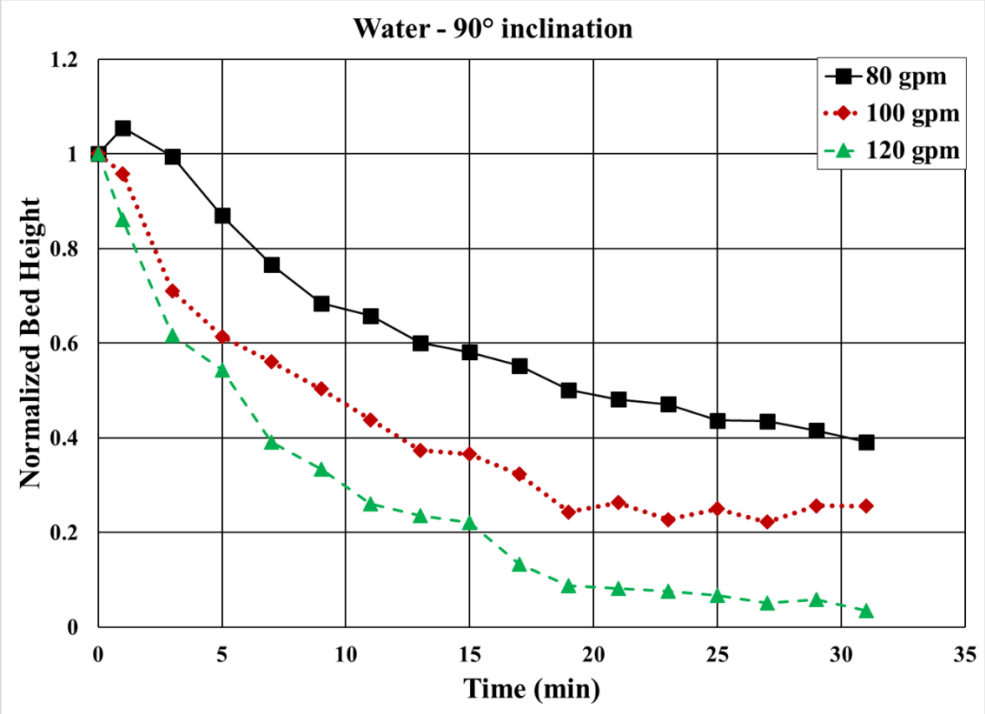

Figure 4.4: Bed erosion curves for water at 90° inclination

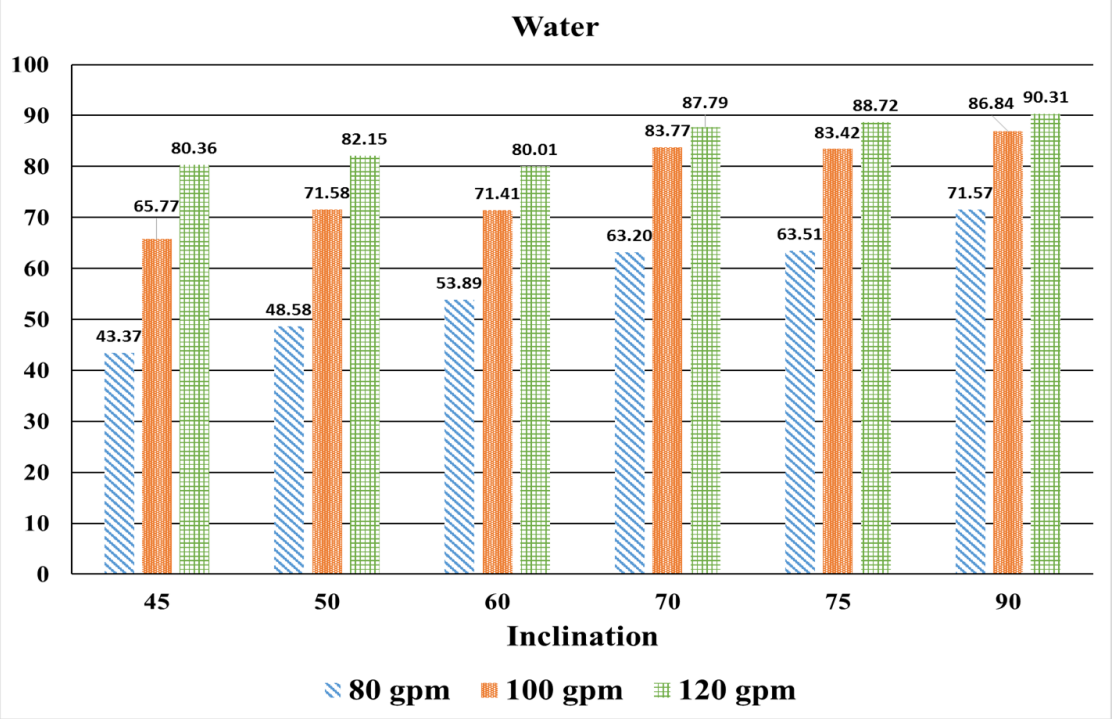

Figure 4.5: Cleanout efficiencies of water

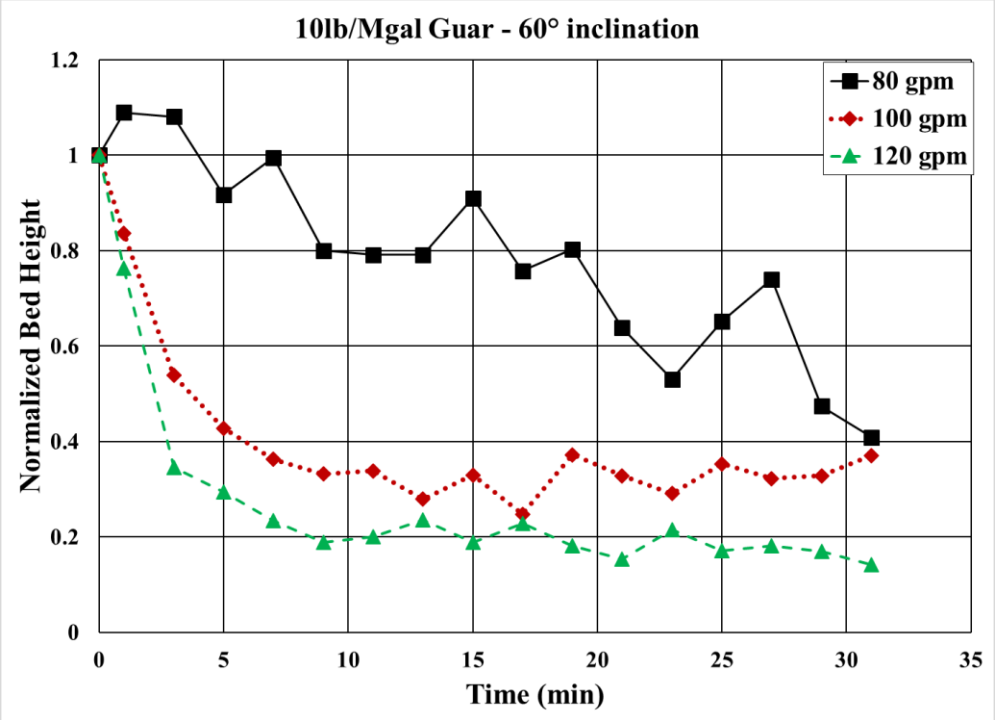

Figure 4.6: Bed erosion curves of 10 lb/Mgal guar at 60° inclination

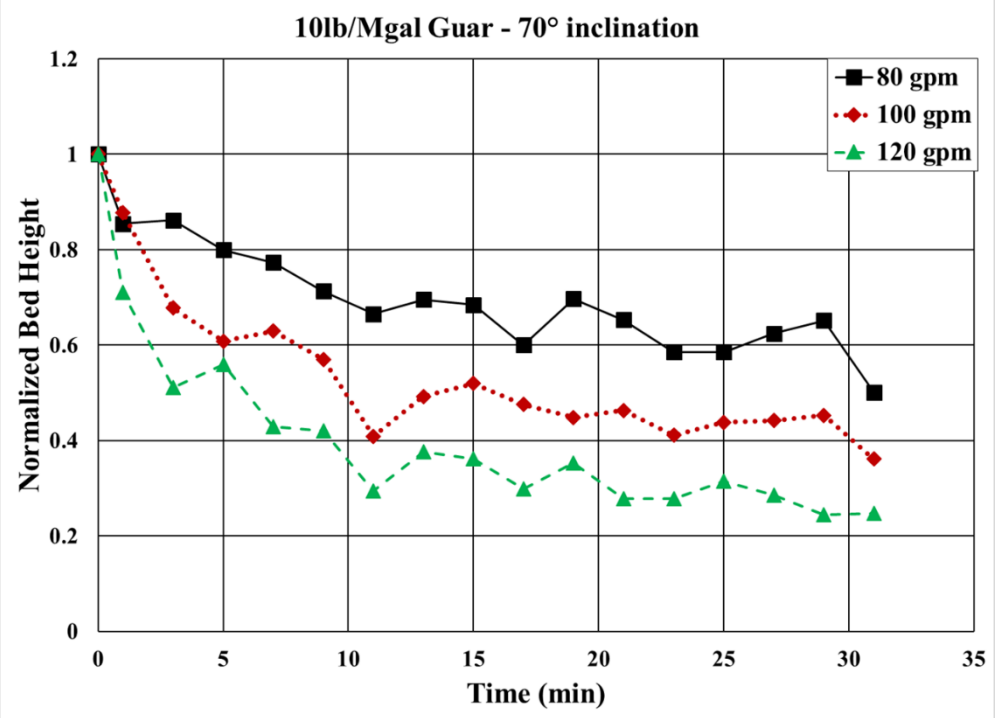

Figure 4.7: Bed erosion curves for 10 lb/Mgal guar at 70° inclination

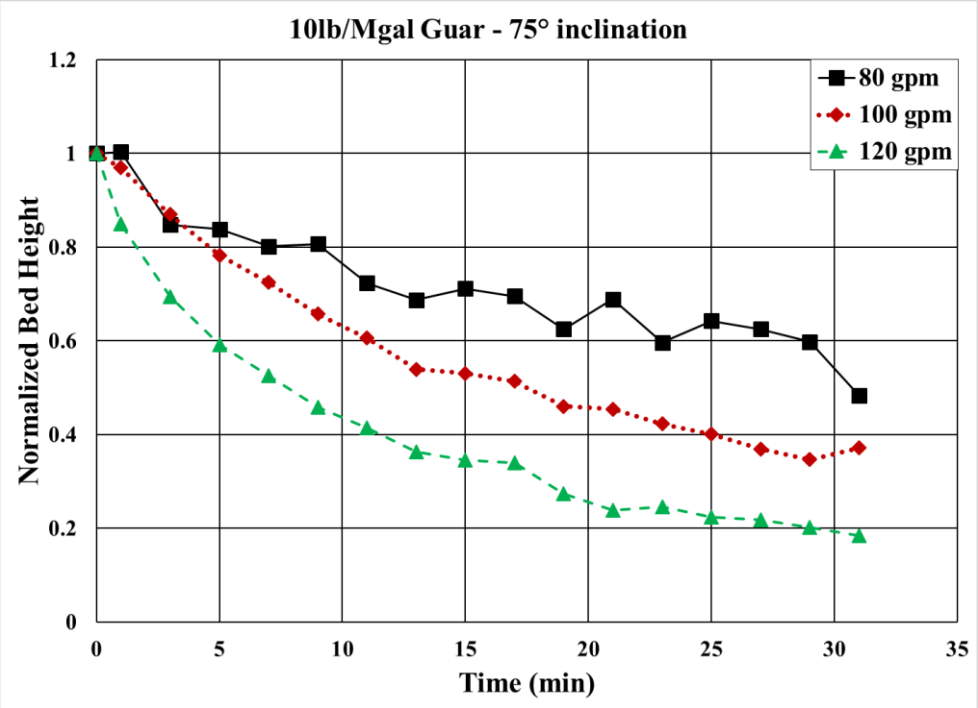

Figure 4.8: Bed erosion curves for 10 lb/Mgal guar at 75° inclination

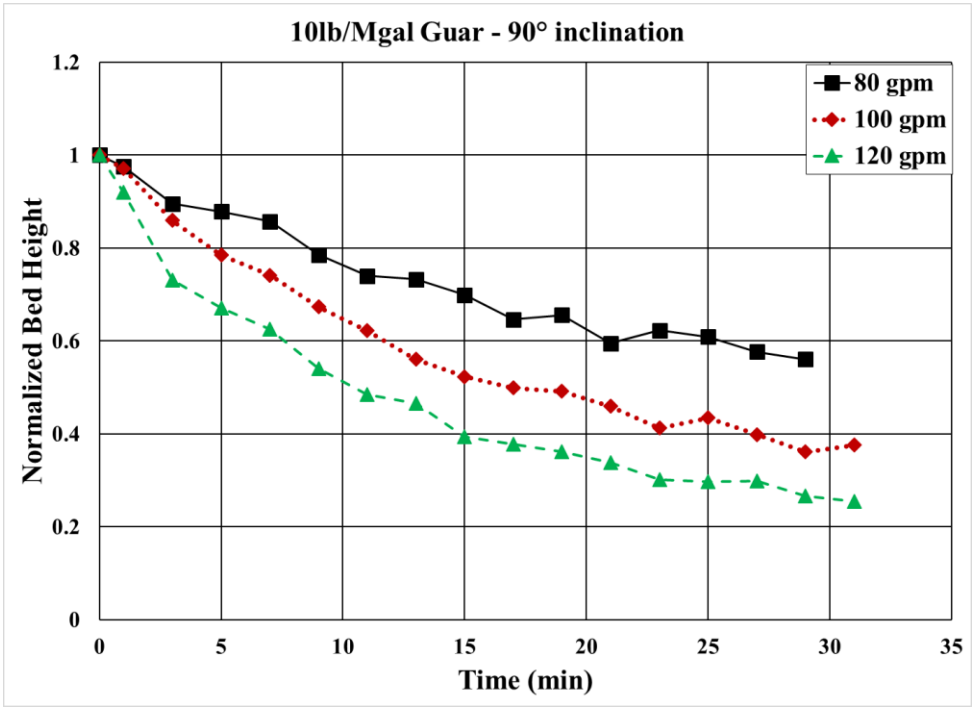

Figure 4.9: Bed erosion curves for 10 lb/Mgal guar at 90° inclination

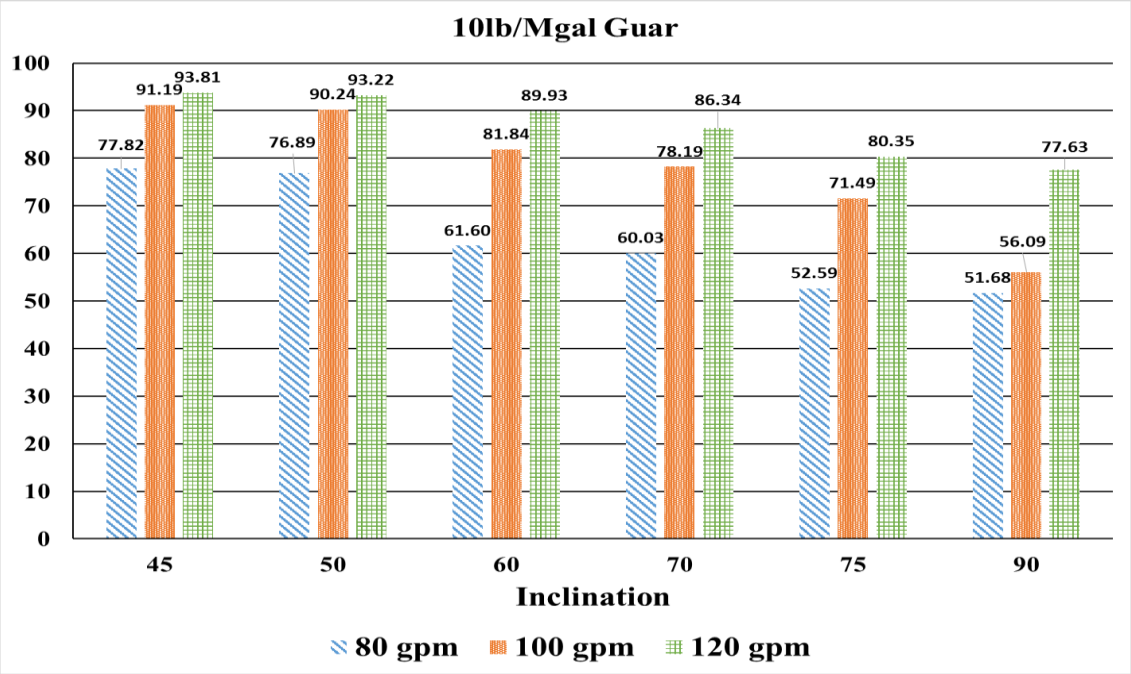

Figure 4.10: Cleanout efficiencies of 10 lb/Mgal guar

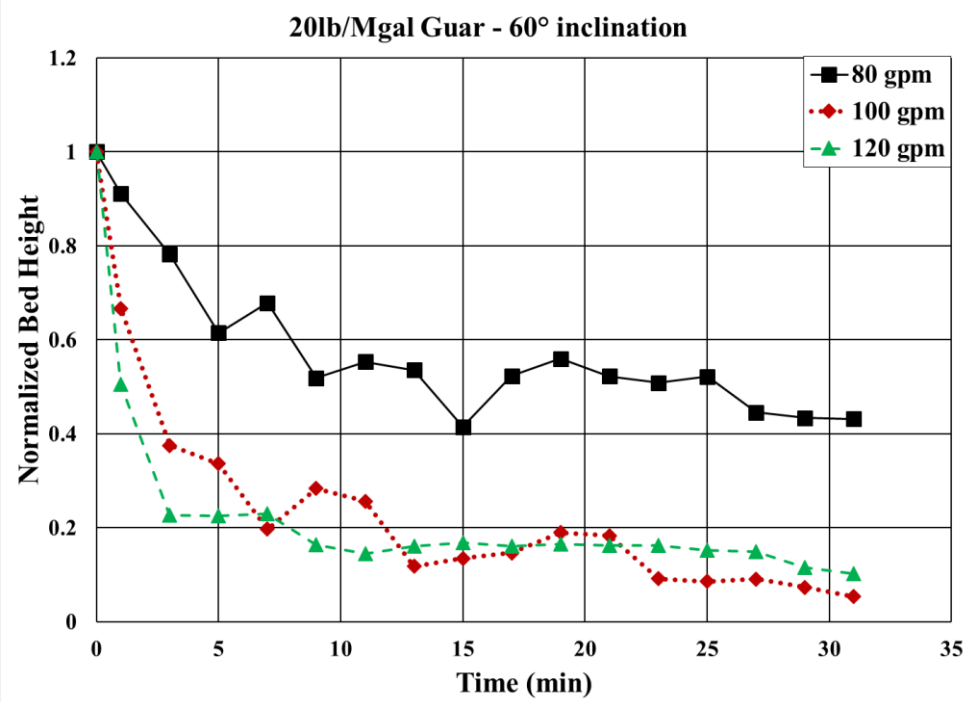

Figure 4.11: Bed erosion curves for 20 lb/Mgal guar at 60° inclination

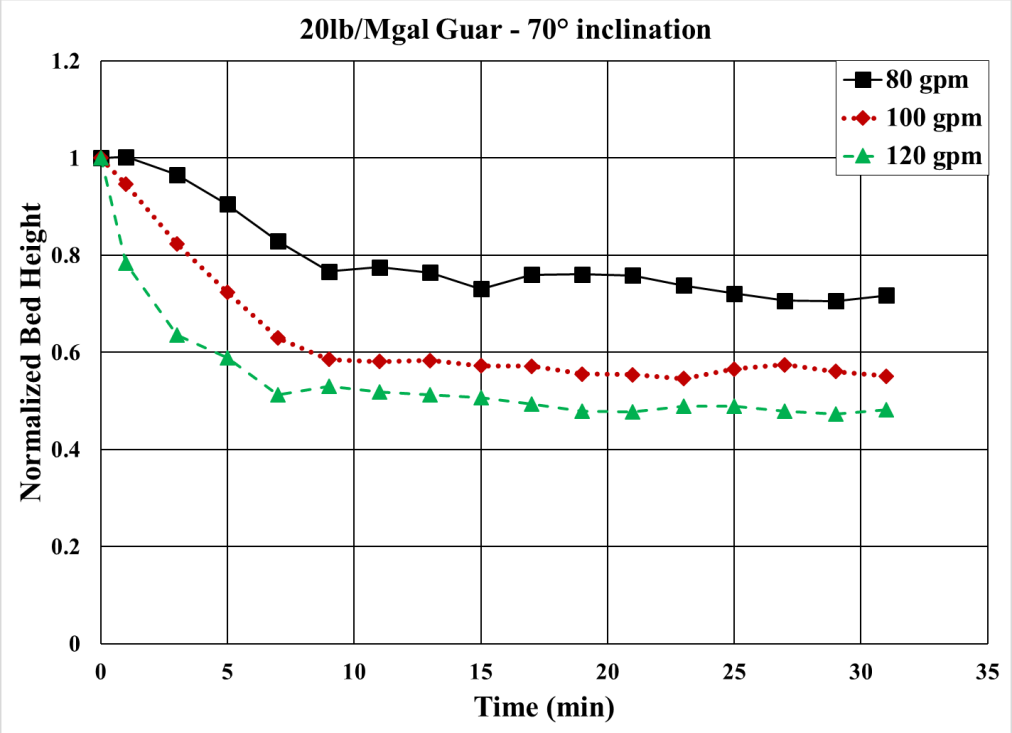

Figure 4.12: Bed erosion curves for 20 lb/Mgal guar at 70° inclination

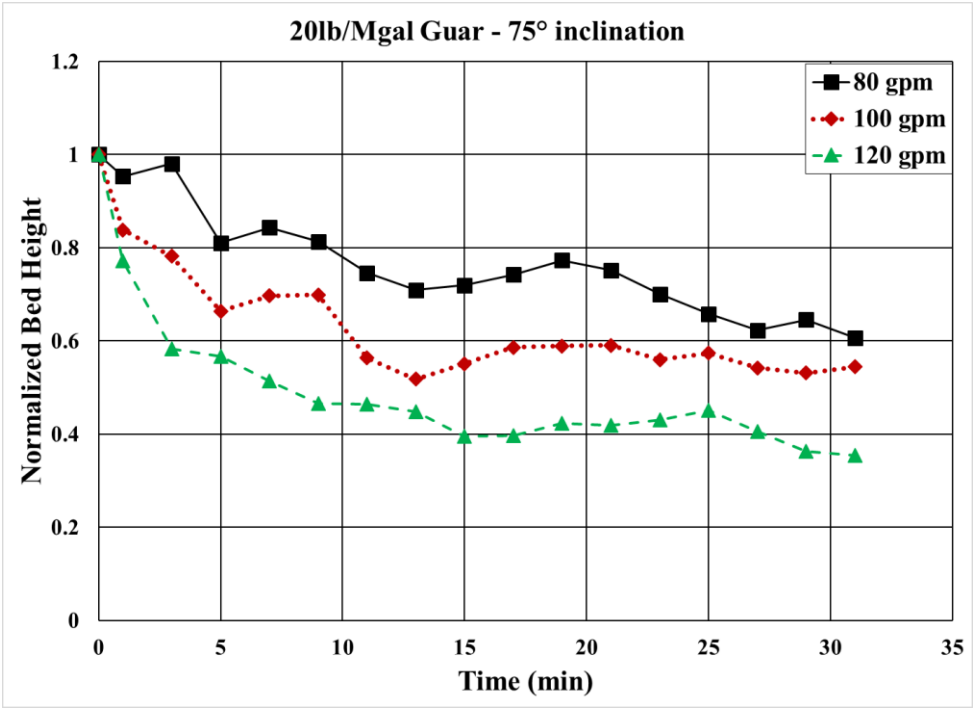

Figure 4.13: Bed erosion curves for 20 lb/Mgal guar at 75° inclination

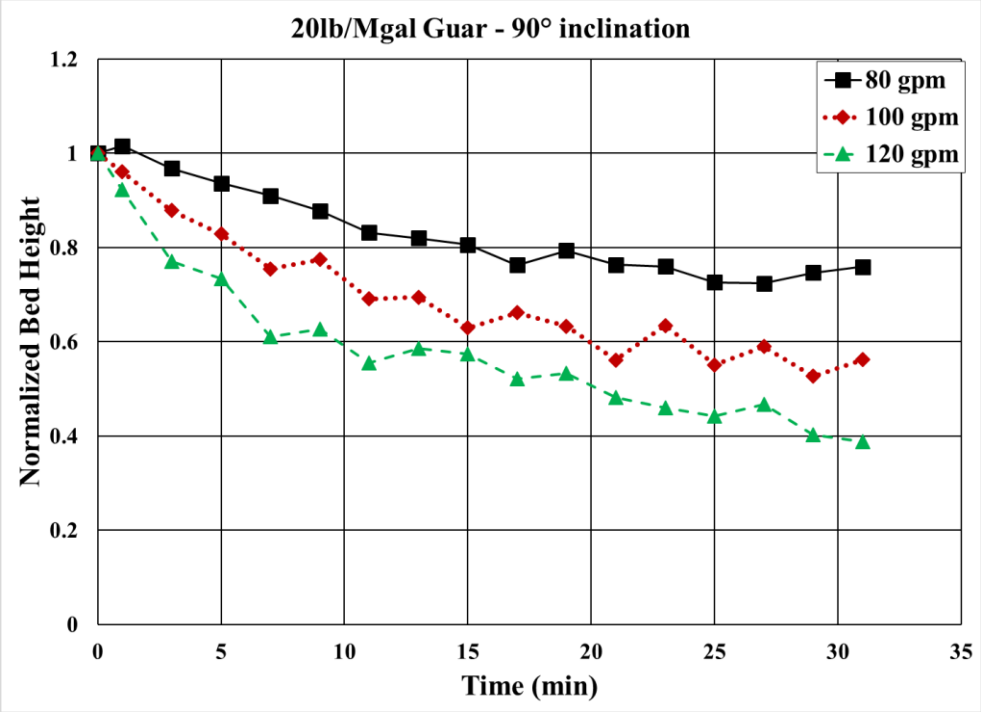

Figure 4.14: Bed erosion curves for 20 lb/Mgal guar at 90° inclination

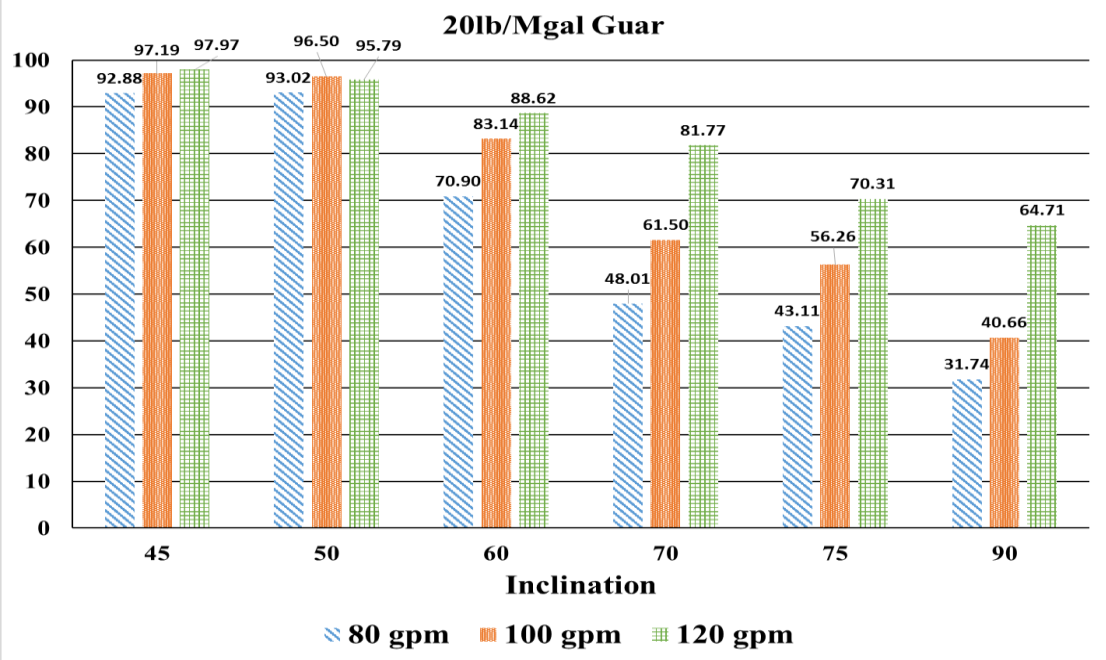

Figure 4.15: Cleanout efficiencies of 20 lb/Mgal guar

4.3 Bed Erosion Curves and Cleanout Efficiency for Various Fluids

Bed erosion curves for three various fluids at flow rates of 80, 100 and 120 gpm and at different inclinations are shown in **Figs. 4.18 through 4.20** (for 60°), **Figs. 4.22 through 4.24** (for 70°), **Figs. 4.26 through 4.28** (for 75°) and **Figs. 4.30 through 4.32** (for 90°). **Figs. 4.16, 4.17, 4.21, 4.25, 4.29 and 4.33** show the cleanout efficiency of different fluids at inclinations of 45°, 50°, 60°, 70°, 75° and 90°, respectively.

The effect of fluid rheology on bed erosion is a function of flow rate and inclination. Furthermore, there is a need to differentiate between the carrying capacity of the liquid and the hole cleaning effect produced by the flow. Water exhibits better performance than polymeric fluids at 70° to 90° for the flow rates considered. At higher inclination (70° - 90°), the solids bed is stationary and does not have a tendency to slide downward. The shear stress at the bed interface plays the key role in solids transport at high inclination. Hole cleaning is more efficient in highly inclined section if a low viscosity fluid is pumped in a turbulent flow regime rather than high viscosity fluid because, for a given flow rate low viscosity fluids can exert higher interfacial stress than the high viscosity fluids. This trend can be observed from bed erosion curves and also from cleanout efficiency values.

Decreasing the inclination from 70° to 60°, the solids bed tends to slide down due to gravity. At the inclination below 60°, higher drag force (due to a higher flow rate) and higher viscosity in a fluid aid in better cleanout. At 60°, although there is a little difference between cleanout efficiencies of all fluids; in general, fluids with higher viscosity

performed better than those with low viscosity, especially at lower flow rates. Although, the increase in flow rate of low viscosity fluid such as water is able to compensate for the lack of viscosity to certain extent. At 60°, the rate of solids erosion increases with viscosity at all flow rates. The cleanout efficiency also increases with viscosity at all flow rates. This is due to the gravity effect that causes the bed to slide, allowing re-entrainment of the particles into the flow stream and permits the utilization of guar fluid's enhanced suspension ability.

Similarly, fluids with higher viscosity performed better than low viscosity fluids at 45° and 50° and at all flow rates. At these inclinations, the flow rates considered are not high enough to compensate for the reduced viscosity in case of water. Thus, 20 lb/Mgal guar fluid shows better performance than 10 lb/Mgal guar fluid and water.

The amount of solids that can be transported by a given volume of liquid is dependent on the rheological properties of liquid. Guar based fluids are more effective than water in terms of carrying capacity but unable to efficiently erode a stationary bed. Lack of viscosity of low viscosity fluids can be compensated to an extent by increasing the flow rate at intermediate angle of inclination. However, it is essential to keep in mind that CT circulation has a limitation in terms of maximum flow rates that can be pumped.

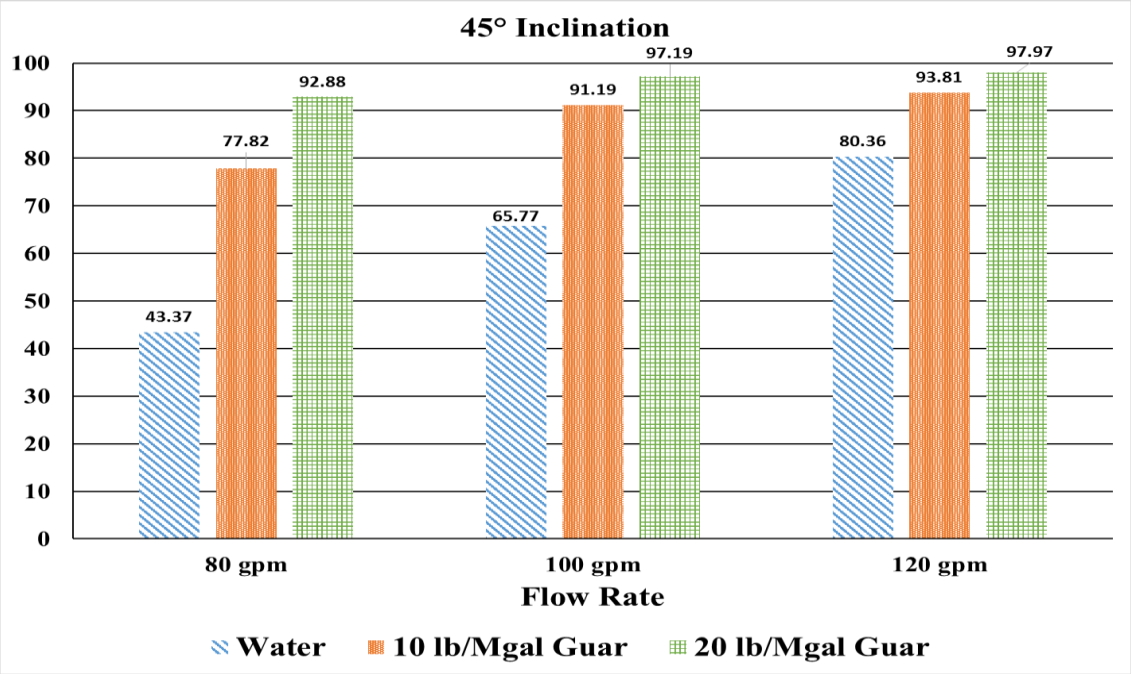

Figure 4.16: Cleanout efficiency of various fluids at 45° inclination

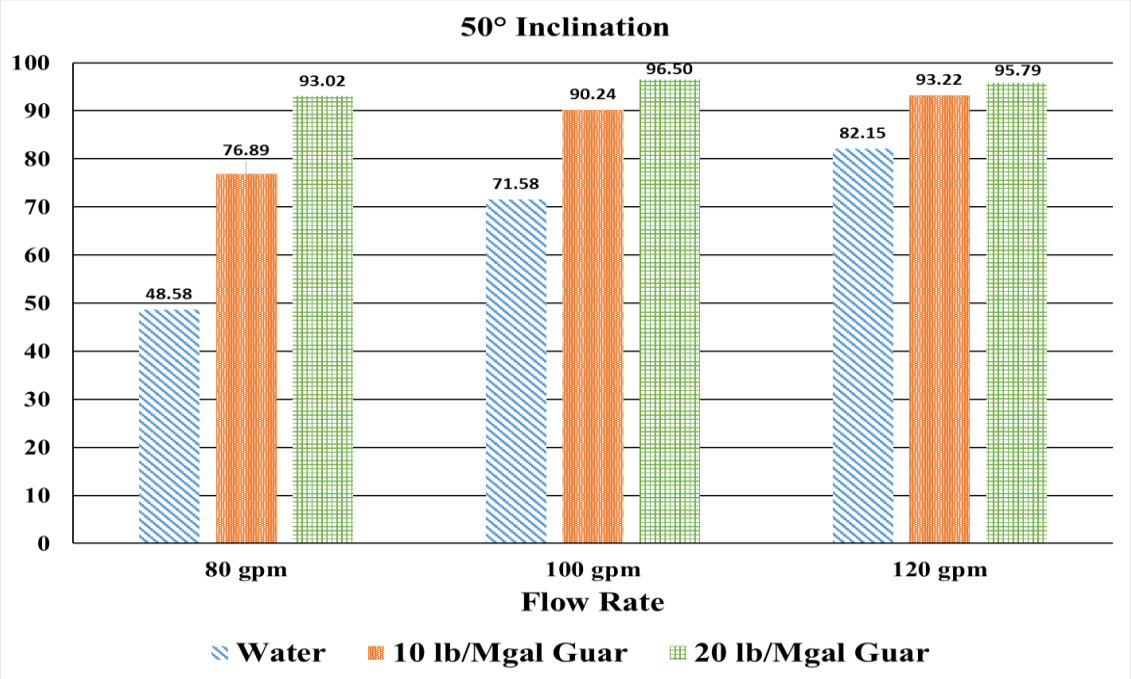

Figure 4.17: Cleanout efficiency of various fluids at 50° inclination

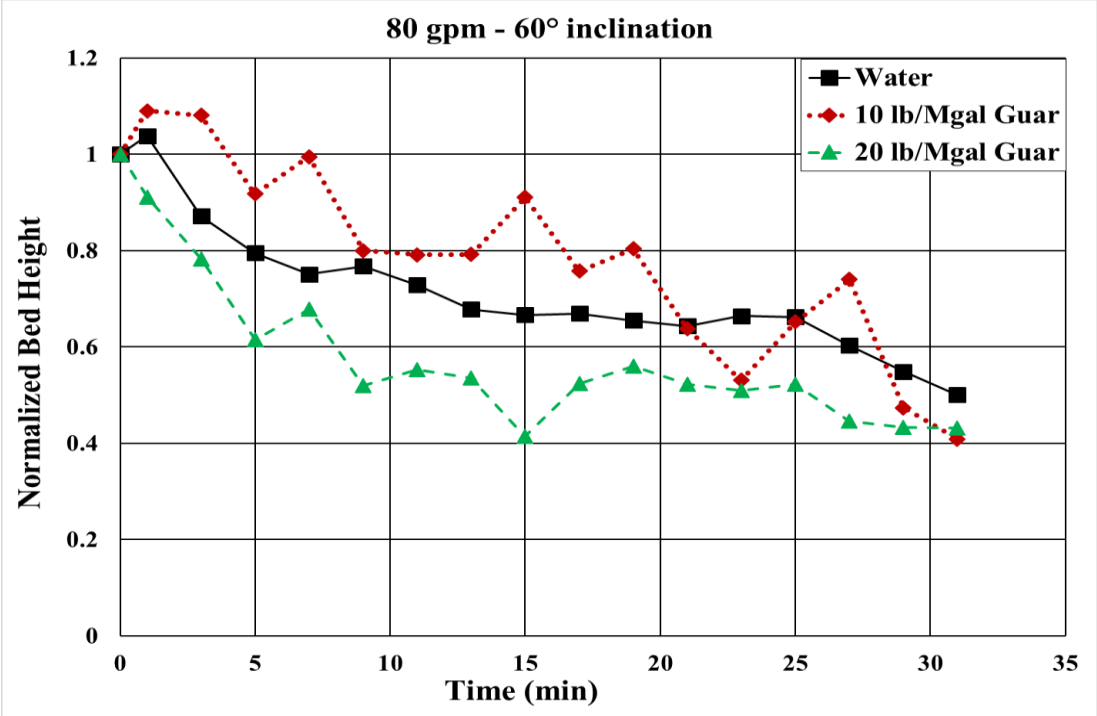

Figure 4.18: Bed erosion curves for various fluids at 60° inclination and 80 gpm

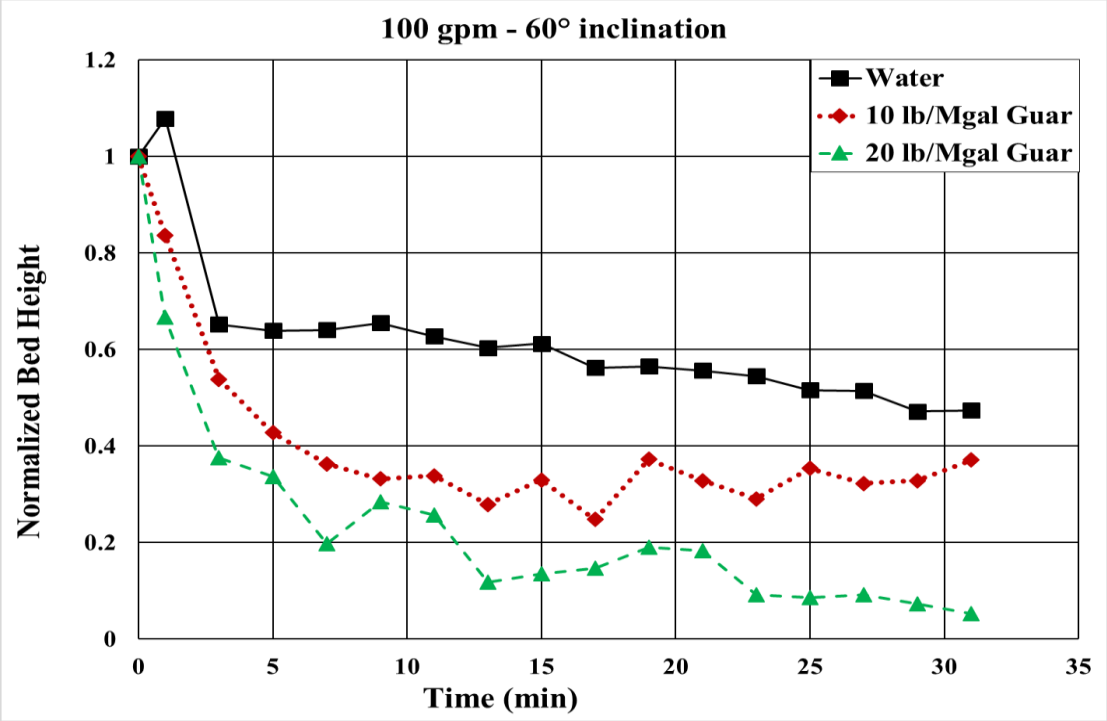

Figure 4.19: Bed erosion curves for various fluids at 60° inclination and 100 gpm

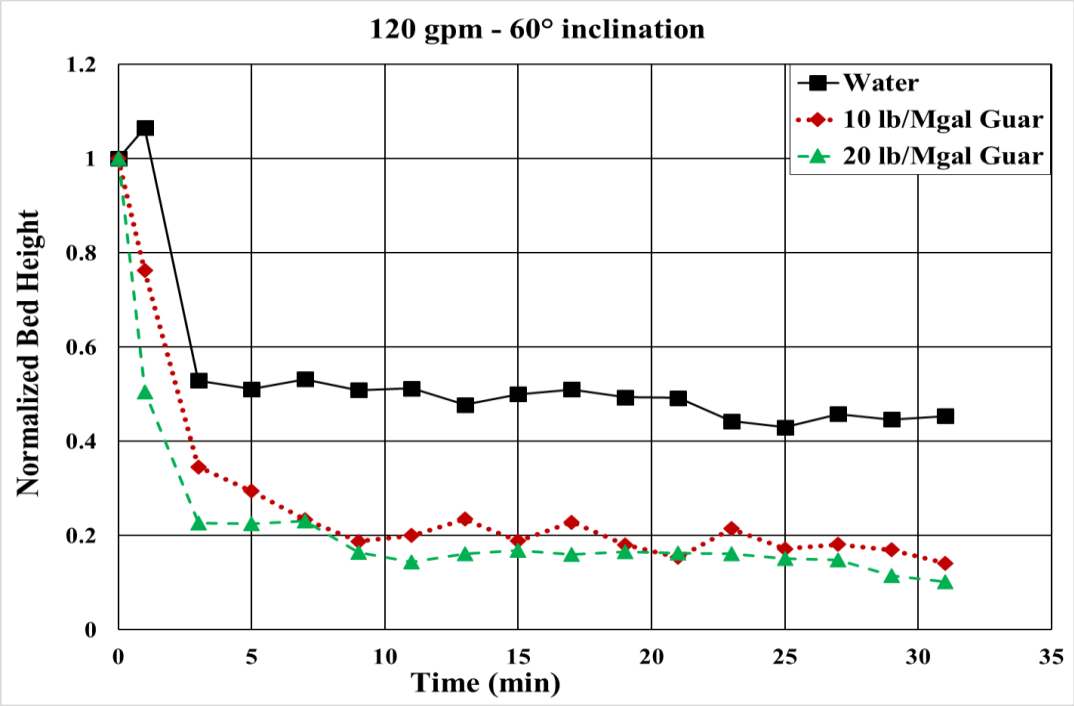

Figure 4.20: Bed erosion curves for various fluids at 60° inclination and 120 gpm

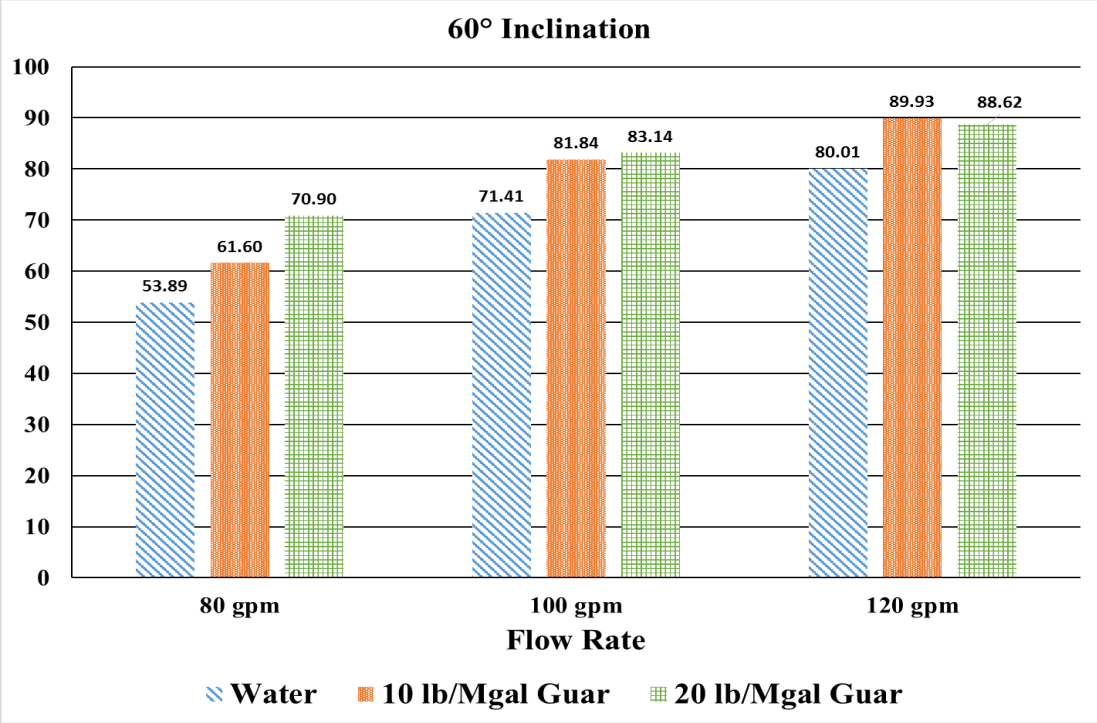

Figure 4.21: Cleanout efficiency of various fluids at 60° inclination

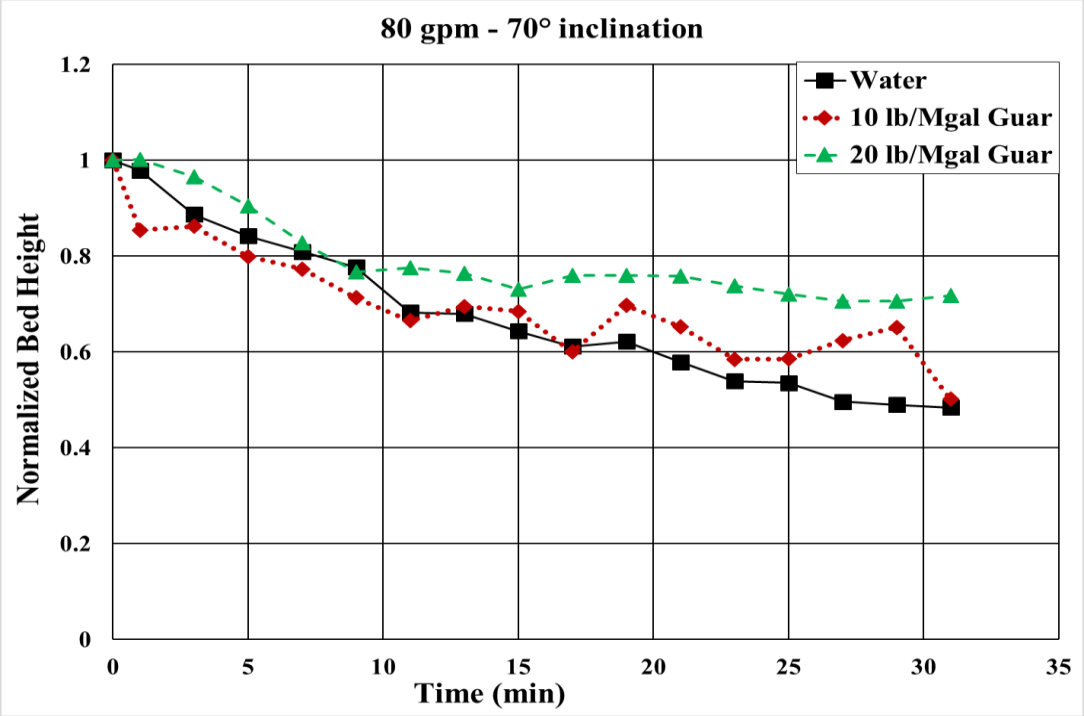

Figure 4.22: Bed erosion curves for various fluids at 70° inclination and 80 gpm

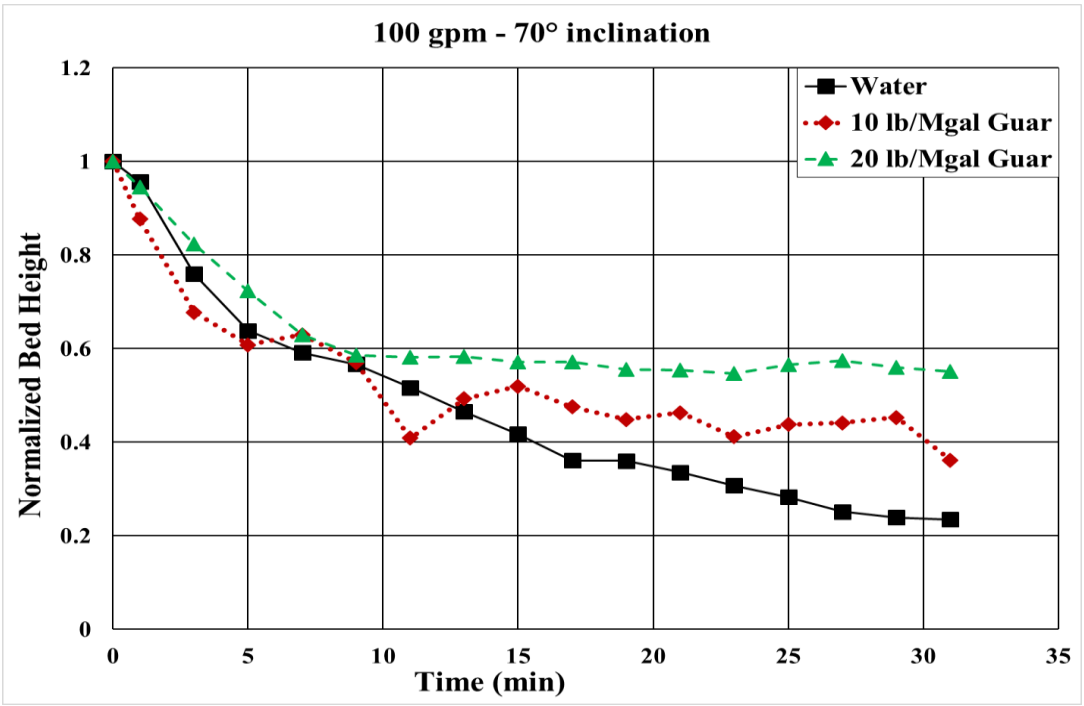

Figure 4.23: Bed erosion curves for various fluids at 70° inclination and 100 gpm

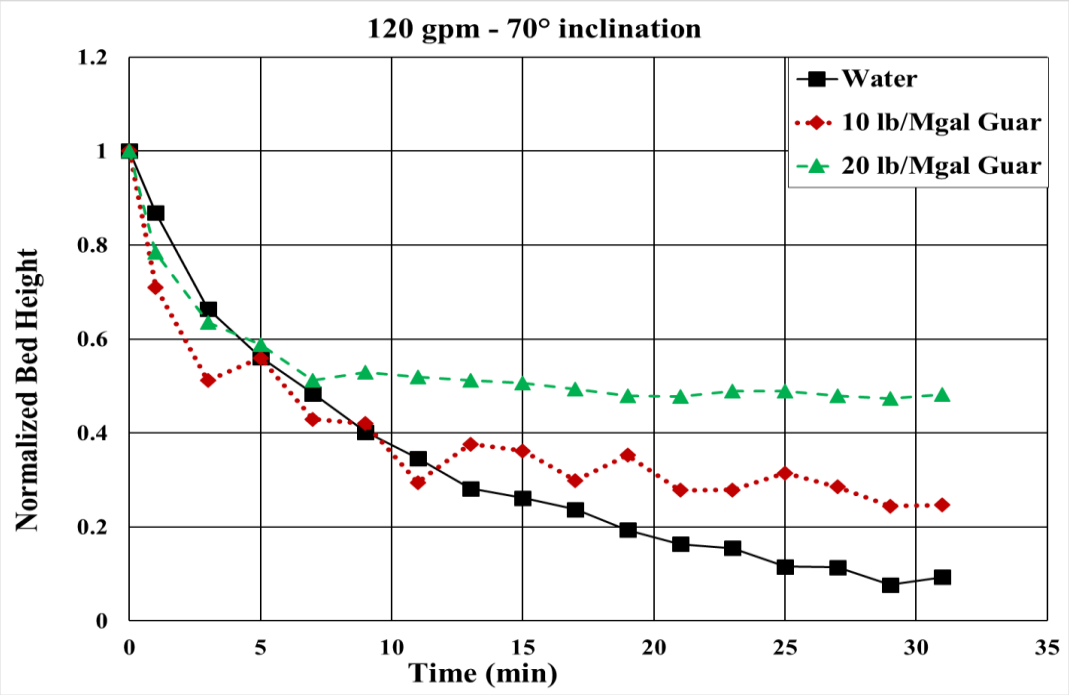

Figure 4.24: Bed erosion curves for various fluids at 70° inclination and 120 gpm

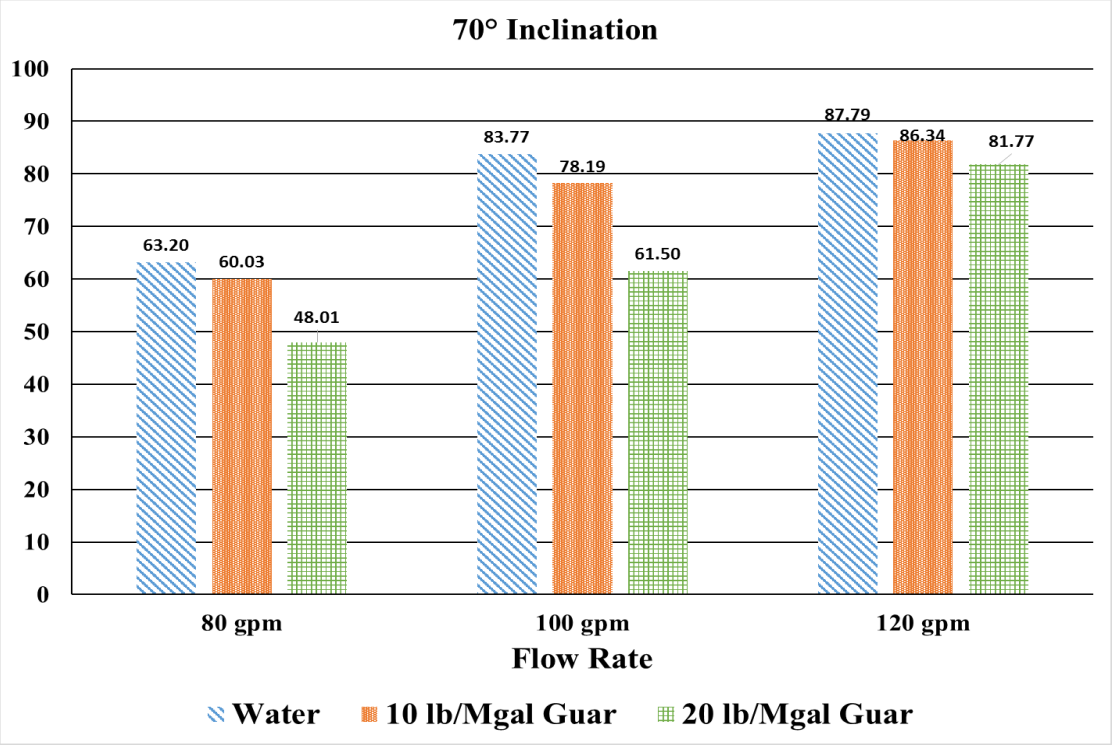

Figure 4.25: Cleanout efficiency of various fluids at 70° inclination

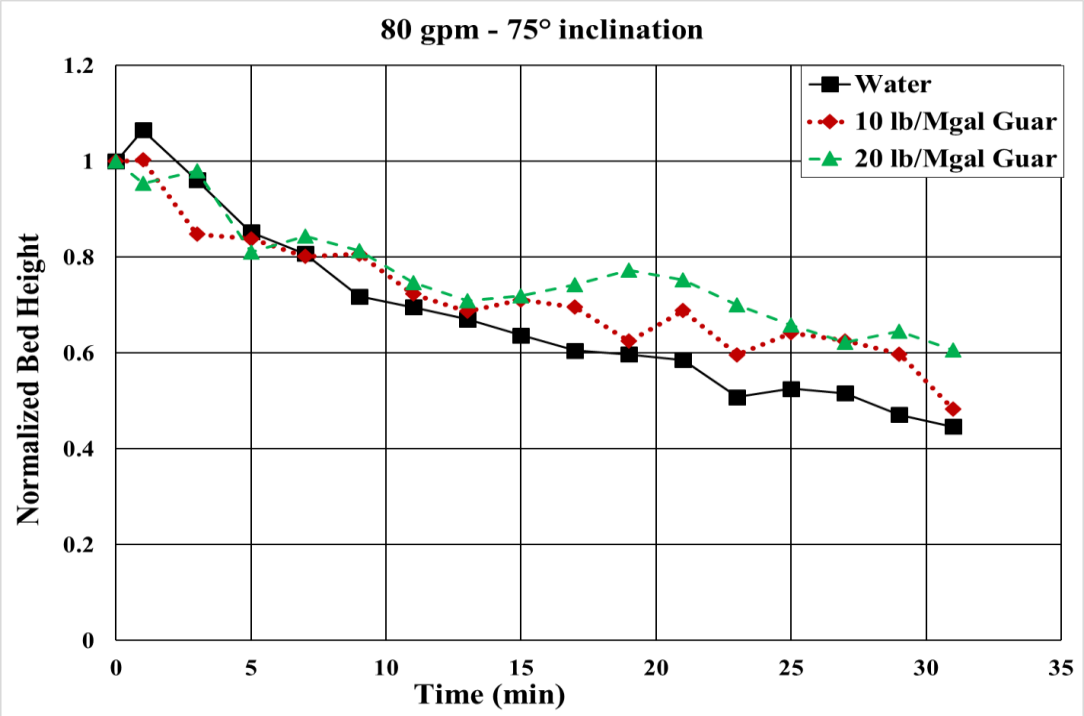

Figure 4.26: Bed erosion curves for various fluids at 75° inclination and 80 gpm

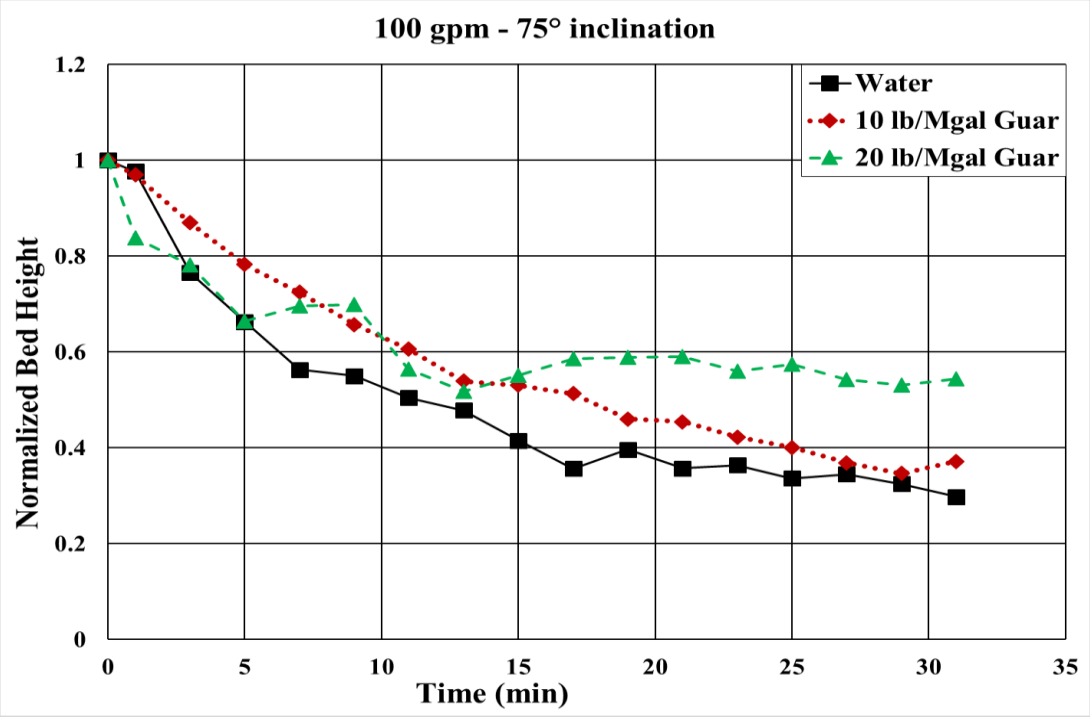

Figure 4.27: Bed erosion curves for various fluids at 75° inclination and 100 gpm

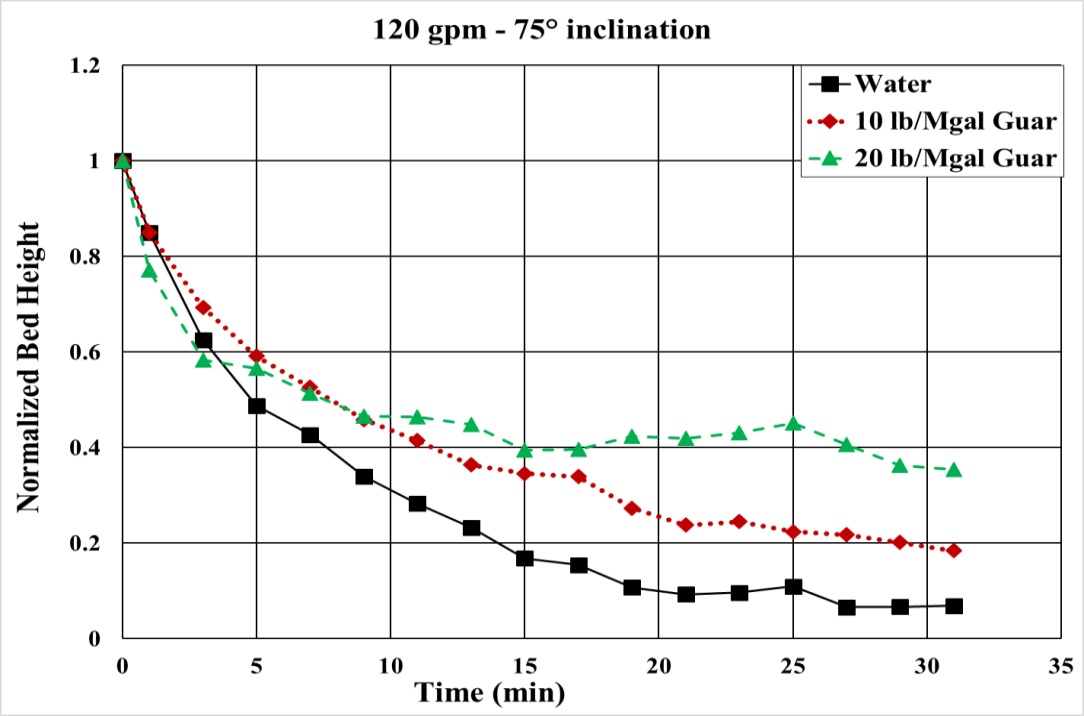

Figure 4.28: Bed erosion curves for various fluids at 75° inclination and 120 gpm

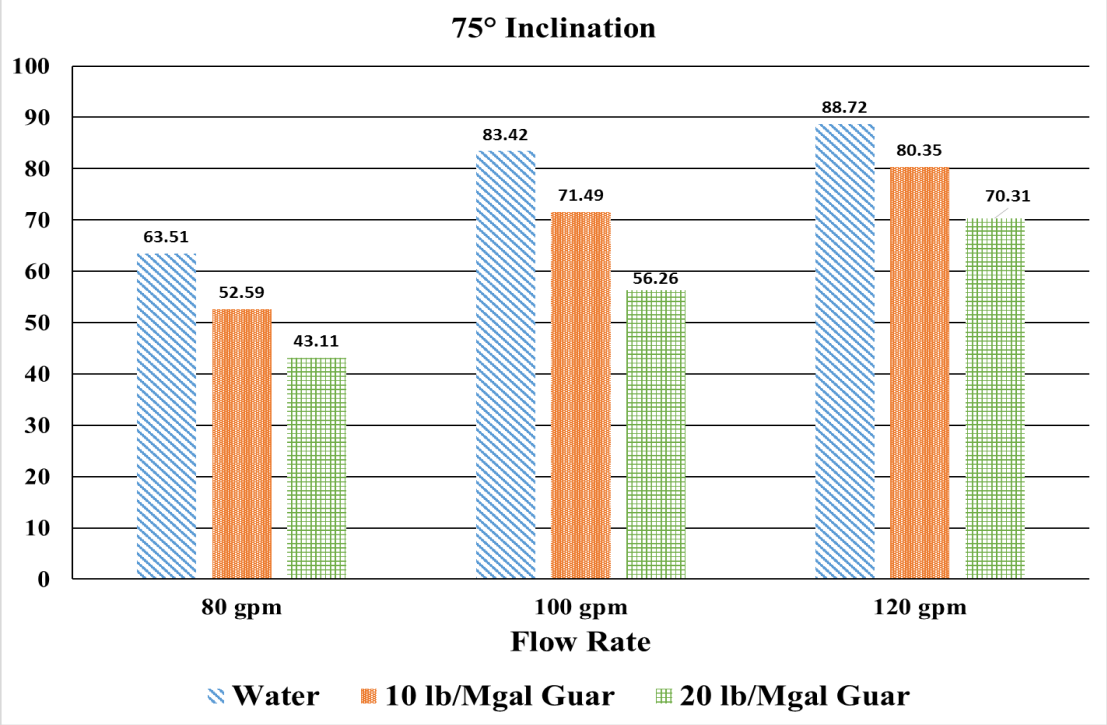

Figure 4.29: Cleanout efficiency of various fluids at 75° inclination

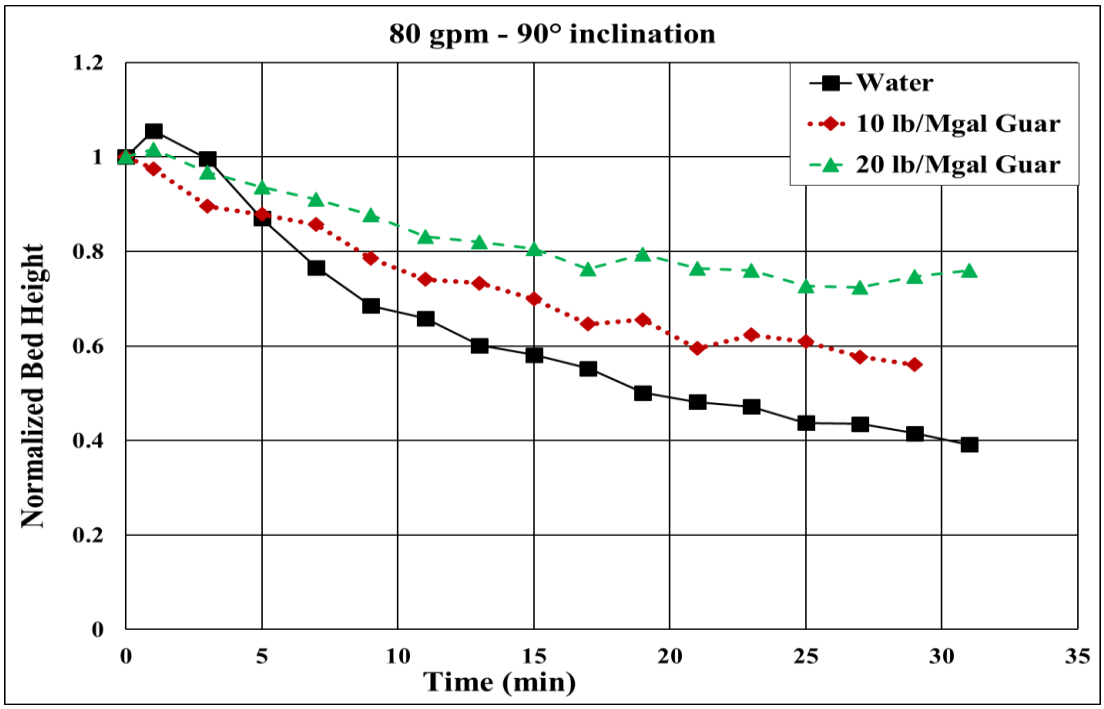

Figure 4.30: Bed erosion curves for various fluids at 90° inclination and 80 gpm

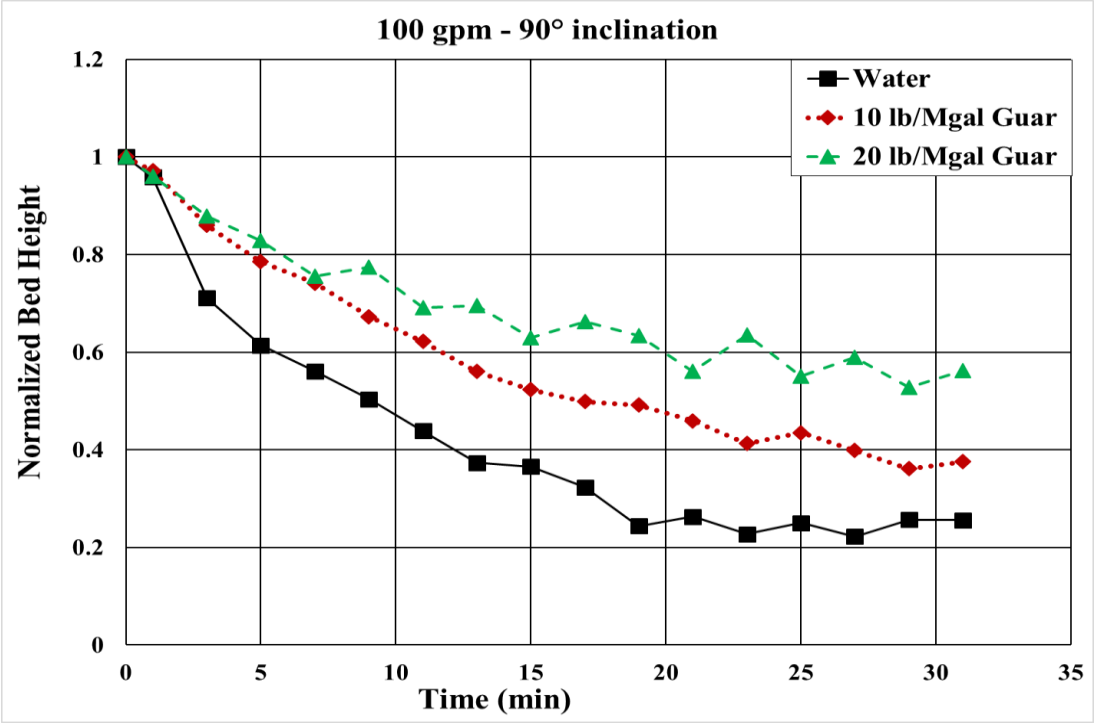

Figure 4.31: Bed erosion curves for various fluids at 90° inclination and 100 gpm

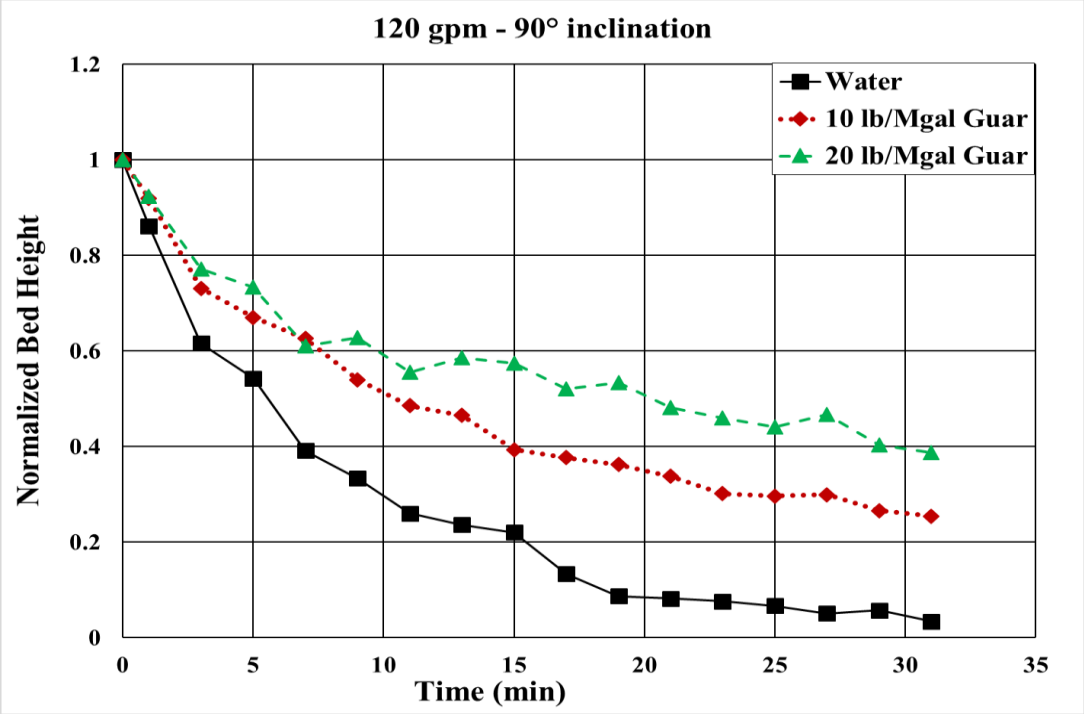

Figure 4.32: Bed erosion curves for various fluids at 90° inclination and 120 gpm

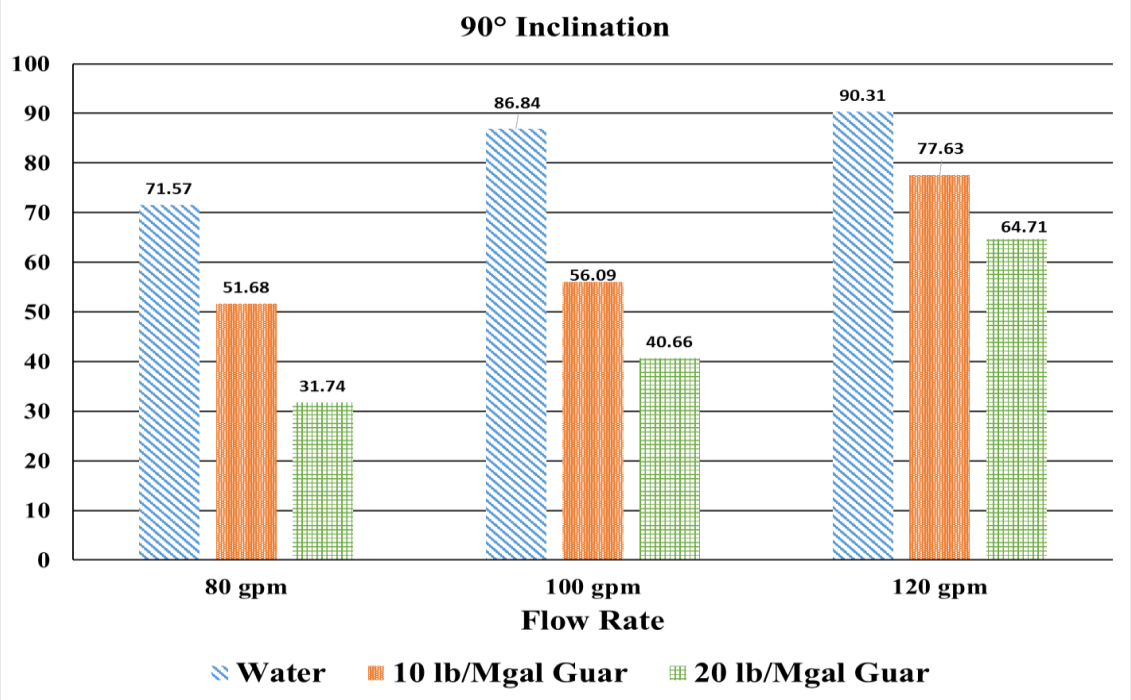

Figure 4.33: Cleanout efficiency of various fluids at 90° inclination

4.4 Cleanout efficiency for various inclinations

The effect of inclination on solids erosion depends on the fluid rheology and flow rate. **Figures 4.34 through 4.36** show the cleanout efficiency at flow rate of 80, 100 and 120 gpm. At all flow rates, the general trend in the cleanout efficiency for water is that it increases with inclination whereas for polymeric fluids it increases with decrease in inclination.

Thus, at higher inclination, lower viscosity fluids perform better whereas at lower inclination, higher viscosity fluids perform better. However, increasing the flow rate can compensate for lower viscosity as can be seen in the case of 120 gpm. The difference in the efficiencies of fluids at high flow rates is less than that at lower flow rates.

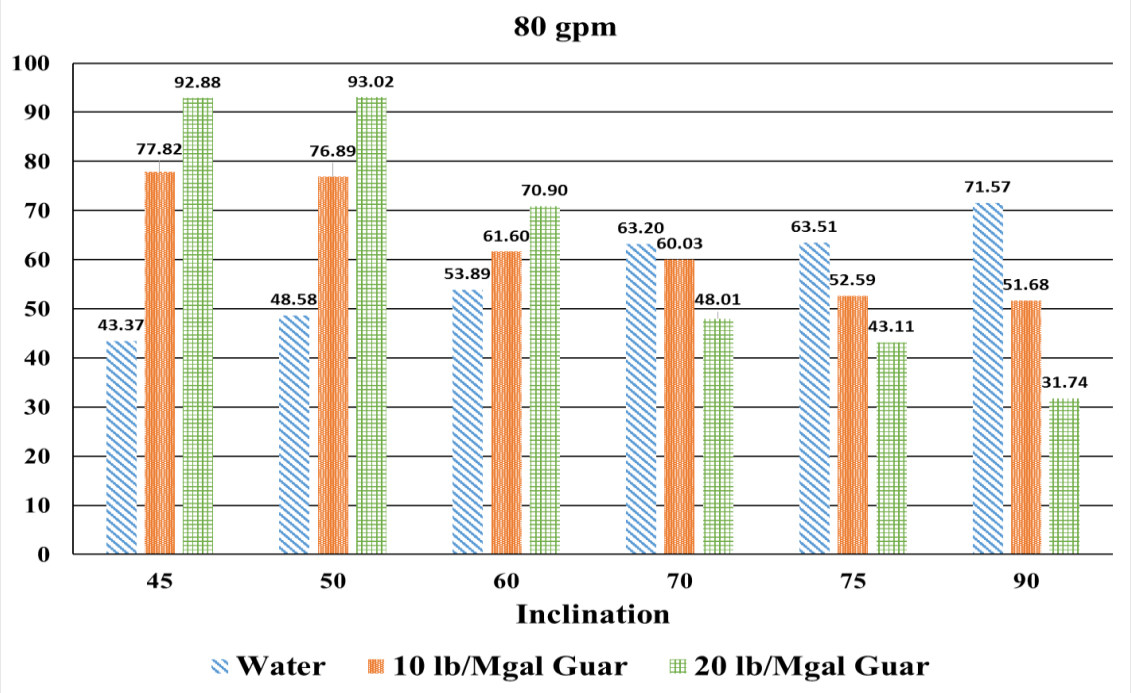

Figure 4.34: Cleanout efficiency of various fluids at 80 gpm

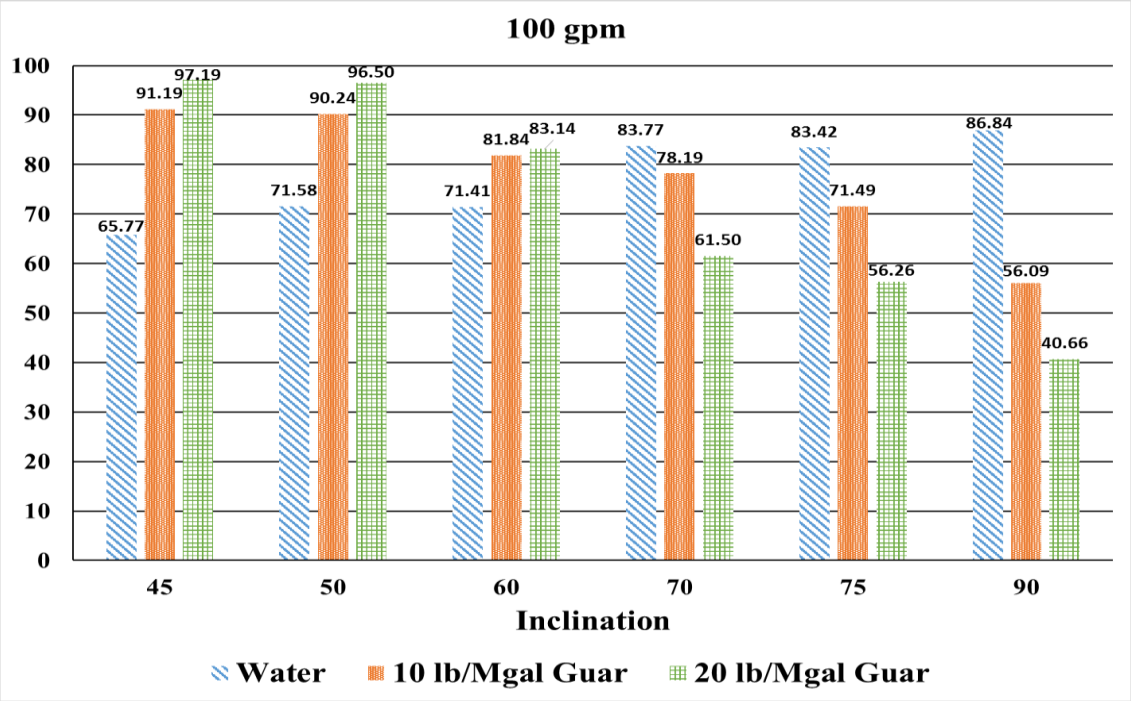

Figure 4.35: Cleanout efficiency of various fluids at 100 gpm

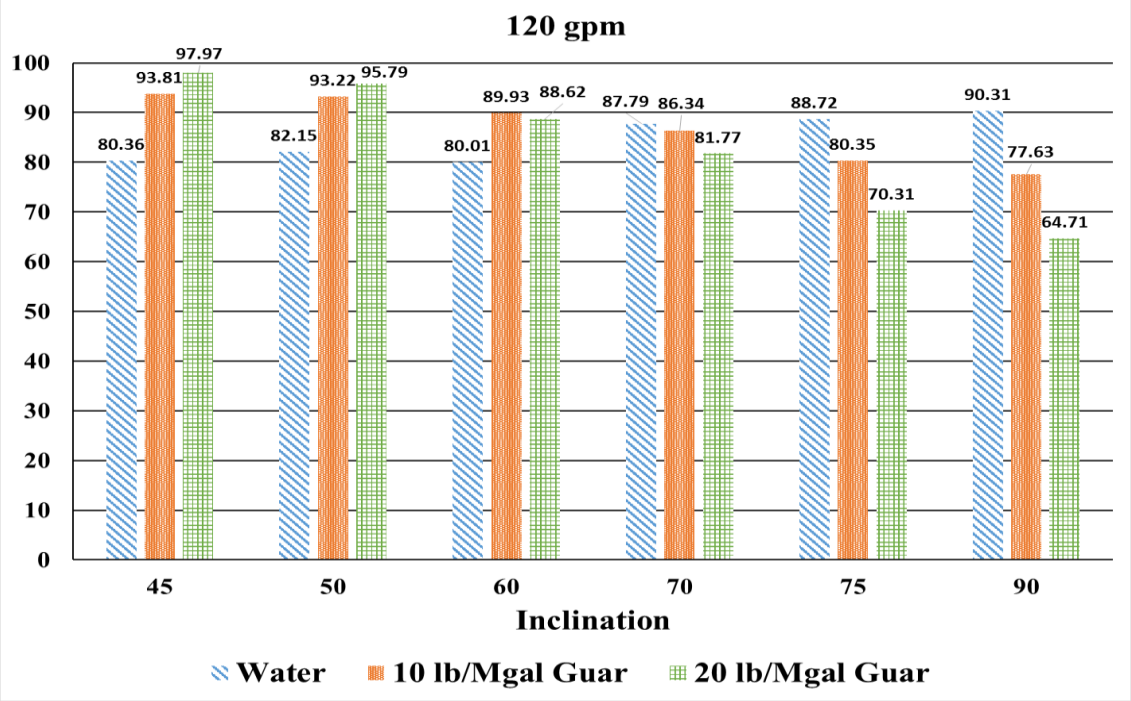

Figure 4.36: Cleanout efficiency of various fluids at 120 gpm

4.5 Critical Angle of Inclination

These results indicate that there exists a critical angle of inclination at which the cleanout efficiency of all fluids at a given flow rate is approximately equal. At inclination higher than the critical angle, low viscosity fluids like water exhibits better cleanout efficiency, whereas, at inclination lower than the critical angle, viscous polymeric fluid is a more suitable candidate.

In order to investigate the critical angle, water was selected as the reference fluid and plots of the ratios of the polymeric fluid efficiency to the base fluid efficiency were generated. Theoretically, the ratio should be unity at critical angle. Since polymeric fluids are more efficient at lower inclination, the ratio should be greater than one and vice versa for the inclination higher than critical angle. **Figure 4.37** represents the ratio of efficiencies of 10 lb/Mgal Guar and water at all flow rates and inclination. It can be seen that irrespective of flow rate, the critical angle exists between 66° and 69° from the vertical. Similarly, **Fig. 4.38** represents the ratio of efficiencies of 20 lb/Mgal Guar and water at all flow rates and inclination. It can be seen that irrespective of flow rate, the critical angle exists between 64° and 67° from the vertical. In terms of field application, this means that the toughest section for hole cleaning is the buildup section (60° to 70°) rather than the vertical or horizontal section.

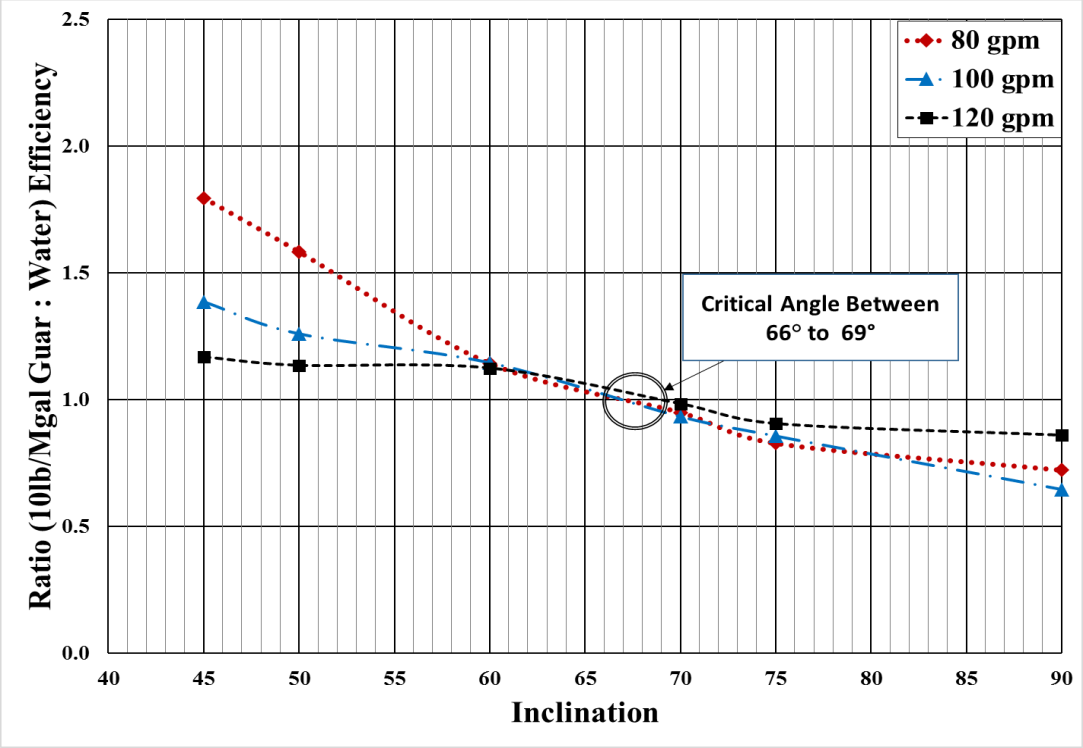

Figure 4.37: Ratio of cleanout efficiencies of 10 lb/Mgal Guar to water

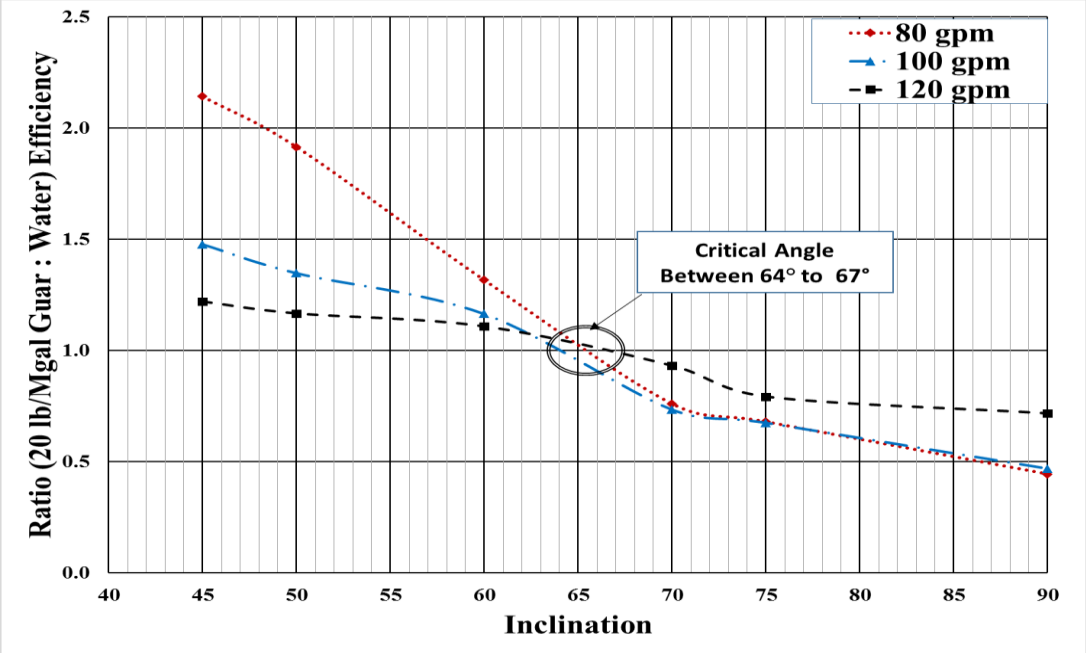

Figure 4.38: Ratio of cleanout efficiencies of 20 lb/Mgal Guar to water

4.6 Discussion

Particle transport is primarily a function of turbulence, drag and lift forces, gravitational, and buoyant forces. Low viscosity fluid like water is able to generate more turbulence as compared to high viscosity fluid. The particle dynamics is substantially different at various inclination.

At higher inclination, saltation dominates the mode of transport of particles. The settled particles are picked up from the low side of the completion section by shear stress generated by fluid eddies on the particle surface. Particles are accelerated and travel horizontally for a short distance before they are deposited back into the bed. This cycle continues until particle is completely out of the horizontal section. The distance travelled by the particles along the horizontal is greatly affected by fluid flow behavior. Fluid flowing within lower turbulent flow regime generates low level of shear stress on to particles and particles tend to stay in the stationary bed for a longer period of time. This renders the entire transport process very slow and tedious. On the contrary, due to the associated high velocity, a fluid flowing in turbulent flow regime can exert higher shear stress on the particles and, with its potential stirring of turbulent eddies, the fluid can pick up particles easily, impart high average speed to particles, and facilitate greater transport distance. It is important to mention that although the average particle velocities are much higher in such cases, particles still settle into the bed as they get decelerated by colliding with walls or other particles. However, generated eddies lift the particles back into the flow stream, and they are rapidly accelerated again. Hence, higher the level of turbulence imparted to fluid, the better it is for the particle transportation process. Higher turbulence

levels are only possible with fluids that present lower viscosity. Naturally, at higher level of turbulence generated, even a low viscosity fluid will generate high frictional losses. This can be addressed with fluid friction pressure reducers that adjust the rheology of the fluid.

On the contrary, at lower inclination, a concept of “downward sliding bed flow” exists (Cano et al. 2016). This concept means that if the flow rate is below a threshold flow rate, the solids bed slides downwards against the flow due to gravity. Hence, the suspension capability of fluid becomes much more important at lower inclination. Polymeric fluid exhibits better cleanout efficiency as it prevents settling of particles and keep them suspended in the flow stream.

CHAPTER 5

DEVELOPMENT OF CORRELATION

5.1 Bed Decay Model

The data of normalized proppant bed height as a function of time was used to improve an already established correlation to predict the circulation time required for a given set of fluid rheology and flow rate. Both exponential and polynomial functions can be used to model the solids bed erosion data. However, the polynomial function predicts the decrease of solids bed height to zero for a given flow rate, which is not always possible. CT application has limitation in terms of maximum flow rate. For the cleanout purpose, the limiting condition is influenced by the fracturing gradient of the formation as well as the burst pressure rating for the CT. If the flow rate is insufficient, there will be a critical sand bed height below which solids will not be removed. The exponential function accurately models this non-linear relationship of decreasing solids bed height with time. The development of solids bed decay model discussed here is a first-order exponential decay model. The model was first used by Adari (1999). However, the tests carried out by Adari were in near horizontal wellbore profile. Another attempt on developing bed decay model was made by Naik (2015). This model is developed to determine the reduction in percentage of bed height by normalizing all the data points. This eliminates one of the empirical parameters used in earlier developed models. Furthermore, the extended model developed incorporates the effect of flow rate and fluid rheology. This

makes the correlation exclusively specific to inclination unlike the previous models that were specific to inclination, fluid type, and flow rate.

Rate of reduction of normalized bed height can be given by the first order differential equation,

$$\frac{d\left[\frac{h(t)}{h_i}-\frac{h_f}{h_i}\right]}{dt} = -\lambda\left[\frac{h(t)}{h_i} - \frac{h_f}{h_i}\right] \quad (5.1)$$

where,

h_f is the steady state bed height;

h_i is the initial bed height;

$h(t)$ is the bed height after time 't';

λ = Reciprocal of time constant, min^{-1};

t = time, min.

Let, $\frac{h(t)}{h_i} - \frac{h_f}{h_i} = X$ (5.2)

Therefore, Eq. 5.1 can be rewritten as,

$$\frac{dX}{dt} = -\lambda X$$

Rearranging,

$$\frac{dX}{X} = -\lambda dt$$

Integrating,

$$\int \frac{dX}{X} = -\int \lambda dt$$

$$\ln[X] = -\lambda t + C$$

or, $X = e^{-\lambda t + C}$ (5.3)

where 'C' is the integration constant.

Substituting for X from Eq. 5.2 into Eq. 5.3,

$$\frac{h(t)}{h_i} - \frac{h_f}{h_i} = e^{-\lambda t + C} \quad (5.4)$$

At time $t = 0$, the bed height, $h(t) = h_i$

Substituting this into Eq. 5.4

$$\left[1 - \frac{h_f}{h_i}\right] = e^{-\lambda(0)} . e^{C}$$

$$C = \ln\left[1 - \frac{h_f}{h_i}\right] \quad (5.5)$$

Substituting 'C' into Eq. 5.4

$$\frac{h(t)}{h_i} - \frac{h_f}{h_i} = \left[1 - \frac{h_f}{h_i}\right] e^{-\lambda t}$$

or,

$$\frac{h(t)}{h_i} = \frac{h_f}{h_i} + \left[1 - \frac{h_f}{h_i}\right] e^{-\lambda t} \tag{5.6}$$

The proposed model therefore, is

$$h_n = \alpha + (1 - \alpha) e^{-\lambda t} \tag{5.7}$$

where,

$h_n = \frac{h(t)}{h_i}$ (normalized bed height at any time, t);

$\alpha = \frac{h_f}{h_i}$ (steady state normalized bed height);

λ = Reciprocal of time constant, min^{-1};

t = time, min.

Time constant, $-(\frac{1}{\lambda})$, is the time at which the normalized bed height is reduced to $\frac{1}{e} = 0.37$ times its initial value.The proposed model is used to fit the experimental data to obtain the regression coefficients α and λ using a statistical software, NCSS version 10. The experimental and predicted bed erosion curve for 10 lbm/Mgal guar fluid tested at 75° inclination and 100 gpm is shown in **Fig 5.1**. Similar analysis was done for all bed erosion tests and the model was observed to fit experimental data very accurately for most of the tests, with absolute deviation of less than 5%. The regression coefficients α and λ

vary with flow rate and fluid rheology. It is found that a logarithmic curve fits the coefficients α as shown in **Fig. 5.2 through 5.5**.

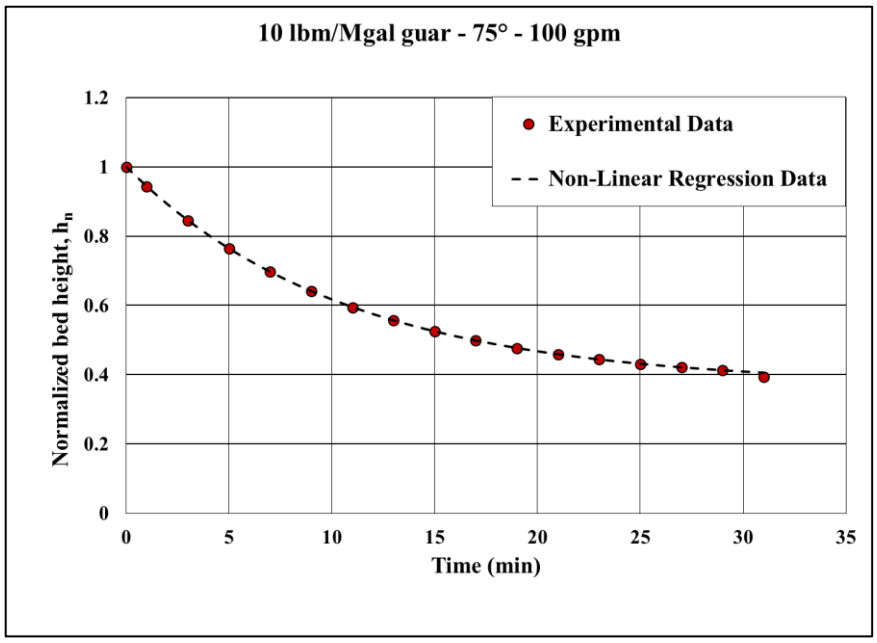

Figure 5.1: Non-linear regression fit data vs. experimental data

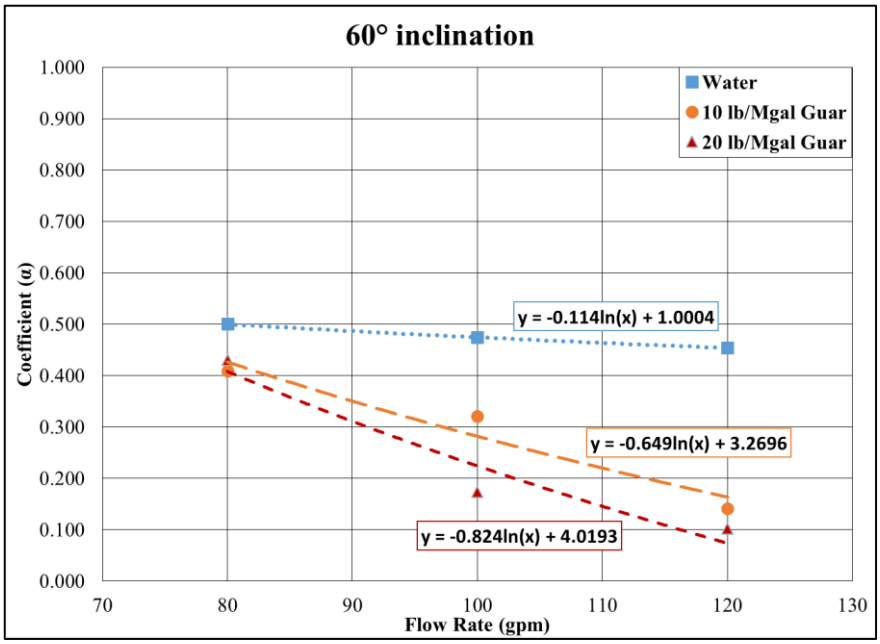

Figure 5.2: Coefficient 'α' as function of flow rate (60° inclination)

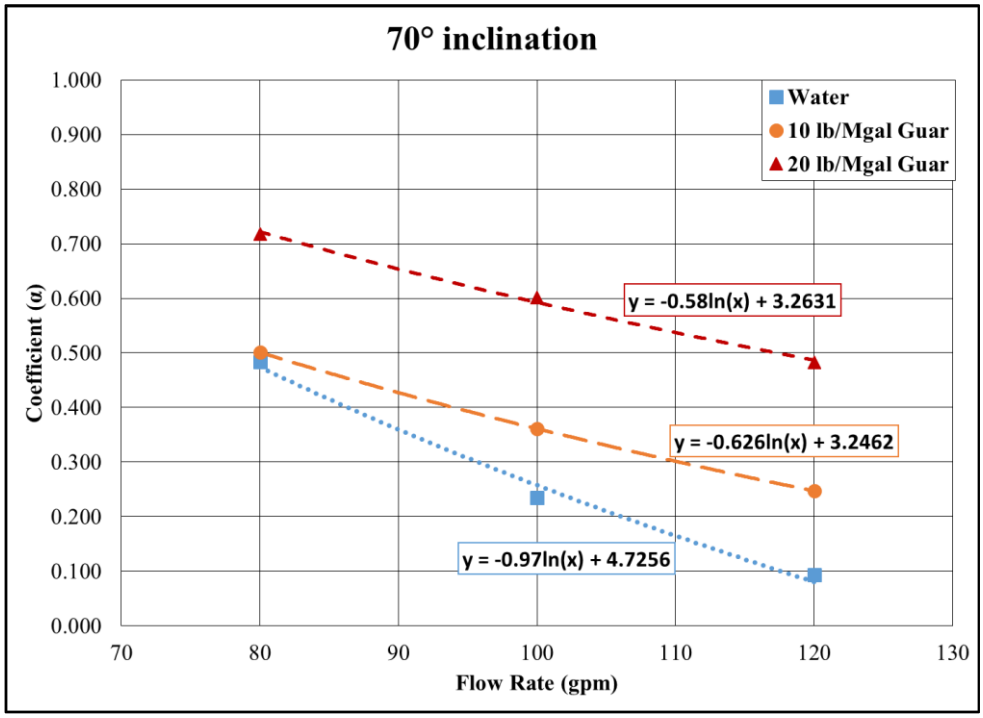

Figure 5.3: Coefficient 'α' as function of flow rate (70° inclination)

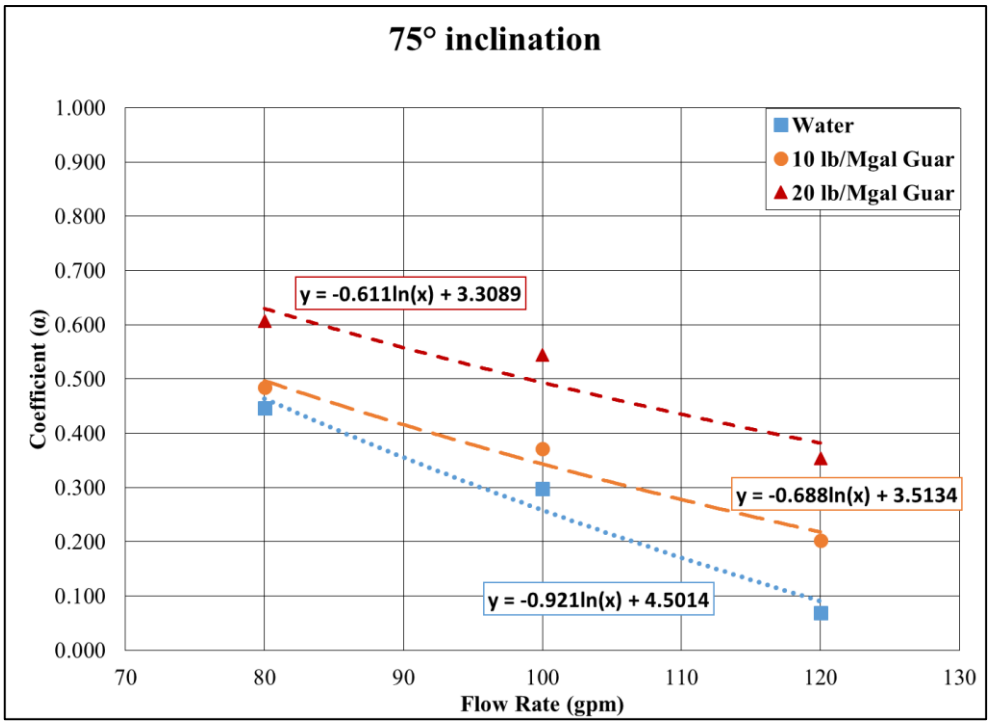

Figure 5.4: Coefficient 'α' as function of flow rate (75° inclination)

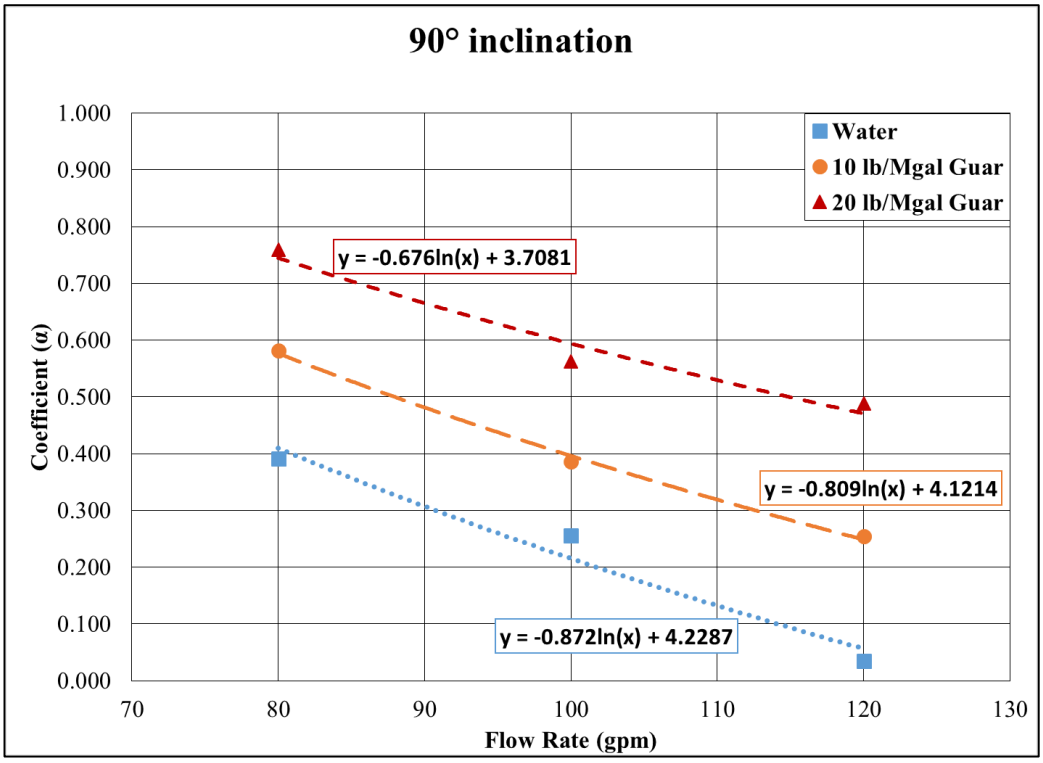

Figure 5.5: Coefficient '$\boldsymbol{\alpha}$' as function of flow rate (90° inclination)

For a fixed inclination and fluid rheology, α can be estimated from the flow rate using the following relation:

$$\alpha = -A_1 \ln(Q) + A_2 \tag{5.8}$$

where,

Q = flow rate, gpm

A_1, A_2 = empirical rheological parameters

Equation 5.8 needs further development to include the effect of fluid rheology. The coefficients A_1 and A_2 are dependent on the fluid rheology. Power law rheology is

considered in this study, as it is widely used to approximate polymer based fluids. The mud rheology parameters A_1 and A_2 are obtained for different fluid systems and are related to power law rheological parameters, n (flow behavior index) and μ_a (apparent viscosity at 511 sec^{-1}) by defining a dimensional group called fluid rheology parameter given by,

$$\kappa = \frac{n}{\mu_a(in\ cP)} \tag{5.9}$$

n = flow behavior index, dimensionless

μ_a = apparent viscosity of non-Newtonian fluids at 511 s^{-1}, cP

For water, $n = 1$ and $\mu_a = 1$ cP.

Figures 5.6 to 5.9 are the plots relating A_1 and A_2 as a function of κ for various inclination. In general, both A_1 and A_2 are polynomial functions of κ and can be expressed as:

$$A_1 = a_{11}\kappa^2 + a_{12}\kappa + a_{13} \tag{5.10}$$

$$A_2 = a_{21}\kappa^2 + a_{22}\kappa + a_{23} \tag{5.11}$$

a_{xy} = empirical inclination specific constants

The inclination specific constants $a_{11}, a_{12}, a_{13}, a_{21}, a_{22},$ and a_{23} are tabulated in **Table 5.1**.

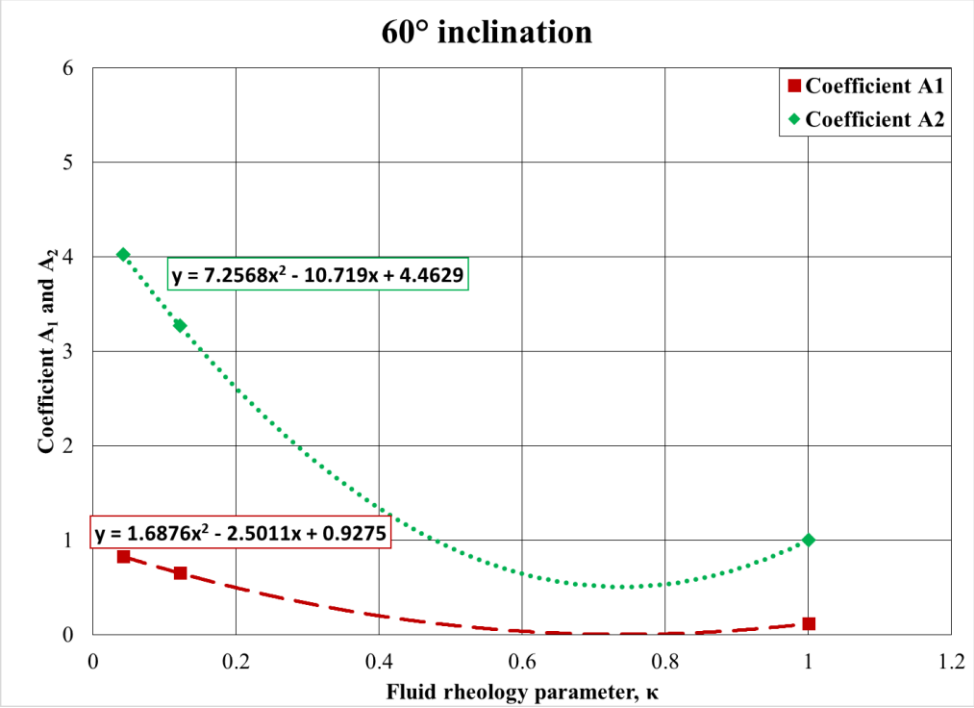

Figure 5.6: Coefficient A_1 and A_2 as function of κ (60° inclination)

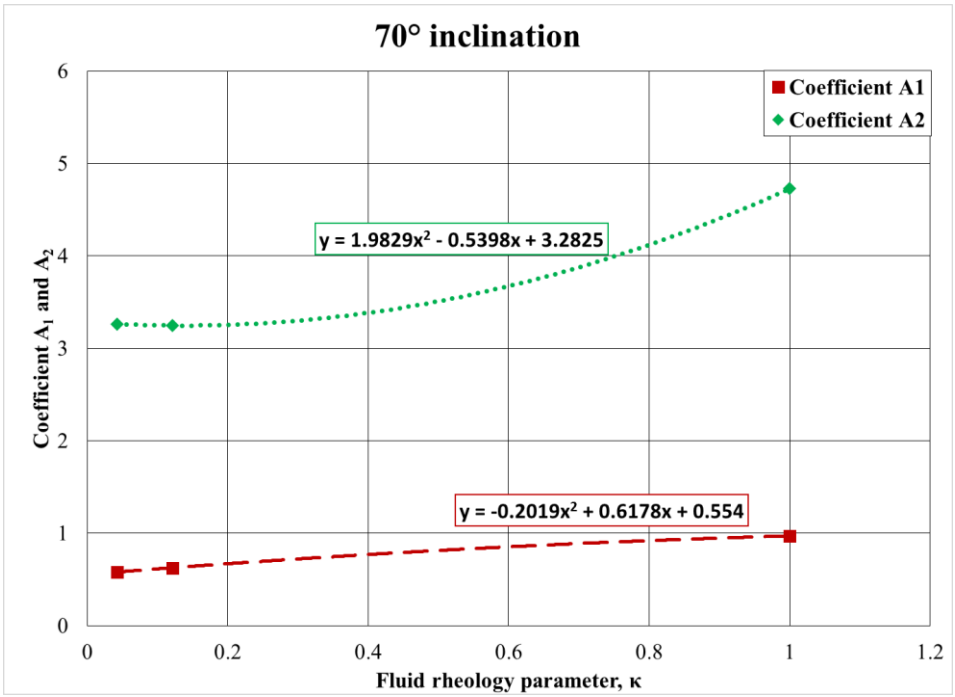

Figure 5.7: Coefficient A_1 and A_2 as function of κ (70° inclination)

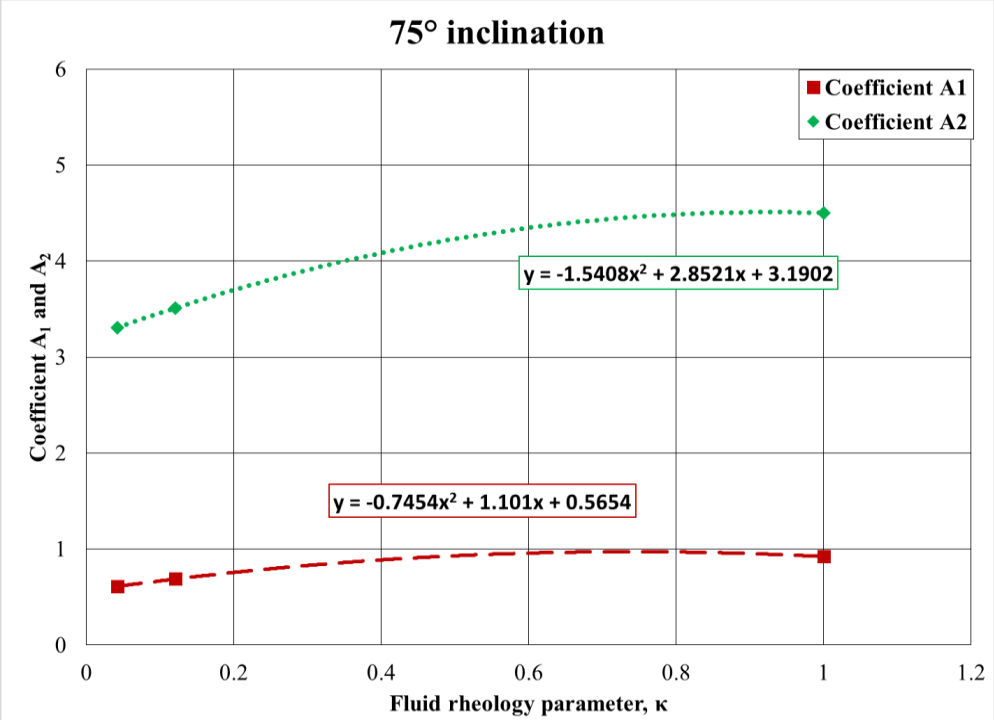

Figure 5.8: Coefficient A_1 and A_2 as function of κ (75° inclination)

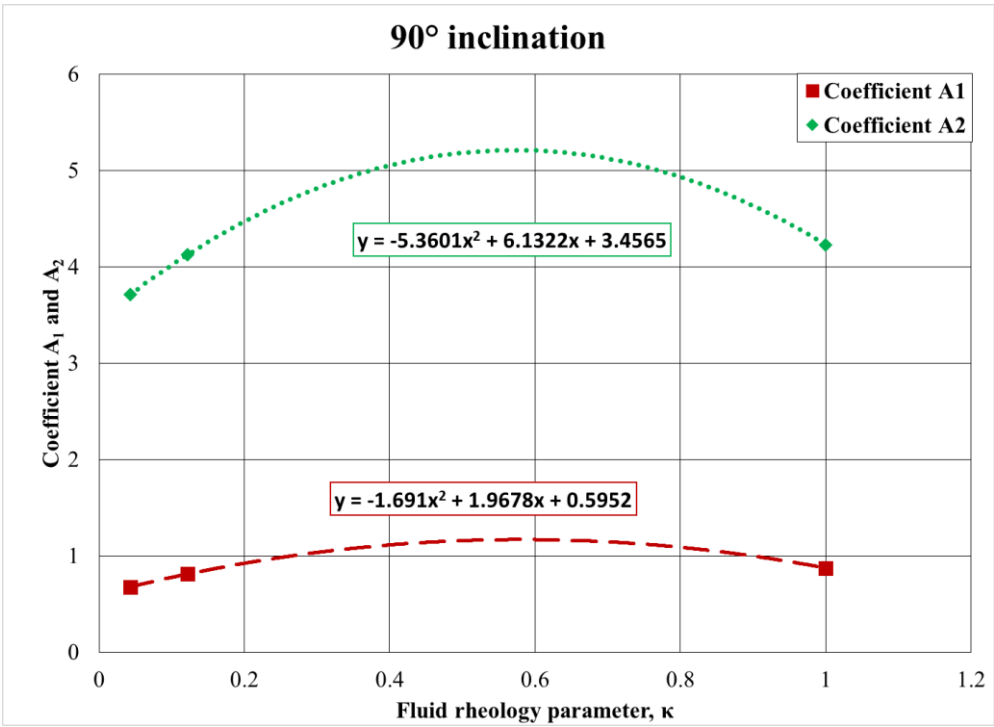

Figure 5.9: Coefficient A_1 and A_2 as function of κ (90° inclination)

Similar procedure can be adopted to find λ. It is found that a logarithmic curve fits the coefficients λ as shown in **Fig. 5.10 through 5.13**.

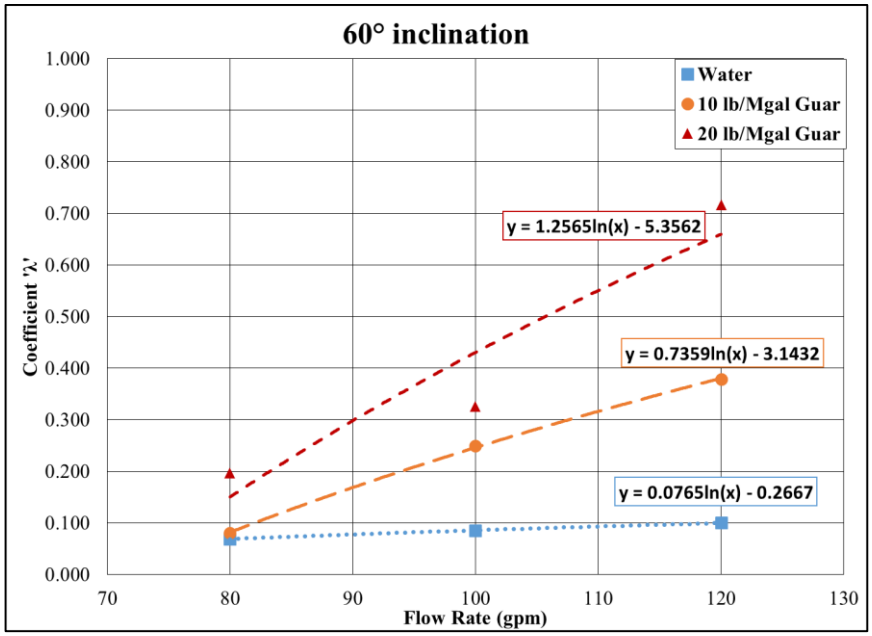

Figure 5.10: Coefficient 'λ' as function of flow rate (60° inclination)

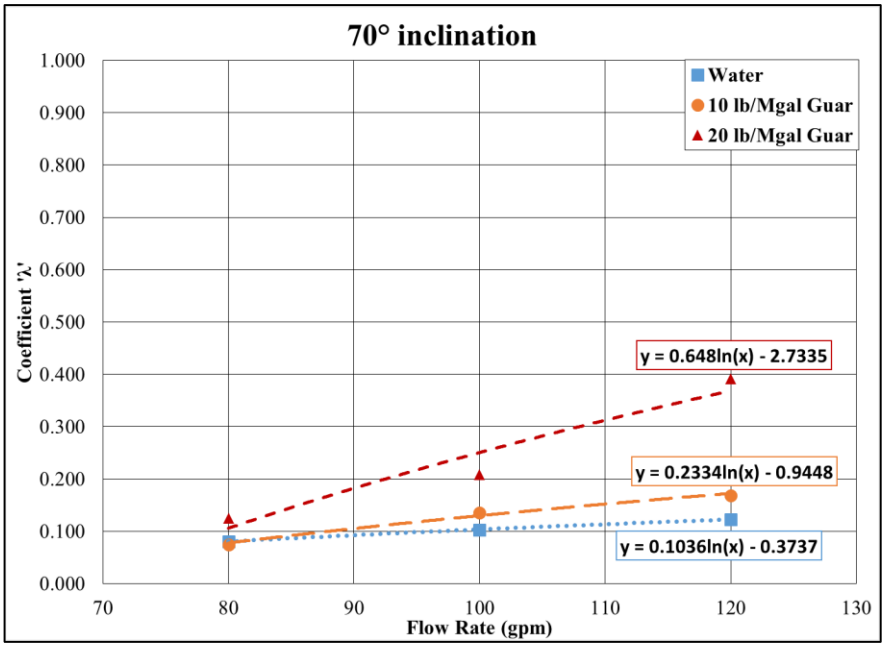

Figure 5.11: Coefficient 'λ' as function of flow rate (70° inclination)

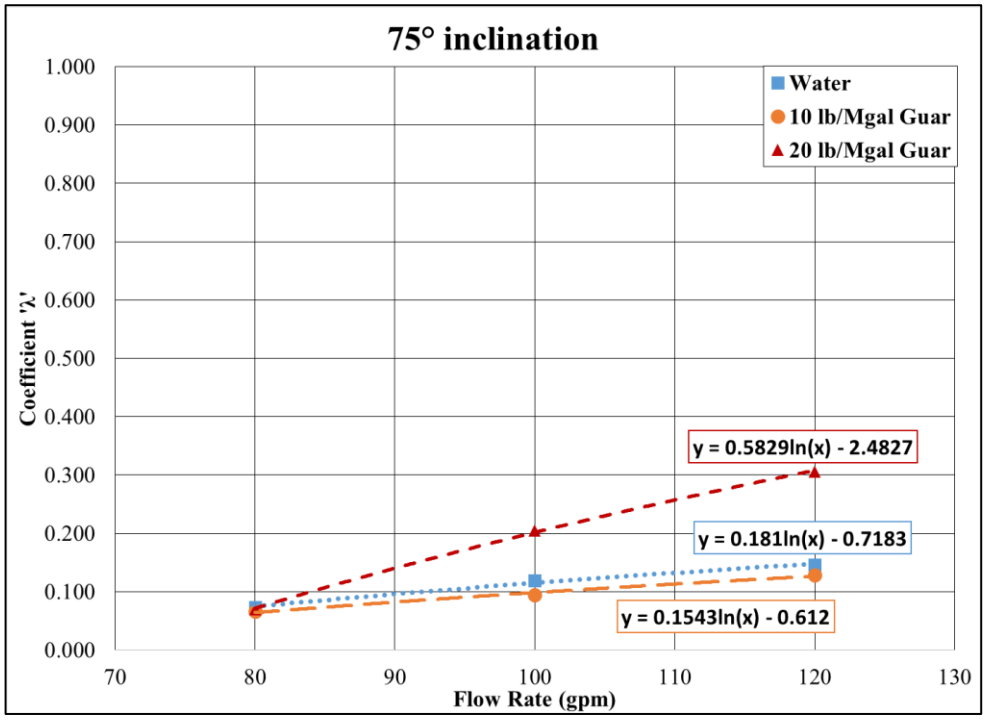

Figure 5.12: Coefficient 'λ' as function of flow rate (75° inclination)

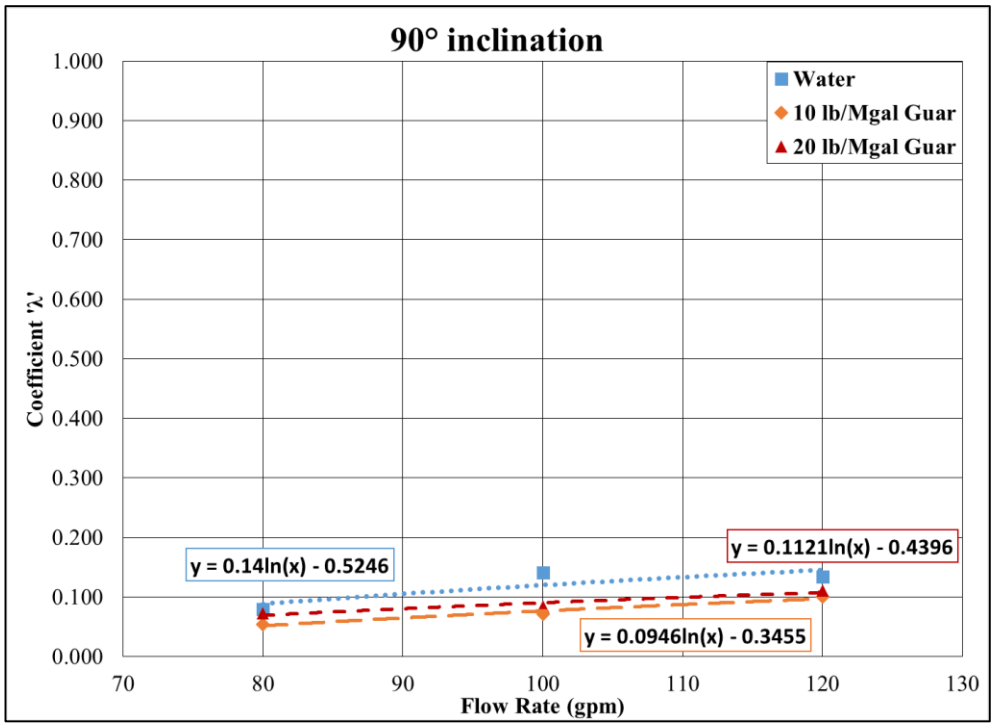

Figure 5.13: Coefficient 'λ' as function of flow rate (90° inclination)

For a fixed inclination and fluid rheology, λ can be estimated from the flow rate using following relation:

$$\lambda = B_1 \ln(Q) - B_2 \tag{5.12}$$

B_1, B_2 = empirical rheological parameters

Analogous to A_1 and A_2, the coefficients B_1 and B_2 are dependent of fluid rheology factor κ. **Figures 5.14 to 5.17** are the plots relating B_1 and B_2 as a function of κ for various inclination. In general, both B_1 and B_2 are polynomial functions of κ and can be expressed as:

$$B_1 = b_{11}\kappa^2 + b_{12}\kappa + b_{13} \tag{5.13}$$

$$B_2 = b_{21}\kappa^2 + b_{22}\kappa + b_{23} \tag{5.14}$$

b_{xy} = empirical inclination specific constants

The inclination specific constants $b_{11}, b_{12}, b_{13}, b_{21}, b_{22}$, and b_{23} are tabulated in **Table 5.1**.

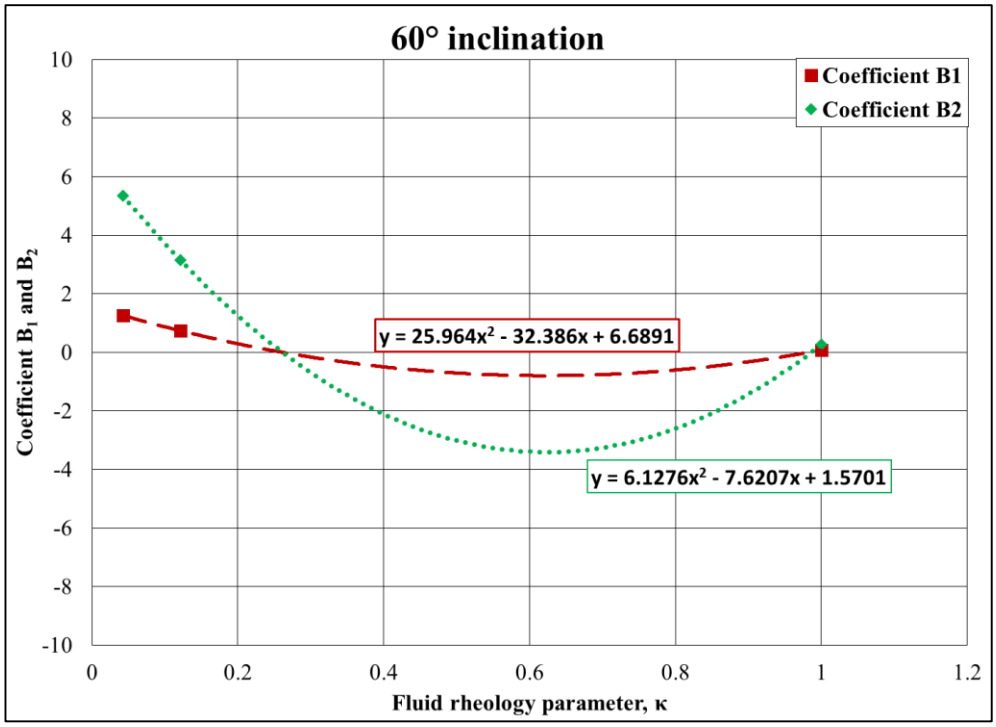

Figure 5.14: Coefficient B_1 and B_2 as function of κ (60° inclination)

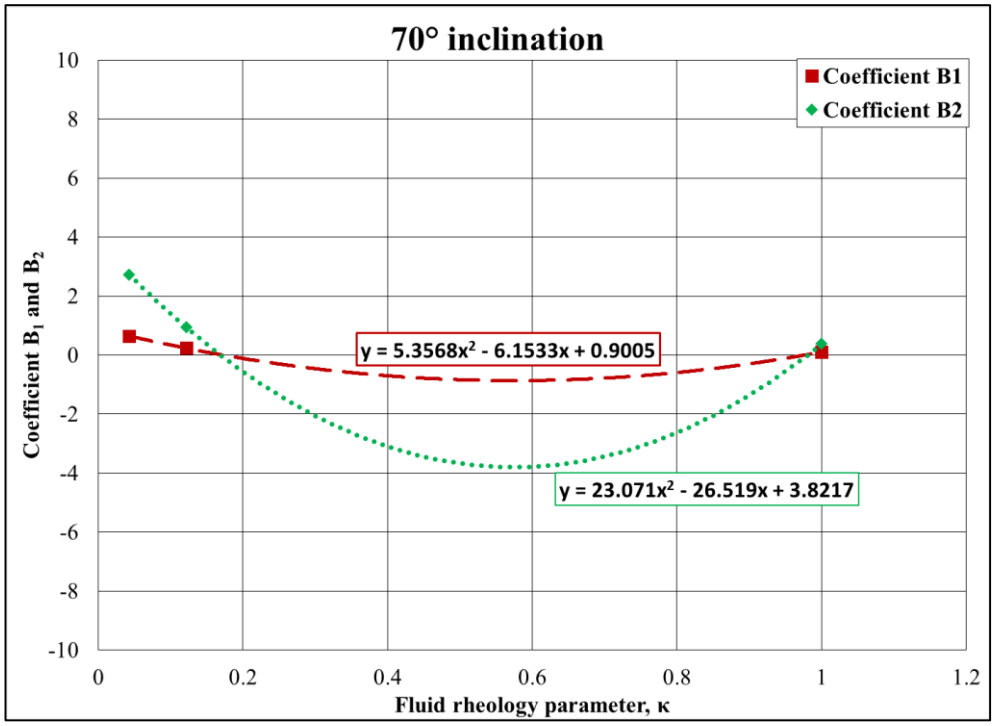

Figure 5.15: Coefficient B_1 and B_2 as function of κ (70° inclination)

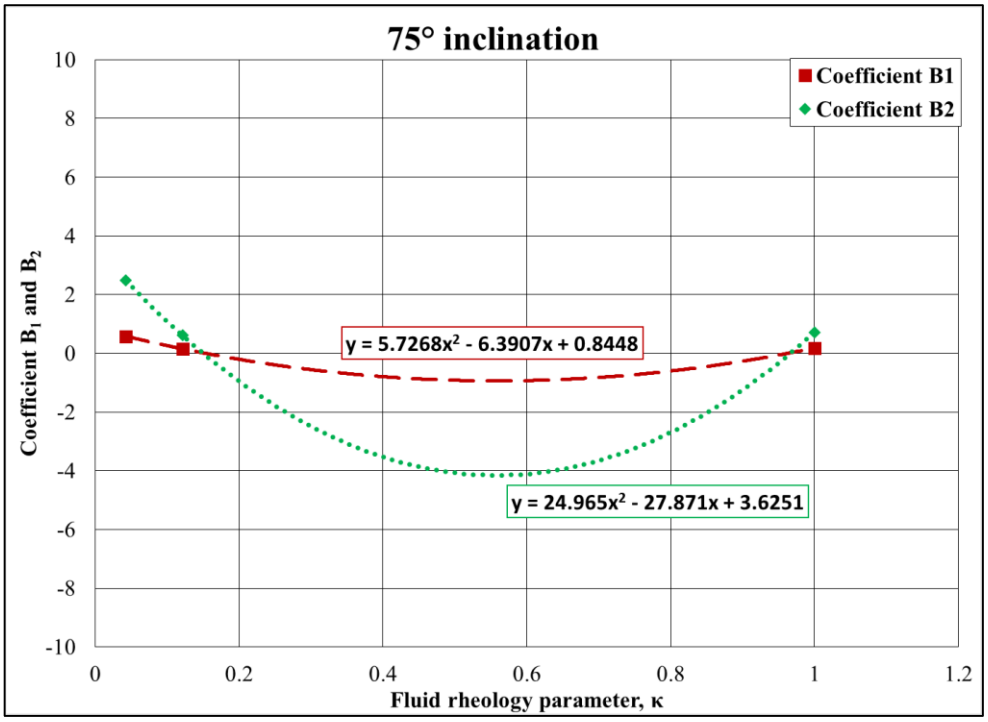

Figure 5.16: Coefficient $\boldsymbol{B_1}$ and $\boldsymbol{B_2}$ as function of $\boldsymbol{\kappa}$ (75° inclination)

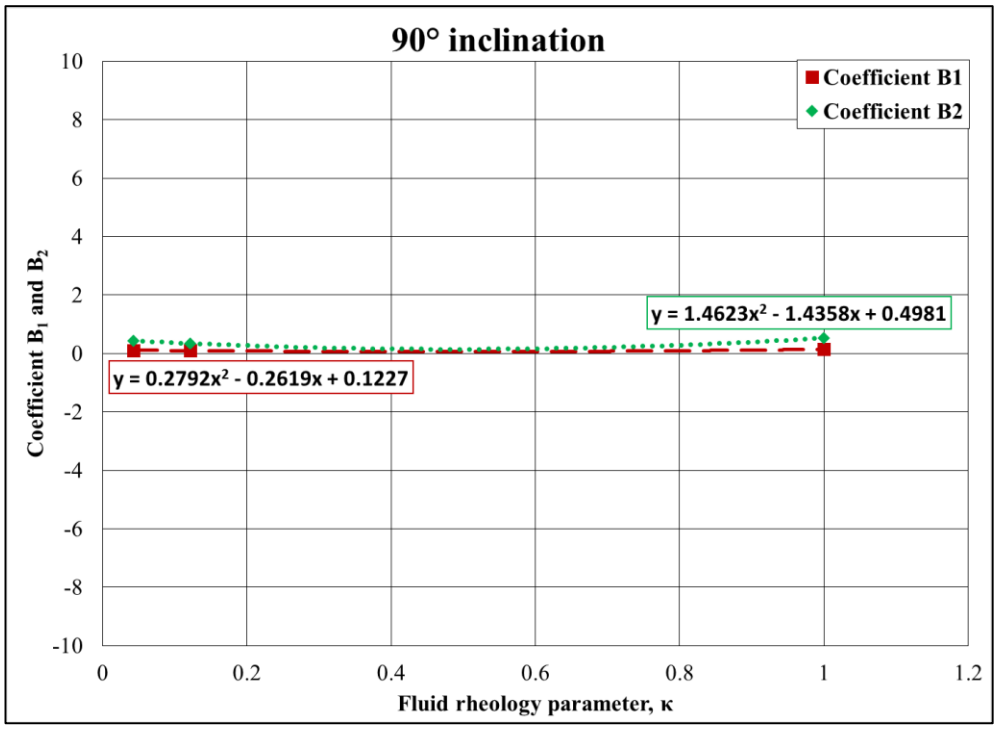

Figure 5.17: Coefficient $\boldsymbol{B_1}$ and $\boldsymbol{B_2}$ as function of $\boldsymbol{\kappa}$ (90° inclination)

Table 5.1: Inclination specific constant $\boldsymbol{a_{xy}}$ and $\boldsymbol{b_{xy}}$

Inclination	60	70	75	90
$\mathbf{a_{11}}$	1.68	-0.20	-0.74	-1.69
$\mathbf{a_{12}}$	-2.50	0.62	1.10	1.97
$\mathbf{a_{13}}$	0.93	0.55	0.56	0.59
$\mathbf{a_{21}}$	7.26	1.98	-1.54	-5.36
$\mathbf{a_{22}}$	-10.72	-0.54	2.85	6.13
$\mathbf{a_{23}}$	4.46	3.28	3.19	3.45
$\mathbf{b_{11}}$	6.13	5.36	5.73	0.28
$\mathbf{b_{12}}$	-7.62	-6.15	-6.39	-0.26
$\mathbf{b_{13}}$	1.57	0.90	0.84	0.12
$\mathbf{b_{21}}$	25.96	23.07	24.96	1.46
$\mathbf{b_{22}}$	-32.39	-26.52	-27.87	-1.43
$\mathbf{b_{23}}$	6.69	3.82	3.62	0.50

Hence, the final bed erosion model (specific to each angle of inclination) is given by,

$$Normalized\ Bed\ Height, h_n(t) = f(Q, n, \mu_a, t) \tag{5.15}$$

It is found that values of α and λ obtained with non-linear regression of the experimental data match closely with the predicted values obtained using Eqs. 5.8 and 5.12 as shown in **Fig. 5.18 and 5.19**. An exact match would result in a unity slope. The experimental data, predicted bed using values of α and λ from the linear regression, and the predicted data using model from Eq. 5.15 for the bed erosion curve with 10 lbm/Mgal guar fluid tested at 75° inclination and 100 gpm is shown in **Fig 5.20**.

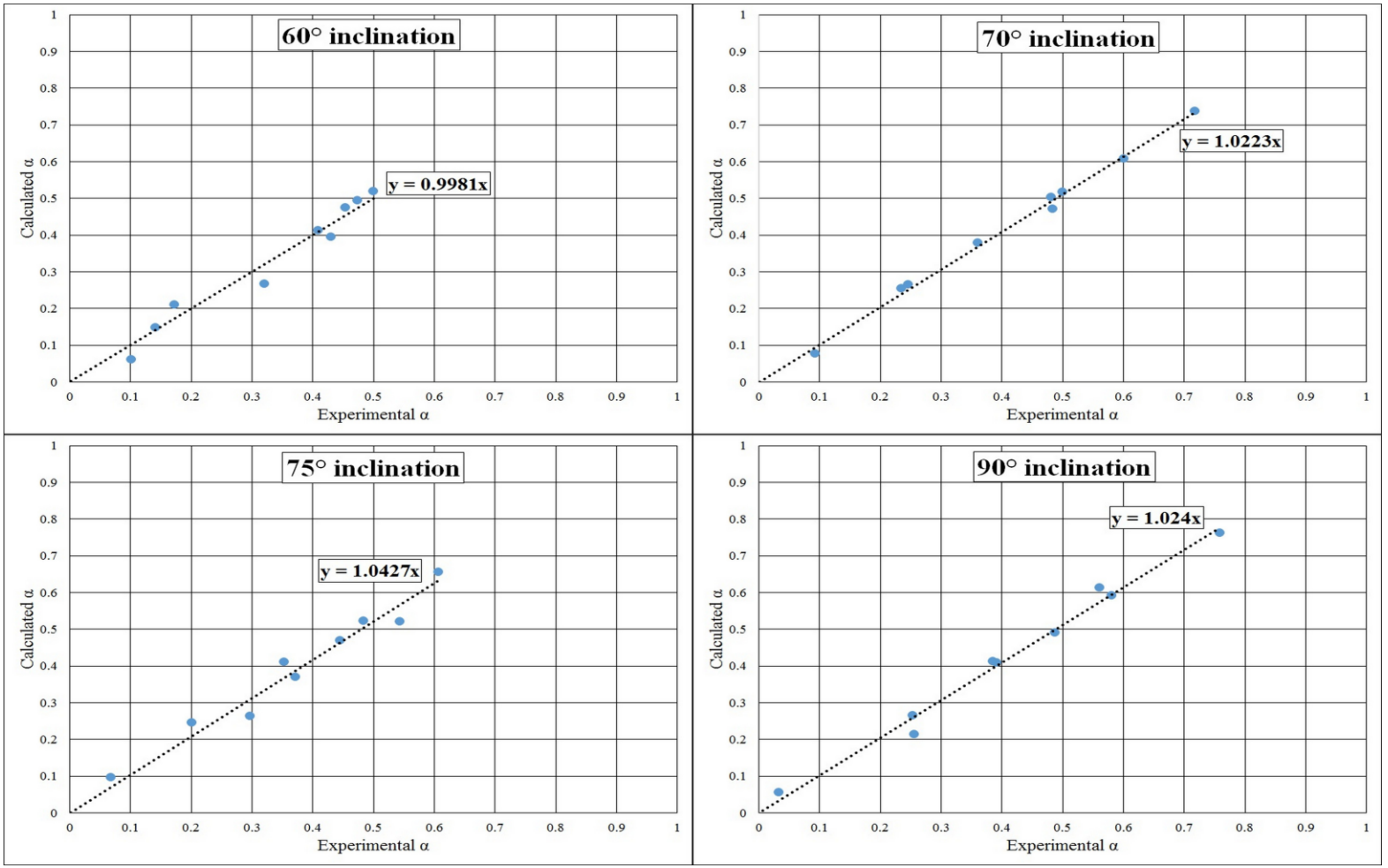

Figure 5.18: Experimental α vs. Predicted α for various inclinations

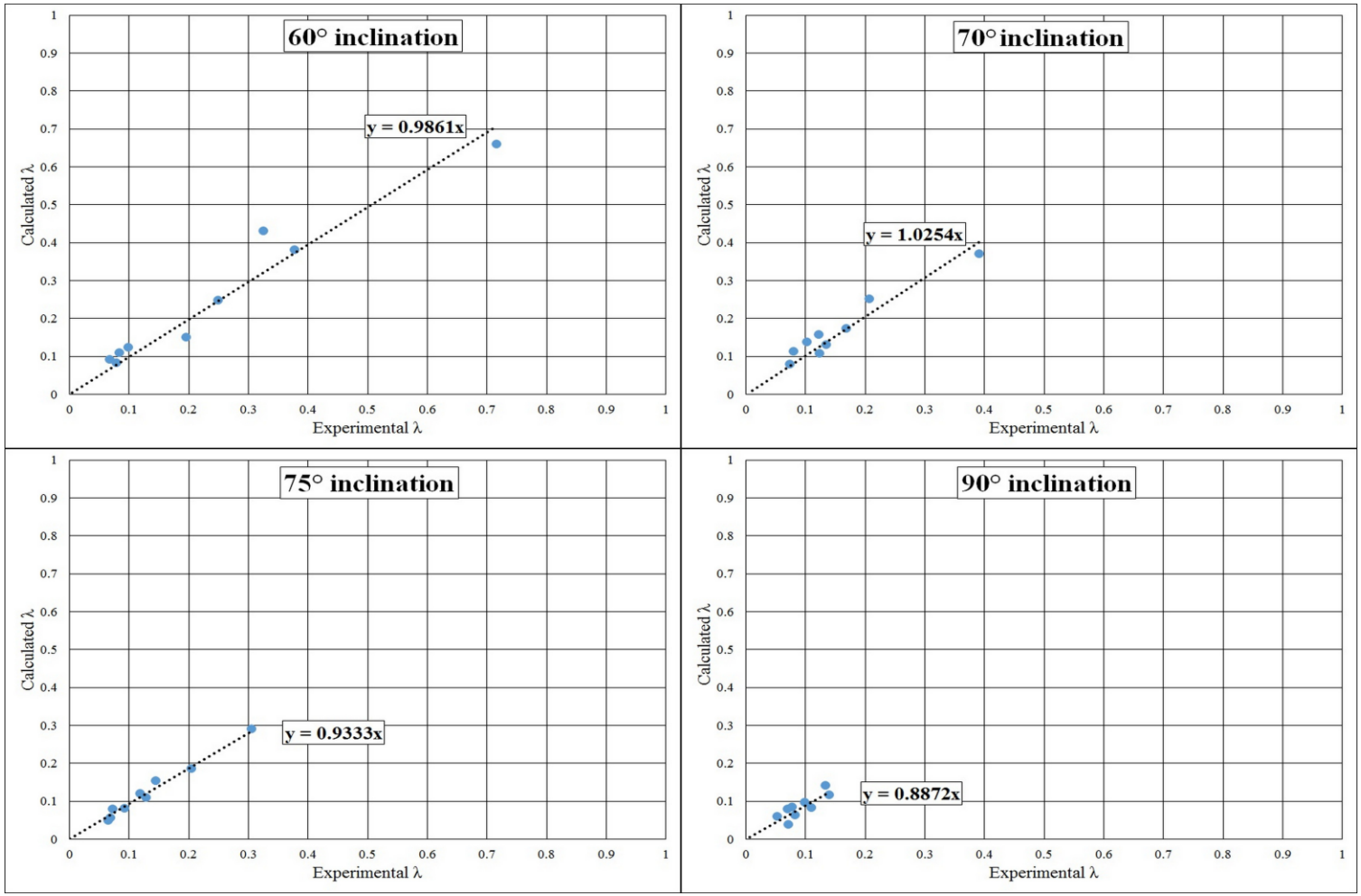

Figure 5.19: Experimental $\boldsymbol{\lambda}$ vs. Predicted $\boldsymbol{\lambda}$ for various inclinations

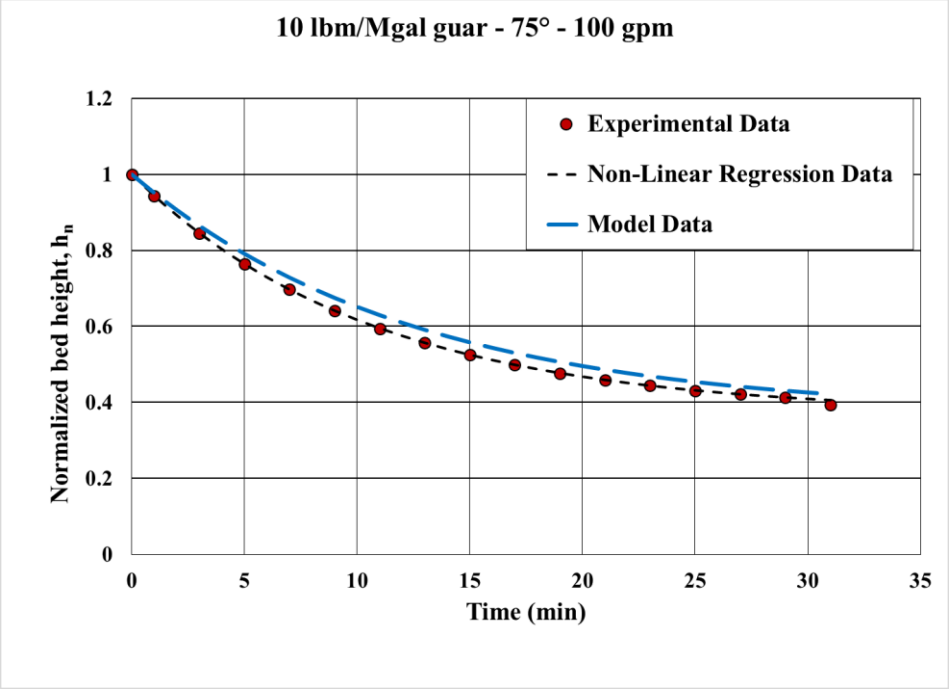

Figure 5.20: Model fit vs. Non-linear regression fit data and Experimental data

5.2 Limitations of the Model

Since the correlation is based on the linear regression, all the factors affecting the cleanout process should be incorporated. However, during the experiments, parameters such as annular configuration, proppant size and density, eccentricity, etc. were maintained constant. The limitations of the model are listed below:

- The correlations were developed with the data obtained from wellbore geometry of 5-in. ID hole, 2.375-in. OD CT with eccentricity of 1.0.
- The model is only valid for the fluid flow in turbulent flow regime and within flow rate range of 80 gpm to 120 gpm. The experiments were conducted to simulate the field condition; and hence, all tests were carried out in the turbulent flow regime.

- Effect of particle size and particle density is not taken into consideration while developing the model. The empirical correlations are only valid for 20/40 mesh ceramic proppant having specific gravity = 1.75.
- It is assumed that the steady state bed height is obtained after 30 minutes. In other words, the normalized bed height does not change for circulation time greater than 30 minutes irrespective of flow rate, inclination and fluid type.
- The test section was slightly more than half-filled with proppant along the entire length before initiating the bed erosion. This corresponds to average initial bed height of 2.75-in. across the test section. The correlations developed can predict the reduction in bed height for a given initial bed height less than or equal to the experimental initial bed height (approximately 2.75-in.). The model will under predict the reduction of bed height for initial conditions such as $3/4^{th}$ cross section of the well bore initially filled with solids or wellbore completely filled with solids.

CHAPTER 6

FIELD APPLICATION OF THE STUDY

6.1 Results from Bed Erosion Curves

The present study establishes the importance of inclination angle, flow rate, fluid rheology and circulation time on cuttings transport mechanism. During cleanout operation in the field, it may not be possible to generate the most ideal condition that result in maximum cleanout. However, results from this study can help design optimum cleanout job based on field operational limit.

An important observation made in this study was that for a fluid pumped at a given flow rate; if the well section is at constant inclination, most of the sand is cleaned in initial few minutes. For instance, it can be observed in Fig. 4.19 that 90% of the bed height in eroded within 15 minutes if 20 lbm/Mgal guar fluid is pumped at 100 gpm. There is insignificant change in the bed height reduction after 15 minutes. For field application, this means that the most efficient hole cleaning period is the first few minutes. After cleaning the hole for a while, pumping at a higher fluid rate will result in more efficient cleaning rather than maintaining a constant circulation rate. This happens because the bed height is reduced after a certain cleaning period and the in-situ liquid velocity decreases. Therefore, the shear force acting at the bed interface is reduced. In order to generate a high enough shear force at the interface to efficiently erode the cuttings bed, a higher flow rate is required.

The results also reflect that in general, the toughest section for hole cleaning is the range of 60° to 70° inclination. The highest in-situ velocity is required for efficient cleanout within this range. The cuttings bed tends to become unstable and slides downward along the wellbore. Therefore, it is better to avoid the longer length of wellbore section falling within this range of inclination.

6.2 Using the Correlation to Predict Bed Height

This section details the procedure for calculating circulation time using the exponential bed decay model for a given inclination. Since the developed correlation is being illustrated, it is assumed that the annular wellbore configuration, solids size and density, and cleanout fluids are similar to those used in our study.

Problem:

A section of wellbore at an inclination of 60° having initial proppant bed thickness of 3-in. is to be cleaned using 10 lbm/Mgal Guar (n=0.644, K_v=0.001019 lbf.sec^n/ft^2) having apparent viscosity of 5.31 cP at 511 sec^{-1} shear rate.

If the fluid is circulated at the flow rate of 100 gpm,

a) What percentage of the bed will be cleaned in 25 mins?
b) What is the bed height at the end of 25 mins?
c) What is the steady state bed height?
d) How much time will be required to achieve 90% of maximum possible cleanout?

Solution:

1. Bed erosion model, $h_n(t) = \alpha + (1-\alpha)e^{-\lambda t}$ (6.1)

2. Determination of rheology parameter

   - Rheology parameter $\kappa = \frac{n}{\mu_a} = \frac{0.644}{5.31} = 0.121$ cP^{-1} (6.2)

3. Determination of A_1, A_2, B_1 and B_2

   - From Table 5.1, at 60° inclination,

     $a_{11} = 1.68$; $a_{12} = -2.50$; $a_{13} = 0.93$

     $a_{21} = 7.26$; $a_{22} = -10.72$; $a_{23} = 4.46$

     $b_{11} = 6.13$; $b_{12} = -7.62$; $b_{13} = 1.57$

     $b_{21} = 25.96$; $b_{22} = -35.39$; $b_{23} = 6.69$

   - $A_1 = a_{11}\kappa^2 + a_{12}\kappa + a_{13}$

     $A_1 = (1.68)(0.121)^2 + (-2.5)(0.121) + (0.93) = 0.652$ (6.3)

   - $A_2 = a_{21}\kappa^2 + a_{22}\kappa + a_{23}$

     $A_2 = (7.26)(0.121)^2 + (-10.72)(0.121) + (4.46) = 3.27$ (6.4)

   - $B_1 = b_{11}\kappa^2 + b_{12}\kappa + b_{13}$

     $B_1 = (6.13)(0.121)^2 + (-7.62)(0.121) + (1.57) = 0.737$ (6.5)

   - $B_2 = b_{21}\kappa^2 + b_{22}\kappa + b_{23}$

     $B_2 = (25.96)(0.121)^2 + (-35.39)(0.121) + (6.69) = 3.15$ (6.6)

4. Determination of α and λ

   - $\alpha = -A_1 \ln(Q) + A_2 = -(0.652)\ln(100) + (3.27) = 0.2674$ (6.7)

   - $\lambda = B_1 \ln(Q) - B_2 = (0.737)\ln(100) - (3.15) = 0.244$ min^{-1} (6.8)

Solution to part a)

Substituting the values of α and λ from Eqs. 6.7 and 6.8 into Eq. 6.1 for time t=25 mins,

$h_n = (0.2674) + (1 - 0.2674)e^{-(0.244)(25)}$

$h_n = 0.269$

Therefore, percentage reduction in bed height = (1- 0.269)*100 = 73%

Solution to part b)

After time, t = 25 minutes, $h_n = 0.269$.

Therefore, $\frac{h_{25\,min}}{h_{initial}} = 0.269$

Or, $h_{25\text{ mins}} = 0.269 * 3 = 0.81$-in.

Solution to part c)

Normalized steady state bed height = α

$\alpha = 0.2674$

$\alpha = \frac{h_{steady\ state}}{h_{initial}} = 0.2674$

$h_{steady\ state} = 0.2674 * 3 = 0.80$-in.

Solution to part d)

Maximum possible cleanout in terms of bed height reduction occurs at time, $t \to \infty$.

At $t \to \infty$; $h_{steady\ state} = 0.80$-in.

Therefore, in time $t = \infty$, $3 - 0.8 = 2.2$-in. of bed is cleaned out.

Hence, it is required to find the time when $0.9 * 2.2 = 1.98$-in. of the bed is cleaned out.

So, $h_{(90\%)} = 3$-in. $- 1.98$-in. $= 1.02$-in.

$h_{n(90\%)} = \frac{1.02}{3} = 0.34$

$h_{n(90\%)} = \alpha + (1 - \alpha)e^{-\lambda t_{90}}$

$0.34 = 0.2674 + (1 - 0.2674)e^{-(0.244)t_{90}}$

upon solving, we get $t_{90} \approx 9.5$ minutes.

Therefore, 90% of maximum possible sand cleanout at 100 gpm occurs within first 9.5 minutes.

CHAPTER 7

CONCLUSIONS AND RECOMMENDATIONS

7.1 Conclusions

1. Solids bed erosion tests were conducted with fresh water, 10 lbm/Mgal guar and 20 lbm/Mgal guar fluids each at flow rate of 80, 100 and 120 gpm and inclination of 50° and 70° in 34 ft long test section.

2. Selected solids bed erosion tests were repeated with fresh water, 10 and 20 lb/Mgal guar fluids each at various flow rate and inclination to produce a better quality cleanout test data.

3. With increasing flow rate, the solids erosion rate and cleanout efficiency increase for all fluids and inclination considered. Increase in flow rate improves interfacial stress acting on the solids bed. Higher interfacial stress indicates higher force acting to transport solids, leading to improved solids transport. The fluid drag and lift on suspended solids also increases with increasing flow rate leading to improved solids transport.

4. The amount of solids that can be transported by a given volume of liquid is dependent on the rheological properties of the liquid. Guar based fluids are more effective than water in terms of carrying capacity but unable to efficiently erode a stationary bed.

5. Water performance is better compared to polymeric fluids at 90° and 75° for the flow rates considered. Decreasing inclination from 70° to 60°, the solids bed tends to slide down due to gravity. At the inclination below 60°, higher drag force (due to a higher flow rate) and higher viscosity in a fluid aids in better cleanout. Fluids with higher viscosity perform better than low viscosity fluids at 45° and 50° and at all flow rates.

6. For all flow rates considered, the rate of solids erosion for water increases with inclination whereas for polymeric fluids it increases with decrease in inclination.

7. The particle dynamics is substantially different at various inclination. At higher inclination, saltation dominates the mode of transport of particles. At lower inclination, solids bed tends to slide downwards against the flow due to gravity.

8. There exists a critical inclination angle at which all fluids have similar performance. It was studied that irrespective of the flow rate, this critical angle exists between 66° and 69° when 10 lb/Mgal Guar is compared with water; and between 64° and 67° when 20 lb/Mgal Guar is compared with water. In general, the critical inclination angle exists between 60° and 70° irrespective of the fluid and flow rate.

9. The reduction in normalized bed height with time is modeled using an exponential decay equation. Non-linear regression was used to determine the steady state normalized bed height (α) and reciprocal of time constant (λ). These parameters were observed to be a function of fluid rheology and flow rate. A system of

empirical equations was developed for every inclination to predict the bed height at any time within applicable range of fluid rheology and flow rate.

7.2 Recommendations

1. Bed erosion tests with various particle properties, annular configuration and wellbore length should be conducted to quantify their effect on wellbore cleanout.

2. A dimensionless correlation should be developed to incorporate the effect of various parameters on the solids transport mechanism. An accurate model requires that tests be conducted by varying these parameters autonomously.

3. Tests should be conducted to determine the critical deposition velocity and critical re-suspension velocity for different fluids at different inclination.

4. Mode of solids transport and dune formation should be quantitatively analyzed to better understand particle dynamics within the flow.

NOMENCLATURE

A_1, A_2	Empirical rheological parameter for calculation of α
A_p	Projected area of the solid particle
a	Bed arc length measured from top, in.
a_{xy}	Inclination specific constants to calculate α
B_1, B_2	Empirical rheological parameters for calculation of λ
b	Bed arc length measured from the bottom, in.
b_{xy}	Inclination specific constants to calculate λ
C_D	Drag coefficient, dimensionless
C_L	Lift coefficient, dimensionless
D_b	Diameter of the bob, mm
D_c	Diameter of the cup, mm
d_h	Hydraulic diameter, in.
d_s	Solids diameter, in.
F_b	Buoyancy force

F_d	Drag force
F_g	Gravitational force
F_L	Lift force
g	Acceleration due to gravity, m/s^2
h	Vertical bed height, in.
h_c	Corrected vertical bed height, in.
h_i	Initial bed height, in.
h_f	Final or steady state bed height, in.
h_n	Normalized bed height, dimensionless
$h(t)$	Bed height at any time, in.
K_V	Viscometer consistency index, $lbf\text{-}s^n/ft^2$
m	Mass of a solid particle
m_{30}	Dry weight of proppant cleaned out during a 30 min. test duration, lbm
m_{flush}	Dry weight of proppant flushed out of the test section after each test, lbm
N	Spring factor (0.2 for a $1/5^{th}$ spring)

n	Flow behavior index, dimensionless
Q	Flow rate, gpm
Re	Reynolds number, dimensionless
r	Radius of the outer pipe, in.
t	Circulation time, min
u	Fluid velocity
V_s	Volume of the solid particle
x	Difference between radius of outer pipe and vertical bed height, in.

GREEK SYMBOLS

α	Steady state normalized bed height, dimensionless
β	Ratio of bob to cup diameter, dimensionless
$\dot{\gamma_w}$	Wall shear rate, sec^{-1}
θ	Angle of inclination
θ_i	Viscometer dial reading at i^{th} rpm
κ	Rheology parameter, cP^{-1}
λ	Reciprocal of time constant, min^{-1}
μ	Dynamic fluid viscosity, cP
μ_a	Apparent fluid viscosity, cP
ρ_f	Fluid density
ρ_s	Solids density
τ_w	Wall shear stress, lbf/ft^2

REFERENCES

Acrivos, A., and Herbolzheimer, E. 1978. Enhanced Sedimentation in Settling Tanks with Inclined Walls. Journal of Fluid Mechanics (1979), vol. 92, part 3, 435-457.

Adari, R.B. 1999. Development of Correlations Relating Bed Erosion to Flowing Time for Near Horizontal Wells. MS thesis, University of Tulsa, USA.

Boycott A.E. 1920. Sedimentation of Blood Corpuscles. Nature, January 22.

Cano, V., Cardona, W.G., Murphy, C., and de Araujo, M. 2016. Improved CT Cleanout and Milling Procedures Utilizing Only Non-Viscous Cleanout Fluids. Presented at SPE/ICoTA Coiled Tubing & Well Intervention Conference & Exhibition, Houston, Texas, USA, 22-23 March 2016. SPE 179070

Cho, H., Shah, S. N., and Osisanya, S.O. 2000. A Three-Layer Modeling for Cuttings Transport with Coiled Tubing Horizontal Drilling. Presented at SPE Annual Technical Conference and Exhibition, Dallas, Texas, USA, 1-4 October. SPE 63269.

Clark, R. K., and Bickham, K. L. 1994. A Mechanistic Model for Cuttings Transport. Presented at SPE Annual Technical Conference and Exhibition, New Orleans, Louisiana, USA, 25-28 September. SPE 28306.

Duan, M., Miska., S.Z., Yu, M. et al. 2008. Transport of Small Cuttings in Extended Reach Drilling. SPE Drilling and Completion 23 (3): 258-265. SPE 104192.

Duan, M., Miska, S. Z., Yu, M., Takach, N., and Ahmed, R. 2007. Critical Conditions for Effective Sand-Sized Solids Transport in Horizontal and High-Angle Wells. Presented at SPE Production and Operations Symposium, Oklahoma City, Oklahoma, USA, 31 March – 3 April. SPE 106707.

Ford, J.T., Gao, E., Oyeneyin, M.B., Peden, J.M., Larrucia, M.B., and Parker, D. 1996. A New MTV Computer Package for Hole-Cleaning Design and Analysis. SPE Drilling & Completion, September, 168-172. SPE 26217.

Gavignet, A. A., and Sobey, I. J. 1989. Model Aids Cuttings Transport Prediction. Journal of Petroleum Technology 41(9): 916-921. SPE 15417.

Halow, J.S. 1971. Incipient Rolling, Sliding and Suspension of Particles in Horizontal and Inclined Turbulent Flow. Chemical Engineering Science (1973), Vol. 28, 1-12.

Jacob, A.E. 2013. Investigation of Stationary Cuttings Bed Height in Washout. MS thesis, Norwegian University of Science and Technology, Norway.

Jalukar, L.S. 1993. A Study of Hole Size Effect on Critical and Sub-critical Drilling Fluid velocities in Cuttings Transport for Inclined Wellbores. MS Thesis, University of Tulsa, USA.

Kamp, A. M., and Rivero, M. 1999. Layer Modeling for Cuttings Transport in Highly Inclined Wellbores. Presented in Latin American and Caribbean Petroleum Engineering Conference, Caracas, Venezuela, 21-23 April. SPE 53942.

Kelessidis, V. C., and Mpandelis, G. E. 2004. Hydraulic Parameters Affecting Cuttings Transport for Horizontal Coiled Tubing Drilling. Presented at 7th National Congress on Mechanics, Chania, Greece, 24-26 June.

Larsen, T.I.F. 1990. A Study of the Critical Fluid Velocity in Cuttings Transport for Inclined Wellbores. MS thesis, University of Tulsa, USA.

Li, J., and Walker, S. 1999. Sensitivity analysis of Hole Cleaning parameters in Directional Wells. Presented at SPE/ICoTA Coiled Tubing Roundtable, Houston, Texas, 25-26 May. SPE 54498.

Li, J., Walker, S., and Aitken, B. 2002. How to Efficiently Remove Sand from Deviated Wellbores with a Solids Transport Simulator and a Coiled Tubing Cleanout Tool. Presented at the SPE Annual Technical Conference and Exhibition, San Antonio, Texas, 29 September-2 October, 2002. SPE 77527.

Li, J., Wilde, G., and Crabtree, A.R. 2005. Do Complex Super-Gel Liquids Perform Better than Simple Linear liquids in Hole Cleaning with Coiled Tubing? Presented at the SPE/ICoTA Coiled Tubing Conference and Exhibition, The Woodlands, Texas, 12-13 April. SPE 94185.

Li, J., and Wilde, G. 2005. Effect of Particle Density and Size on Solids Transport and Hole Cleaning with Coiled Tubing. Presented at SPE/ICoTA Coiled Tubing Conference and Exhibiton, The Woodlands, Texas, 12-13, April. SPE 94187.

Li, J., Misselbrook, J.G., and Seal, J. 2010. Sand Cleanout with Coiled Tubing: Choice of Process, Tools or Fluids? Journal of Canadian Petroleum Technology 49 (8): 69-82. SPE 113267.

Li, J., and Luft, B. 2014. Overview of Solids Transport Study and Application in Oil-Gas Industry: Theoretical Work. Presented at International Petroleum Technology Conference, Kuala Lumpur, Malaysia, 10-12 December 2014. IPTC 17832.

Martins, A.L., Sa, C. H. M., Lourenco, A. M. F., and Campos, W. 1996. Optimizing Cuttings Circulation in Horizontal Well Drilling. Presented at the International Petroleum Conference & Exhibition of Mexico, Villahermosa, Mexico, 5-7 March. SPE 35341

Martins, A.L., Silva, R.A., and Costa, F.G. 2003. Effect of Non-Newtonian Behavior of Fluids in the Re-Suspension of a Drilled Cuttings Bed. Annual Transactions of The Nordic Rheology Society, Vol. 11, 49-56.

Martins, A. L., and Santana, C. C. 1992. Evaluation of Cuttings Transport in Horizontal and Near Horizontal Wells-A Dimensionless Approach. Presented at the SPE Latin America Petroleum Engineering Conference, Caracas, Venezuela, 8-11 March. SPE 23643.

Martins, A. L., Santana, M., Gaspari, E., and Campos, W. 1998. Evaluating the Transport of Solids Generated by Shale Instabilities in ERW Drilling. Presented at the SPE International Conference on Horizontal Well Technology, Calgary, Alberta, Canada, 1-4 November. SPE 50380.

Naik, S. 2015. Effect of Fluid Rheology and Flow Rate on Wellbore Cleanout Process in Horizontal and Directional Wells. PhD dissertation, University of Oklahoma, USA.

Nguyen, D., and Rahman, S.S. 1998. A Three Layer Hydraulic Program for Effective Cuttings Transport and Hole Cleaning in Highly Deviated and Horizontal Wells. SPE Drilling and Completion 13 (3):182- 189. SPE 51188.

Nir, A., and Acrivos, A. 1989. Sedimentation and Sediment Flow on Inclined Surfaces. Journal of Fluid Mechanics (1990) vol. 212, 139-153.

Ozbayoglu, M. E., Miska, S. Z., Reed, T. et al. 2004. Analysis of the Effects of Major Drilling Parameters on Cuttings Transport Efficiency for High-Angle Wells in Coiled Tubing Drilling Operations. Presented at SPE/ICoTA Coiled Tubing Conference and Exhibition, Houston, Texas, 23-24 March. SPE 89334.

Ozbayoglu M.E., Saasen, A., Sorgun, M., and Svanes, K. 2008. Effect of Pipe Rotation on Hole Cleaning for Water-Based Drilling Fluids in Horizontal and Deviated Wells. Presented at the IADC/SPE Asia Pacific Drilling Technology Conference and Exhibition, Jakarta, Indonesia, 25-27 August. IADC/SPE 114965

Ozbayoglu, M. E., and Sorgun, M. 2010. Frictional Pressure Loss Estimation of Non-Newtonian Fluids in Realistic Annulus with Pipe Rotation. Journal of Canadian Petroleum Technology 49 (12): 57-64.

Ozbayoglu, M. E., Reza, E.O., Ozbayoglu M.A., and Ertan, Y. 2010. Estimation of "Very-Difficult-to-Identify" Data for Hole Cleaning, Cuttings Transport and Pressure

Drop Estimation in Directional and Horizontal Drilling. Presented at the IADC/SPE Asia Pacific Drilling Technology Conference and Exhibition, Ho Chi Minh City, Vietnam, 1-3 November. IADC/SPE 136304

Rolovic, R., Weng, X., Hill, S., Robinson, G., Zemlak, K., and Nejafov, J. 2004. An Integrated System Approach to Wellbore Cleanouts with Coiled Tubing. Presented at SPE/ICoTA Coiled Tubing Conference and Exhibition, Houston, Texas, USA, 23-24 March. SPE 89333.

Santana, M., Martins, A.L., and Sales Jr., A., 1998. Advances in the Modeling of the Stratified Flow of Drilled Cuttings in High Angle and Horizontal Wells. Presented at the International Petroleum Conference and Exhibition of Mexico, Villahermosa, Mexico, 3-5 March. SPE 39890.

Sifferman, T. R., & Becker, T. E. 1992. Hole Cleaning in Full-Scale Inclined Wellbores. SPE Drilling Engineering 7 (2):115-120. SPE 20422.

Walker, S., and Li, J. 2000. The Effects of Particle Size, Fluid Rheology, and Pipe Eccentricity on Cuttings Transport. Presented at SPE/ICoTA Coiled Tubing Roundtable, Houston, Texas, 5-6 April. SPE 60755.

Xiaofeng, S., Kelin, W., Tie, Y., Yang, Z., Shuai, S., and Shizhu, L. 2013. Review of Hole Cleaning in Complex Structured Wells.The Open Petroleum Engineering Journal, 6, 25-32.

Xu, Z.J., and Michaelides, E.E. 2005. A Numerical Simulation of Boycott Effect. Chemical Engineering Communications, 192:4, 532-549

Yu, M., Melcher, D., Takach, N., Miska, S., and Ahmed, R. 2004. A New Approach to Improve Cuttings Transport in Horizontal and Inclined Wells. Presented at SPE Annual Technical Conference and Exhibition, Houston, Texas, USA, 26-29 September. SPE 90529

APPENDIX A

LASER PARTICLE SIZE ANALYSIS

The 20/40 US mesh ceramic proppant employed to deposit the solids bed was re-used for several tests. During bed deposition, proppant passing through the centrifugal pump can get damaged by the impellers of the centrifugal pump rotating at very high speed. Hence, particle size analysis was carried out in order to verify the consistence of proppant size for all tests.

A.1 Equipment Used

The Beckman Coulter LS 13 320

This is a particle size analyzer that measures the size distribution of particles suspended either in a liquid or in dry powder form by using the principles of light/laser scattering. The LS 13 320 (**Fig. A.1**) measures particle size distribution by measuring the pattern of light scattered by the particles in the sample. This pattern of scattered light is often called a scattering pattern or scattering function. More specifically, a scattering pattern is formed by light intensity as a function of scattering angle. Each particle's scattering pattern is characteristic of its size. The pattern measured by the LS 13 320 is the sum of the patterns scattered by each constituent particle in the sample.

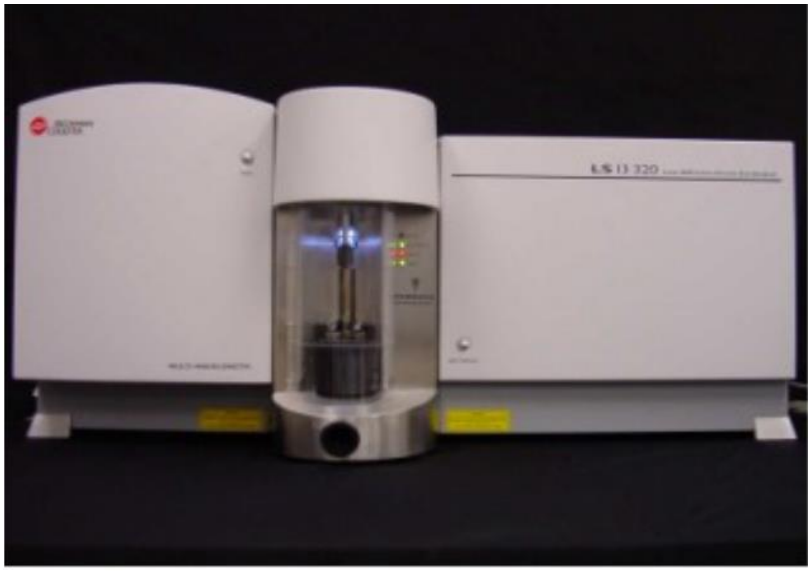

Figure A.1: The Beckman Coulter LS 13 320 Laser Particle Size Analyzer

This equipment was preferred over conventional sieve analysis technique because it requires smaller sample size (20 gms of sand) as compared to sieve analysis (100 gms of sand). Also, this equipment is more automated as compared to sieve analysis with respect to generating output results.

A.2 Samples Tested

Random Sample taken:

1. From the new unused batch of sand
2. From the batch of sand reused for 36 Tests
3. From the batch of sand reused for 63 Tests

A.3 Results

Figure A.2 represents the size distribution for all the samples tested.

Unused batch of sand

The sand used in the CT cleanout testing is 20/40 US mesh sand. The results for this batch demonstrate that 98% of sand distribution lies between 400 microns (40 US mesh) to 840 microns (20 US mesh).

Sand after 36 Tests

Each test always has certain amount of proppant lost during flushing of lines, drying of sand, cleaning the sieve, etc. In order to maintain the constant weight of sand in initial feed, certain amount of unused sand is mixed after every test. Due to this, there was only marginal change in the size distribution of the sand after 36 tests. The results depict that more than 97% of particle size distribution lies with 20/40 mesh range.

Sand after 63 Tests

After 63 tests, 97.4% of particle size distribution lies with 20/40 mesh range. The value increased marginally from that after 36 tests since it was decided to add more amount of unused sand for each test.

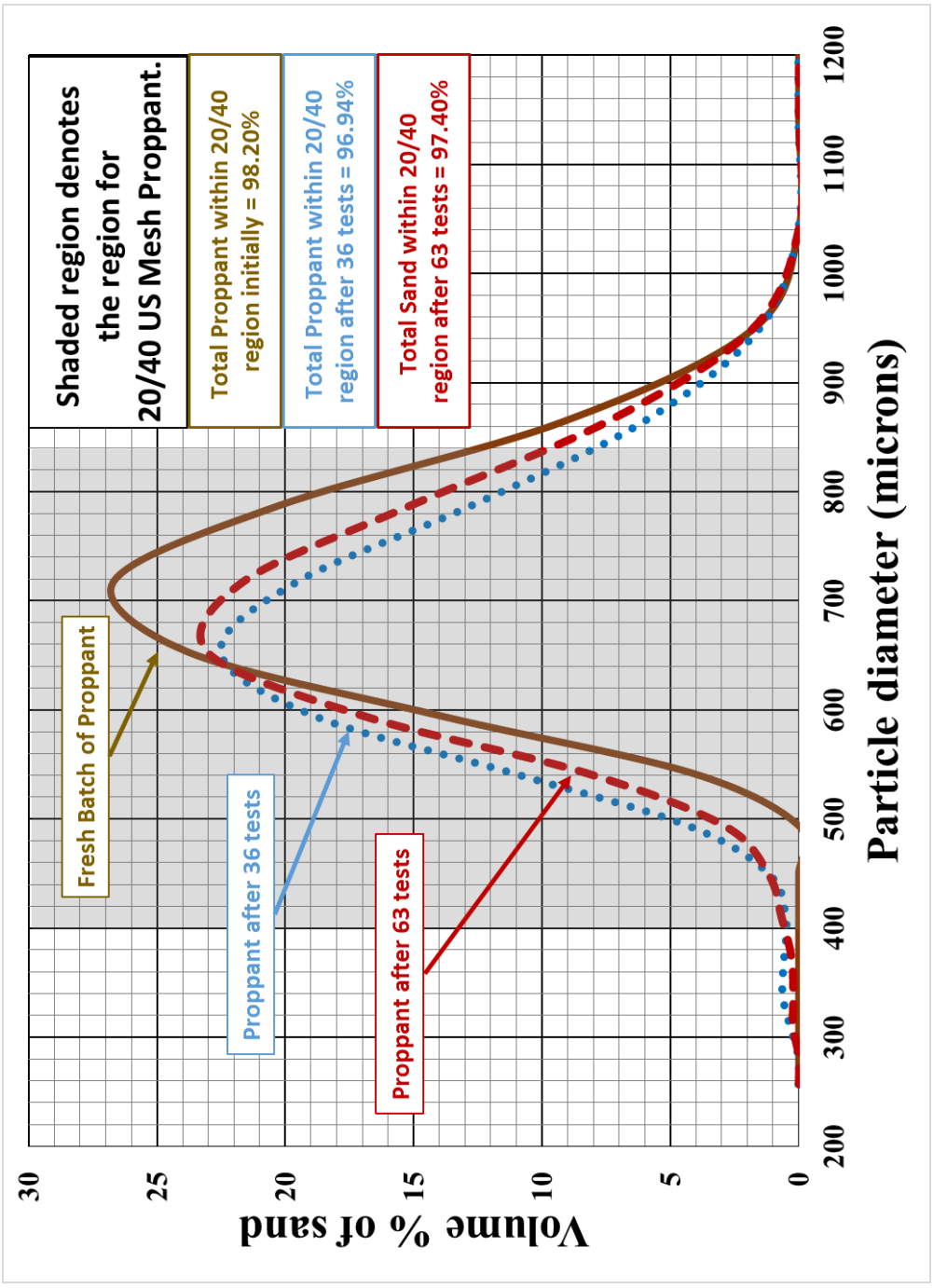

Figure A.2: Comparison of particle size distribution of 20/40 mesh proppant